

**HOT SURFACE IGNITION TEMPERATURE OF DUST LAYERS
WITH AND WITHOUT
COMBUSTIBLE ADDITIVES**

by
Haejun Park

A Thesis
Submitted to the Faculty
of the
WORCESTER POLYTECHNIC INSTITUTE
in partial fulfillment of the requirements for the
Degree of Master of Science
in
Fire Protection Engineering
May 2006

APPROVED:

Professor Robert G. Zalosh, Advisor

Joseph A. Senecal, Kiddie-Fenwal, Inc., Co-advisor

Professor Kathy A. Notarianni, Head of Department

Abstract

An accumulated combustible dust layer on some hot process equipment such as dryers or hot bearings can be ignited and result in fires when the hot surface temperature is sufficiently high. The ASTM E 2021 test procedure is often used to determine the Hot Surface Minimum Ignition Temperature for a half inch deep layer of a particular dust material. This test procedure was used in this thesis to study possible effects of combustible liquid (such as lubricating oil) and powder additives in the dust layer as well as air flow effects.

The following combustible dusts were used: paper dust from a printing press, Arabic gum powder, Pittsburgh seam coal, and brass powder. To develop an improved understanding of the heat transfer, and oxygen mass transfer phenomena occurring in the dust layer, additional instrumentation such as a second thermocouple in the dust layer, an oxygen analyzer and gas sampling line, and an air velocity probe were used in at least some tests.

Hot Surface Minimum Ignition temperatures were 220°C for Pittsburgh seam coal, 360°C for paper dust, 270°C for Arabic gum powder, and > 400°C for brass powder. The addition of 5-10 weight percent stearic acid powder resulted in significantly lower ignition temperature of brass powder. When combustible liquids were added to the dust layer, the ignition temperatures did not decrease regardless of the liquids' ignitibility because the liquids seemed to act as heat absorbents. Although air velocity on the order of 1 cm/s did not affect test results, much larger

air velocities did affect the results. With 33 cm/s downward airflow at the elevation of the surface of the layer, Pittsburgh seam coal was not ignited at 230°C which was 10°C higher than the 220°C hot surface ignition temperature without airflow. Based on the results and data from the additional instrumentations, modifications of the ASTM E2021 test procedure are recommended.

Acknowledgement

I heartily thank my parents and family. As farmers, they must have had hard times both in physically and financially. They were willing to support me when I decided to study abroad and have prayed for my health and safety more than anyone else.

I would like to thank my academic and thesis advisor, Professor, Robert G. Zalosh, for his excellent guidance and support. He has shown concrete trust on me throughout the period while I have worked on the tests and thesis write-up. He provided me with scholarships and helped me not to suffer financial hardship. He supported me not only financially but also spiritually. His work ethic and passion for the field of fire protection engineering at his old age has been always a good motivation to me, and even more I thought him as a role model in my life. Now he is retiring at the end of this semester, 2006 fall, giving me the honor to be his last M.S. thesis student, I truly want to pray for his health for the rest of his life.

I also would like to thank Dr. Joseph A. Senecal of Kidde-Fenwal, Inc., thesis co-advisor, for reviewing my thesis and giving me good advice on the test procedures and the results.

I also want to thank all other FPE professors and staffs for their professionalism and support for students.

Table of contents

Abstract	ii
Acknowledgement	iv
Table of contents	v
Nomenclature	vii
List of tables	viii
List of figures	ix
1. Introduction	13
2. Literature review	15
2.1. Previous study of hot surface ignition.....	15
2.2. ASTM E 2021-01, IEC 61241-2-1 and other test methods	18
2.3. Ignition Handbook by Vytenis Babrauskas	21
2.4. Self heating, and Frank-Kamenetskii's theory	23
2.4.1. Self-heating theory.....	23
2.4.2. Steady state theory for symmetrically cooled bodies	25
2.4.3. Steady state theory for unsymmetrically cooled bodies	27
3. Problem statement and assumptions	29
3.1. Problem statement.....	29
3.2. Assumptions.....	31
4. Testing	32
4.1. Test objectives.....	32
4.2. Test description	33
4.2.1. Equipment layout	33
4.2.2. Test procedure	38
4.2.3. Test environment.....	39
4.3. Uncertainty and experimental error	40
4.3.1. Test equipment inherent errors.....	40
4.3.2. Experimental errors.....	46
4.4. Test material properties.....	50
4.4.1. Dust.....	50
4.4.2. Combustible liquids and contaminants	51
4.5. Preliminary test	53

4.5.1. Pittsburgh seam coal	56
4.5.2. Brass powder.....	59
4.5.3. Analysis and summary	59
4.6. Ignition temperatures of dust alone.....	60
4.6.1. Newspaper dust.....	60
4.6.2. Gum Arabic powder.....	65
4.6.3. Analysis and summary	69
4.7. Ignition temperatures of dust with combustible liquids	71
4.7.1. Newspaper dust.....	71
4.7.2. Gum powder with ketone-based liquid solution	87
4.7.3. Analysis and summary	93
4.8. Comparisons of ignition temperatures with and without combustible liquids	95
4.8.1. Newspaper dust.....	95
4.8.2. Gum Arabic powder.....	101
4.9. Ignition temperature of Brass powder with stearic acid.....	103
4.10. Oxygen concentration in the Pittsburgh seam coal layer	109
4.10.1. When ignition occurred.....	112
4.10.2. When ignition did not occur.....	115
4.10.3. Analysis and summary	116
4.11. Air flow effects on ignition temperature of Pittsburgh seam coal layer	119
4.11.1. Without air flow, and with inherent air flow on the bench	123
4.11.2. With downward air flow.....	125
4.11.3. Analysis and summary	127
5. Application of test results to ASTM E2021 Standard	128
6. Conclusions and Recommendations	131
References	134
Appendix A	136
Appendix B	142

Nomenclature

ρ	material density (kg/m ³)
Q	heat of reaction (kJ/kg)
A	pre-exponential factor (/s)
E	apparent activation energy (kJ/mol)
R	universal gas constant (=8.314 J/mol-K)
h	convective heat transfer coefficient (kW/m ² -K)
k	bulk thermal conductivity (kW/m-K)
T _s	layer surface temperature (K)
T ₀	ambient air temperature (K)
T _h	hot plate temperature (K)
T _m	maximum layer temperature (K)
C1	integration constant
C2	integration constants
x	distance from the reference point in the slab
θ	non-dimensional parameter for T
z	non-dimensional parameter for x
δ	non-dimensional parameter for heat generation rate

List of tables

Table 1 : Results of some dust layer ignition tests conducted by Bowes	21
Table 2 : Single-drop hotplate ignition temperatures found by Krasawa et al.	22
Table 3 : Ignition of spills of turbine oil on a hot surface	22
Table 4 : Comparison of test equipment inherent errors and ASTM requirements	45
Table 5 : Average amount of dust to fill half of the ring (0.5 inch thick)	46
Table 6 : Summary of dust properties and provider	50
Table 7 : Flash point and Auto Ignition Temperatures of liquids	52
Table 8 : Max. temperatures of paper dust (3g) with ink (3g) at different hot plate temperatures	78
Table 9 : Comparison of ignition temperatures of paper dust mixture	93
Table 10 : Summary of other test results of gum powder mixture	94
Table 11 : Dust particles' volume fraction and bulk density	96
Table 12 : Summary of brass powder (30g) with different amount of stearic acid addition at 400°C	104

List of figures

Figure 1 : IEC 62141-10 Maximum allowable surface temperature.....	19
Figure 2 : Heat losses and gains, as represented in the Semenov theory	23
Figure 3 : The geometry of a self-heating, in the form of a symmetric slab	25
Figure 4 : The geometry of a self-heating, in the form of unsymmetrically cooled slab	27
Figure 5 : Equipment layout on the test bench in the fire science lab.....	33
Figure 6 : Process and Instrument diagram.....	34
Figure 9 : Temperature controller, hot plate, and Solid State Relay layout.....	37
Figure 10 : Hot plate temperature deviation at 225 °C	41
Figure 11 : Hot plate temperature deviation at 325 °C	42
Figure 12 : Temperature distributions when hot plate temperatures are at 225 °C and 325 °C	42
Figure 13 : Thermocouple position for the hot plate temperature.....	43
Figure 14 : Hot plate temperature when dust layer was placed on it	44
Figure 15 : Dust layer temperatures of Pittsburgh seam coal at 210 °C	48
Figure 16 : Comparison of dust layer temperatures without airflow and on the bench at 210 °C	49
Figure 17 : Pittsburgh seam coal at 210 °C	54
Figure 18 : Pittsburgh seam coal at 210 °C for the first 200 sec	55
Figure 19 : Cracks in the Pittsburgh seam coal dust layer when ignition occurred.....	57
Figure 20 : Pittsburgh seam coal at 210 °C	58
Figure 21 : Pittsburgh seam coal at 220 °C	58
Figure 22 : Paper dust layer right after being leveled at 350 °C.....	60
Figure 23 : Paper dust layer temperature at 350 °C.....	62
Figure 24 : Chars formed on the bottom of paper dust layer at 350 °C	63
Figure 25 : Paper dust layer temperature at 360 °C	63

Figure 26 : Glowing in the paper dust layer at 360 °C	64
Figure 27 : Paper dust at the end of test at 360 °C	64
Figure 28 : Gum powder dust layer temperature at 260 °C	66
Figure 29 : Cracks in the gum powder dust layer at 260 °C	67
Figure 30 : Gum powder dust layer temperature at 270 °C	67
Figure 31 : Glowing in the gum powder dust layer at 270 °C	68
Figure 32 : Gum powder dust layer at the end of test at 270 °C	68
Figure 33 : Paper dust (3g) with Citgo oil (3g) at 400 °C	72
Figure 34 : Paper dust (3g) with Citgo oil (3g) at 400 °C, early stage	72
Figure 35 : Paper dust (3g) with Citgo oil (3g) at 400 °C, at the end of test	73
Figure 36 : Paper dust (3g) with DTE24 (3g) at 400 °C	75
Figure 37 : Paper dust (3g) with DTE24 (3g) at 400 °C, early stage	75
Figure 38 : Paper dust (3g) with DTE24 (3g) at 400 °C, at the end of test	76
Figure 39 : Paper dust (3g) with newspaper printing ink (3g) at 340 °C	78
Figure 40 : Paper dust (3g) with newspaper printing ink (3g) at 350 °C	79
Figure 41 : Paper dust (3g) with newspaper printing ink (3g) at 350 °C, at the end of test	79
Figure 42 : Paper dust (3g) with newspaper printing ink(3g) at 360 °C	80
Figure 43 : Paper dust (3g) with newspaper printing ink (3g) at 360 °C	80
Figure 44 : Paper dust (3g) with n-decane (3g) at 350 °C	82
Figure 45 : Paper dust (3g) with n-decane (3g) at 360 °C	82
Figure 46 : Paper dust (3g) with n-decane (3g) at 360 °C	83
Figure 47 : Paper dust (3g) with kerosene (3g) at 360 °C	85
Figure 48 : Paper dust (3g) with kerosene (3g) at 370 °C	85
Figure 49 : Paper dust (3g) with kerosene (3g) at 370 °C	86
Figure 50 : Gum powder (20g) with ketone-based liquid solution (1g) at 270 °C	88
Figure 51 : Gum powder (20g) with ketone-based liquid solution (4g) at 270 °C	89

Figure 52 : Gum powder (20g) with ketone-based liquid solution(1g) at 270°C , early stage	89
Figure 53 : Gum powder (20g) with ketone-based liquid solution (1g) at 270°C , at the end of test	90
Figure 54 : Gum powder (20g) with ketone-based liquid solution (2g) at 280°C	90
Figure 55 : Gum powder (20g) with ketone-based liquid solution (4g) at 280°C	91
Figure 56 : Gum powder (20g) with ketone-based liquid solution (2g), ignition	91
Figure 57 : Gum powder (20g) with ketone-based liquid solution (2g), at the end of test.....	92
Figure 58 : Paper dust (3g) alone and with ink (3g) at 6mm high at 350°C	97
Figure 59 : Paper dust (3g) alone and with ink (3g) at 6mm high at 360°C	98
Figure 60 : Paper dust (3g) with Citgo oil (3g) and DTE 24 (3g) at 400°C	98
Figure 61 : Paper dust (3g) alone, with ink (3g), and kerosene (3g) at 360°C , first 600s	99
Figure 62 : Gum powder (20g) alone and with ketone-based liquid (4g) at 3mm high at 270°C	102
Figure 63 : Gum powder (20g) alone and with ketone-based liquid (2g) at 3mm high at 280°C	102
Figure 64 : Brass powder (30g) with stearic acid (3g) at 170°C	105
Figure 65 : Brass powder (30g) with stearic acid (3g) at 180°C	106
Figure 66 : Brass powder (30g) with stearic acid (0.6g) at 400°C	106
Figure 67 : Brass powder (30g) with stearic acid (1.2g) at 400°C	107
Figure 68 : Brass powder (30g) with stearic acid (1.8g) at 400°C	107
Figure 69 : Brass powder (30g) with stearic acid (3g) at 400°C	108
Figure 70 : At the end of test of brass powder with 4% stearic acid at 400°C	108
Figure 71 : Oxygen analyzer	111
Figure 72 : Brass tube coved by thermocouple cover at 6mm above the hot plate	111
Figure 73 : Oxygen concentration at 6mm high, Pittsburgh seam coal at 230°C	113
Figure 74 : Pittsburgh seam coal when ignition occurred	114

Figure 75 : Oxygen concentration at 6mm high, Pittsburgh seam coal at 220°C	115
Figure 76 : Oxygen concentrations and temperatures at 6mm above the hot plate	118
Figure 77 : Downward air flow on the hot plate	119
Figure 78 : nozzle shape and air distribution pattern from the nozzle	120
Figure 79 : Air flow velocity measurement.....	121
Figure 80 : Pittsburgh seam coal without air flow at 220 °C	124
Figure 81 : Pittsburgh seam coal temperatures at 6mm high with and w/o air flow at 220°C ..	124
Figure 82 : Comparison of dust layer at 6mm high with and without air flow at 220 °C	126
Figure 83 : Pittsburgh seam coal with 15SLPM downward air flow on the bench at 230 °C	126

1. Introduction

Hot surface ignition temperatures of dust layers refer the minimum surface temperatures which can ignite a certain thickness of dust layers. It has been an issue quite a long time in the fire protection engineering field, since layers of small particles can be easily observed in the coal processing industry, furniture making plant, paper processing plant, and any facilities having hot processes dealing with small particles. Ignition in dust layers can even develop into dust explosions if proper confinement and lifting momentum forming dust clouds are provided. Since dust layers can act as a fuel or explosion medium easily, research has been focused on dusts' ignitability.

However, in some cases, the cause of a fire is not dust alone, but the mixture of combustible liquids. Some combustible liquids such as lubricants, coolants, and grease are not intended to be mixed with dust and others such as adhesives with wood particles or sawdust in furniture making facility are.

For example, there was a real fire related to the hot surface ignition of a dust layer with combustible liquids in a printing press machine. Paper dusts had been accumulated on a bearing and printing ink infiltrated to the casing gap. The dust layer on the bearing ignited causing a fire. The bearing worked as a hot surface and printing ink or certain lubricants acted as added combustible liquids. In this accident not only the dust layer but also the printing ink affected the ignition and subsequent fire development (N. Jackson, 2004).

Other fire scenarios are also possible. In veneer board manufacturing facilities,

if the temperature of a hot plate compressor or pressing roller is uncontrolled, sawdust layer can ignite with gluing bond. Although the temperature controller works properly, the ignition might occur, since the mixture of dust and combustible liquids might have lower ignition temperature than dust alone or liquid alone. Unexpected combustible liquids can be involved in the dust processing and vice versa.

2. Literature review

2.1. Previous study of hot surface ignition

Hot surface ignition temperatures of dust layers have been researched especially by the Bureau of Mines and two major papers were published by Yael Miron and Charles P. Lazzara(1988), and P.C. Bowes and S.E. Townshend(1962).

Yael Miron and Charles P. Lazzara used three types of dust materials: fuels, agricultural dusts, and metal dusts. Coal and oil shale for fuels, lycopodium, cornstarch, and grain dust for agricultural dusts, and brass powder for metal dusts were tested. They analyzed the dust layer ignition temperatures based on the three different aspects: nature of dust, dust layer thickness and particle size.

For the nature of dust, composition of each dust was briefly reviewed and linked to the ignition patterns. In case of coal, it is composed of organic and intertwined inorganic matter and its ignition is a slow, smolder type. Its volatile contents are also very important factor in terms of ignition temperature; the more volatile matter is included, the lower the ignition temperatures are.

For the three agricultural materials, lycopodium reacted similarly to coals, with smolder type ignition. However, cornstarch and grain dust formed char deterring decomposition of other dust particles and then developed to glowing combustion. The coated brass powder with stearic acid or metal stearates showed lower ignition temperature than the other dusts.

For layer thickness, Miron and Lazzara found that the thicker the layer is, the

lower the ignition temperature is. As a dust layer thickness increases, the temperature gradient in the dust layer becomes smaller, which reduces the conduction rate consequently. This results in the local temperature increases, exothermic reaction, and ignition at lower temperature of hot plate.

About the particle size, the more complete oxidation occurred in smaller particle until a certain critical size. If the particle size is much bigger, surface area and rated combustion are too small to overcome the rate of heat dissipation.

P. C. Bowes and S. E. Townshend wrote the paper in 1962 and provided more theoretical aspects on hot surface ignition than Miron and Lazzara's paper. They used sawdust and test method was different in that dust layer was put on the hot plate from the beginning of the test and heated up. The test purpose with sawdust was to see the effects of layer depth, particle size, and packing density and furthermore the thermal combustion theory which used Frank-Kamenetskii's exponential approximation for Arrhenius equation was compared with test data.

The results were that the dust layer depth is the most important factor affecting the ignition temperature and particle size is not important and packing density affected the ignition temperatures of only thin layers. The accordance of test data to the combustion theory was satisfactorily the level of acceptance for most practical purposes.

B. J. Tyler and D. K. Henderson (1987) used sodium dithionite to identify the controlling parameters from both computational and analytical self-heating model. They introduced exothermicity of the test material controlled by the

addition of different amount of inert material, with which each model's results were evaluated. With high exothermic material matched better the two models and less correspondence was observed in low exothermicity. They used 75mm diameter rings having 5 to 40mm heights to hold dust layers. One interesting test they conducted was to provide air flow. They provided downward air flow at the rate of $35\text{dm}^3/\text{min}$ on the dust layer through a glass tube having 1 mm marginal gap all around the ring. With the provision of $35\text{dm}^3/\text{min}$ downward air flow, ignition temperature of 20mm layer was 168°C compared to 175°C with the downward air flow and background temperature decrease just above the dust layer was recorded from 60°C to 35°C .

2.2. ASTM E 2021-01, IEC 61241-2-1 and other test methods

ASTM E2021-01 depicts the standardized test method of hot surface ignition temperature of dust layers. The test method used for this thesis was not much different from ASTM E2021, since the test purpose is to see if there are ignition temperatures' differences with addition of combustible liquids and solids to the dust layers.

IEC 61241-2-1, Electrical apparatus for use in the presence of combustible dust - methods for determining the minimum ignition temperatures of dust, also described the test method for hot surface ignition temperatures of dust layers.

Both ASTM and IEC use 4 inch inner diameter ring in which dusts are filled and 8 inch diameter of hot plate. Compression to the test material inside the ring is not applied in both cases. However, there are different criteria for the dust particle size, layer thickness and ignition symptom.

In ASTM E2021, dust particle size for this test method should be smaller than 75 μm which corresponds to the standard sieve number 200, and IEC requires 100% of particles should be smaller than 200 μm which approximately sieve number 80. Therefore, ASTM E2021 asks to use particles below mesh 200 sieve and IEC does below mesh 80 sieve. About the layer thickness, 12.7 mm (1/2 inch) is applied for ASTM E2021 and other depths can also be used, and 5mm in priority and 12.5 mm or 15 mm can be used as options for IEC. As previously reviewed in 2.1, layer thickness is very important factor in deciding hot surface ignition temperature. The thicker the layers are, the lower the ignition

temperatures are.

Ignition temperature criterion is also different between these two test methods. ASTM accepts glowing, flaming or a temperature rise more than 50 °C above hot plate surface temperature and IEC does glowing, flaming, a temperature of 450 °C, or a temperature more than 250 °C above the hot plate surface temperature.

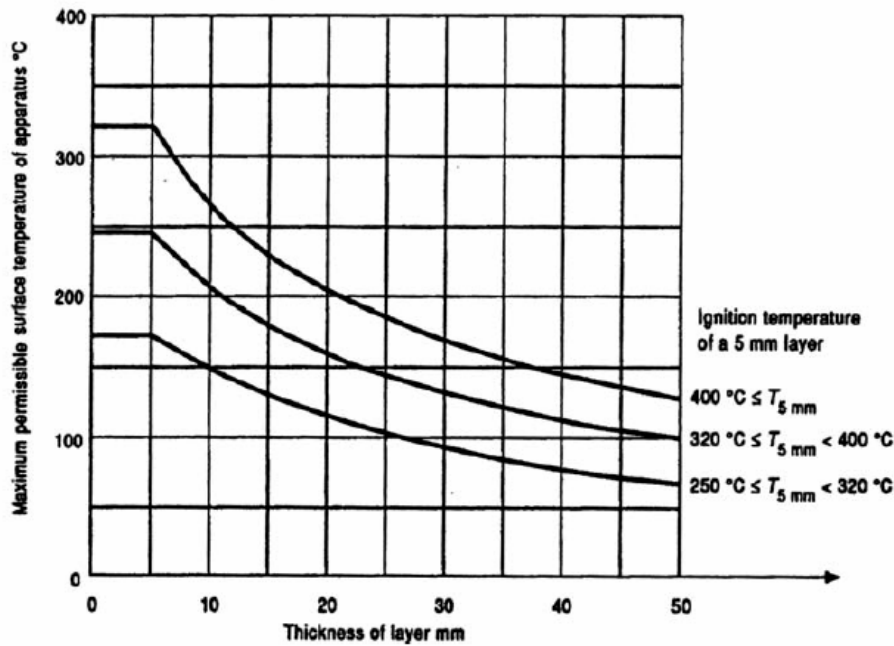


Figure 1 : IEC 62141-10 Maximum allowable surface temperature

IEC 61241-10 has a flow chart to determine the maximum allowable surface temperature for dust layers. If the dust layer thickness is controlled less than 5mm, it recommends the rule 1, and if it is controlled between 5mm and 50mm thick, it recommends the rule 2. Based on the rule 1, there is a figure of requirement of the maximum hot surface temperature for each dust layer thickness between 5mm to 50mm. For example, if a 5mm thick dust layer ignited at 305 °C, the figure 1

dictates the maximum hot surface temperature for 10mm thick layer is 150°C and for 30mm is 95°C. However, Lunn et al. (2001) have confirmed that these extrapolated values are very conservative with large safety margin between the actual hot surface minimum ignition temperatures and the maximum allowable surface temperatures.

Lunn et al. (2001) also developed a test method for dust piles deeper than 50mm from IEC 61241-10. Four liters of dust particles were piled on the heating block via a funnel located 14 cm above the heating block. The block's dimension is 20cm by 10cm by 5cm. The block is connected to the electricity, and its temperature was controlled. This method was developed for the applications in which dust layer thickness can not be controlled or larger than 5mm. Dust's maximum pile height forming a cone shape depends on the material's cohesivity. For example, for 125mm of dust layer in height on the block, 1.5 liters were taken for sawdust, but 10 liters were taken for coal. Through this test method, 25 μm sawdust was ignited at 230°C compared to 340°C at which 5mm thick saw dust layer was ignited on a hot surface based on the IEC 61241-2. The layer thickness was verified as a very important factor in hot surface ignition temperature test as consistent with other researcher's test results.

2.3. Ignition Handbook by Vytenis Babrauskas

Ignition Handbook written by Vytenis Babrauskas contains useful information of various ignition types and test data. Hot surface ignition of dust layers and liquid fuels is also dealt with in detail. Theoretical aspects of hot surface ignition as well as empirical test data are also included.

About the hot surface ignition of dust layers, it cites test results from the paper of Bowes, and the Bureau of Mines. Hot surface ignition temperature test data with beech sawdust, coal, cork, and lycopodium shows that the thicker the layer depth, the lower the ignition temperatures are. This test results are not different from the previous two papers.

Table 1 : Results of some dust layer ignition tests conducted by Bowes

Layer depth (mm)	Ignition temperature(°C)			
	Beech sawdust	Coal	Cork	Lycopodium
5	350	235	350	283
10	315	205	315	261
20	285	173	280	217

Hot surface ignition of combustible liquids is also studied in this book. It cites the test results from the paper of Karasawa et al. (1986), which is single drop hot plate ignition temperature of various combustible liquids.

Hot surface ignition temperatures are typically 200~300°C above the Auto Ignition Temperatures for the liquids listed above. The reason hot surface ignition temperatures are higher than AIT is because it loses heat energy in the form of convection to the surrounding air as opposed to AIT. AIT is surrounded by uniform temperature environment, so that uniform heat flux is provided from all directions. The amount of liquids on a hot surface is also another variable. From the Knowles' test (1965), as the amount of liquid (turbine oil) on a hot surface increases, the hot surface ignition temperature decreases.

Table 2 : Single-drop hotplate ignition temperatures found by Krasawa et al.

	Diethyl ether	n-butanol	heptane	methanol	ethanol
AIT(°C)	195	345	223	470	365
Hot surface Ignition temp. (°C)	670	650	670	690	717

Table 3 : Ignition of spills of turbine oil on a hot surface

	2drops	5ml	30~60ml
Ignition temp. (°C)	450	380	315

In this thesis, two lubricating oils (DTE 24, Citgo oil) and two highly combustible liquids (n-decane, kerosene) were tested with paper dust. The hot surface ignition temperatures of kerosene and lubricating oil are cited from the Skull's test (1951), and it says, 650°C for kerosene and 430°C for lubricating oils, although it does not inform the amount of liquids dropped on the hot plate and the specification of the lubricating oil.

2.4. Self heating, and Frank-Kamenetskii's theory

2.4.1. Self-heating theory

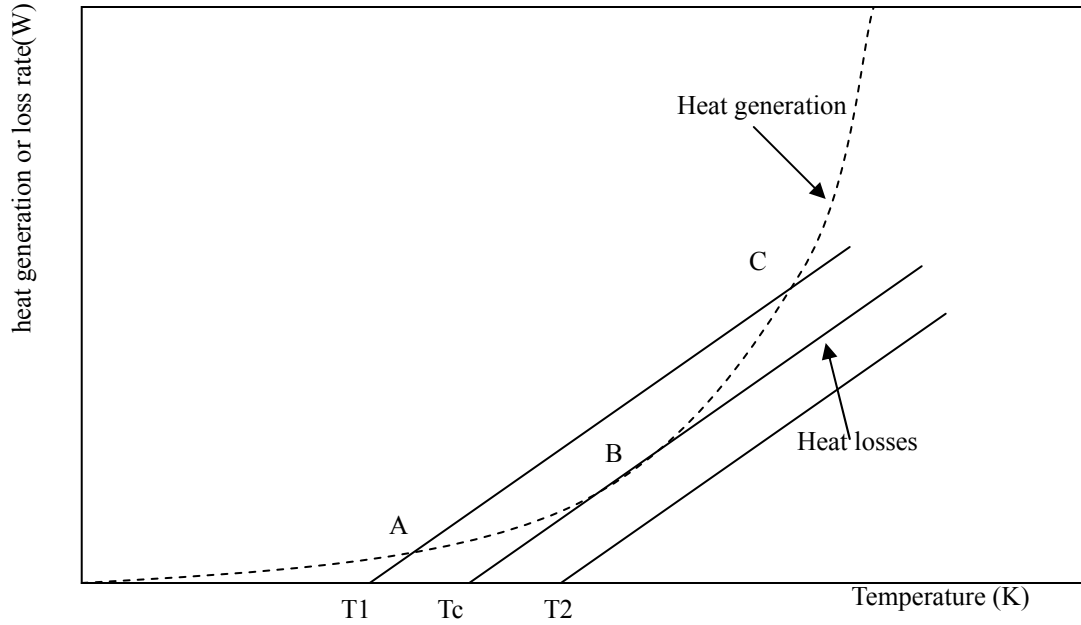


Figure 2 : Heat losses and gains, as represented in the Semenov theory

The shape of heat generation curve in figure 2 was drawn based on the Arrhenius' Law in eq. (2.4.1) Eq. (2.4.1) indicates the heat generation rate per unit volume of dust layer. Heat loss per unit surface area through the top surface of dust layers is in eq. (2.4.2)

$$\dot{q}''' = \rho Q A e^{-E/RT} \quad (2.4.1)$$

$$\dot{q}'' = h(T_s - T_0) \quad (2.4.2)$$

When the hot plate temperature is below T_c , heat loss through convection on the dust layer surface is larger than heat generation inside the dust layer. Therefore, no thermal runaway which is ignition occurs. However, if the hot plate temperature is slightly higher than T_c , heat generation will be larger than heat loss. This corresponds to the hot surface ignition temperature of the dust layer.

If the hot plate temperature is set below T_1 , the dust layer temperature will increase gradually and asymptotically approach to the equilibrium temperature between heat generation and heat loss corresponding to the point A. If the hot plate temperature is set between T_1 and T_c , the dust layer temperature will increase a little bit more than equilibrium temperature but return to the equilibrium temperature making small hump before steady state since heat loss is larger than heat generation. However, if the hot plate temperature is set above T_c , the dust layer temperature will increase continuously and reach ignition.

Theoretically, when the hot plate temperature is at T_c , the dust layer temperature would reach ignition at infinite time, however, in real situation, small increase of heat generation will lead ignition, although there is some period of steady state condition before ignition. Temperature slightly above T_c will be the minimum hot surface ignition temperature of dust layers.

2.4.2. Steady state theory for symmetrically cooled bodies

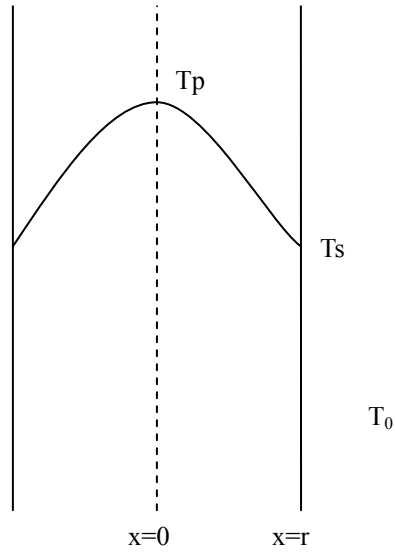


Figure 3 : The geometry of a self-heating, in the form of a symmetric slab

$$k \frac{d^2 T}{dx^2} + \dot{q}''' = \rho C \frac{dT}{dt} \quad (2.4.3)$$

$$-k \frac{d^2 T}{dx^2} = \dot{q}''' \quad (2.4.4)$$

$$\dot{q}''' = \rho Q A e^{-E/RT} \quad (2.4.1)$$

$$\dot{q}''' = h(T_s - T_0) \quad (2.4.2)$$

$$-k \frac{dT}{dx} = h(T_s - T_0) \quad , x = r \quad (2.4.5)$$

$$k \frac{dT}{dx} = h(T_s - T_0) \quad , x = -r \quad (2.4.6)$$

For $\frac{E}{RT_0} \gg 1$,

$$\frac{E}{RT} \approx \frac{E}{RT_0} \left[1 - \frac{T - T_0}{T_0} \right] \quad (2.4.7)$$

$$\theta = \frac{E}{RT_0^2} (T - T_0), \quad (2.4.8)$$

$$z = \frac{x}{r},$$

$$\delta = \frac{E}{RT_0^2} \frac{r^2 \rho Q A}{k} e^{-E/RT_0} \quad (2.4.9)$$

$$\theta = \ln C1 - 2 \ln \left[\cosh(z \sqrt{\delta C1/2} + C2) \right] \quad (2.4.10)$$

Eq. (2.4.3) is the governing equation of heat transfer in slab analysis and eq. (2.4.4) is in steady state condition. Applying eq. (2.4.2) to eq. (2.4.4) leads eq. (2.4.5) and eq. (2.4.6), the boundary condition.

Non-dimensional parameters, θ , z , and δ are introduced for T , and x , and heat generation rate respectively, and the solution of the steady state equation in the form of temperature T is in eq. (2.4.10). However, the important variable for this equation is not the temperature itself, but the δ , since δ is the critical parameter whether ignition occurs or not. For $\delta < \delta_c$, no ignition occurs, and for $\delta > \delta_c$, ignition occurs. The value of δ_c is the dependent of only geometry of the concerned material. δ_c is 0.88 for slab shape, 2.0 for infinite cylinder shape, and 3.32 for sphere.

2.4.3. Steady state theory for unsymmetrically cooled bodies

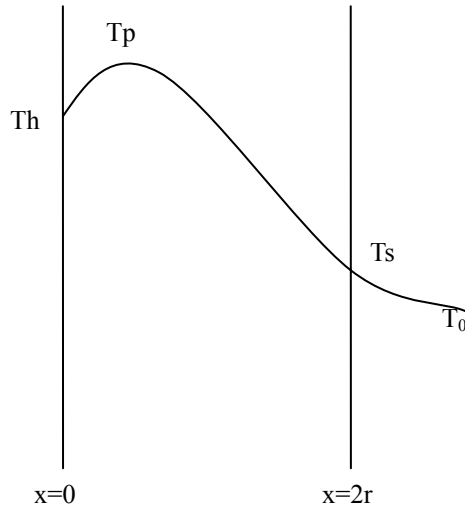


Figure 4 : The geometry of a self-heating, in the form of unsymmetrically cooled slab

Section 2.4.2 was about a slab problem exposed to the uniform environments. However, if one side of the slab is exposed to the constant heat flux, which might be the hot plate, δc value is not the same for the symmetrically cooled slab.

$$\theta = \frac{E}{RT_0^2} (T - T_h) \quad (2.4.11)$$

$$\delta = \frac{E}{RT_h^2} \frac{r^2 \rho Q A}{k} e^{-E/RT_h} \quad (2.4.12)$$

δ is proportional to the r^2 . From the two drawing above, the highest temperature in the symmetrically cooled bodies, when $x=0$ corresponds to the point of T_m (approximately $x=0$) in the drawing above, and $x=r$ in the first drawing can corresponds to $x=2r$ in second drawing. Therefore, δc value for

un-symmetrically cooled body is 4 times smaller than the case of symmetrically cooled body, which is 0.22. Another different from symmetrically cooled case is T_h . T_h is another variable in the equation for δ . Therefore, δ_c in this case is not the only function of geometry, but also include T_h variable which is the hot plate temperature in our case. At a certain hot plate temperature when $\delta < \delta_c$, ignition can not occur and a slight higher hot plate temperature when $\delta > \delta_c$, ignition can occur. Specific value of δ_c will not be measured, but T_h will be decided based on the several tests in this paper.

3. Problem statement and assumptions

3.1. Problem statement

Combustible liquids can be often mixed with dust layers on a hot surface. Motors used to drive a pump, or any type of mechanical equipment has lubricants and nearby process oils can easily leak in many industrial facilities. There are quite a lot of possible hot surfaces. It might be related to the interim works or inherent process. If the industry deals with powder, or dust particles which might be flour, paper dust, grain dust, or even metal dust, there is possibility of fire from the mixture of dusts and combustible liquids.

The roles of combustible liquids in ignition or decomposition process of dust particles are important. Ignition Handbook by Babrauskas states that usually hot surface ignition temperatures of liquids are much higher than their flash points or even auto ignition temperatures, because heat energy is not provided from all direction in case of hot surface test. Heat is only provided from the bottom surface, and upper surface of combustible liquids are open to air allowing loss of heat energy via convection. However, what if combustible liquids are partially contained by dust particles holding up heat energy inside dust layer otherwise dissipated to the ambient air? What if catalytic chemical reaction occurs under a high temperature between dust particles and combustible liquids? In these cases, the ignition temperatures would decrease or time to ignition would become shorter.

On the other hand, if combustible liquids take heat away from the dust layer in the form of vaporization, or if combustible liquids help heat transfer better than porous dust layer particle alone, or if the chemical reaction is anti-catalytic, the ignition temperature would increase, or time to ignition would become longer.

Another question explored in this thesis is the effect of small concentration of a second powder on the surface ignition of the primary powder. For example, powdered brass is often coated with stearic acid for improved metallurgical processing. Therefore, it is of interest to determine how the addition of stearic acid affects the hot surface ignition temperature of brass powder.

3.2. Assumptions

Ignition temperature of a dust layer with addition of a combustible liquid might increase or decrease compared to that of dust layer alone. If the ignition temperature is increased, which means more heat flux is needed for ignition, the combustible liquids would work as a heat sink or having some chemical effects deterring decomposition or oxidation of dust particles. If the ignition temperature decrease, mixed combustible liquids would work as a catalyst for exothermic reactions or decreasing heat transfer loss. For example, combustible liquids located between dust particles can hold heat provided by hot surface or generated in the dust layer, and this accumulated heat energy would help ignition of the dust layer at lower temperature of hot surface.

Time to ignition of dust layers might be increased since a certain portion of heat provided from a hot plate would be taken away in the form of heat of vaporization of combustible liquids. The longer the time to ignition is, the more heat is taken away.

Similar consideration and questions are applicable to the addition of a second powder, such as stearic acid addition to brass powder.

4. Testing

4.1. Test objectives

The first objective is to determine the effect of combustible liquid additives on the measured hot surface ignition temperatures for various dust materials. Two hydraulic oils, n-decane, and kerosene were mixed with paper dust, and ketone-based liquid solution was mixed with Arabic gum powder for this objective.

Another part of this objective is to determine effects of powder additives. Toward this end, different amounts of stearic acid powder were added to the brass powder layer to check the differences of the hot surface ignition temperature of brass powder.

The second objective is to develop an improved understanding of the heat transfer and oxygen mass transfer phenomena that occur during the ASTM E2021 test. In order to accomplish this objective, the tests were run with additional instrumentation in at least some of the tests. The additional instrumentation include a second thermocouple in the dust layer, an oxygen analyzer and gas sampling line, and an air velocity probe.

4.2. Test description

4.2.1. Equipment layout

Test equipment consists of three major components; one is temperature controlling devices including solid state relay, another is a hot plate, and the other is a thermometer, and a computer to record the temperature changes of thermocouples. Figure 5 shows the actual test equipment arrangement on the test bench.

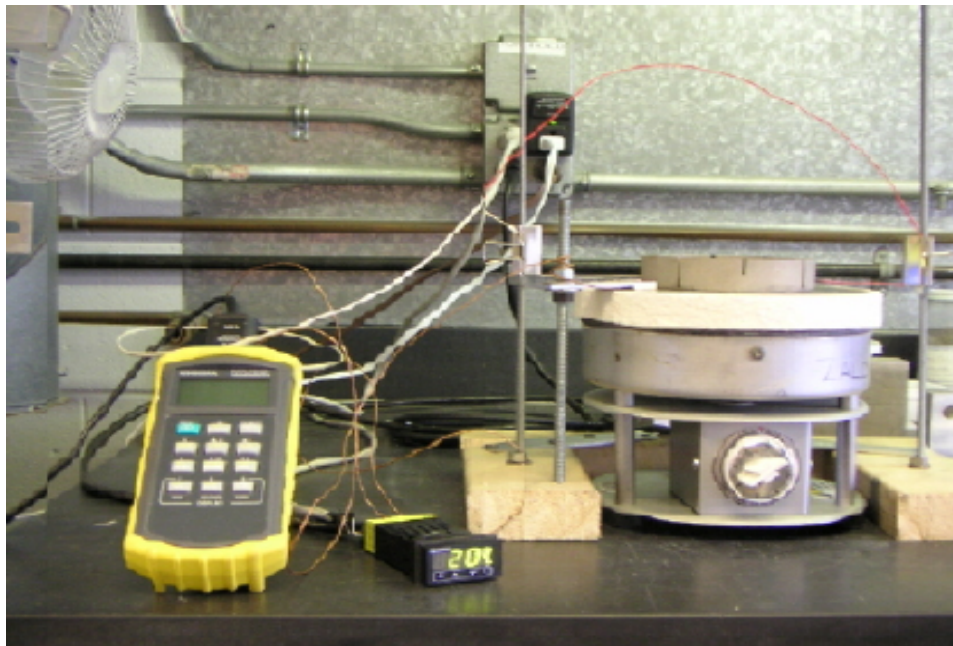


Figure 5 : Equipment layout on the test bench in the fire science lab

4.2.1.1. Process diagram

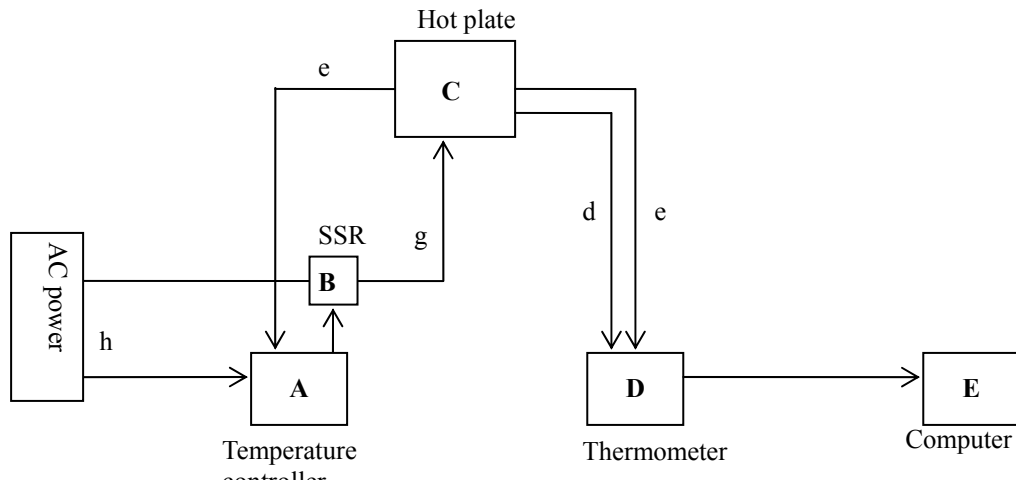


Figure 6 : Process and Instrument diagram

A : Temperature controller, CN 8592, Omega engineering

(This is to control the hot plate temperature and maintain the temperature at a set point during the test period)

B : SSR(Solid State Relay), SSRL240DC25, Omega engineering

(This is to turn it on/off the hot plate to control the temperature cooperating with temperature controller of CN 8592)

C : Hot plate, ROPH-144, Omega engineering, Max. Temperature of 875°F(468°C)

D : Thermometer, HH506RA, Omega engineering

(This is to check the temperatures and transfer them to the computer using its own temperature recording software)

E : Computer : temperatures are recorded as a excel spreadsheet in the computer.

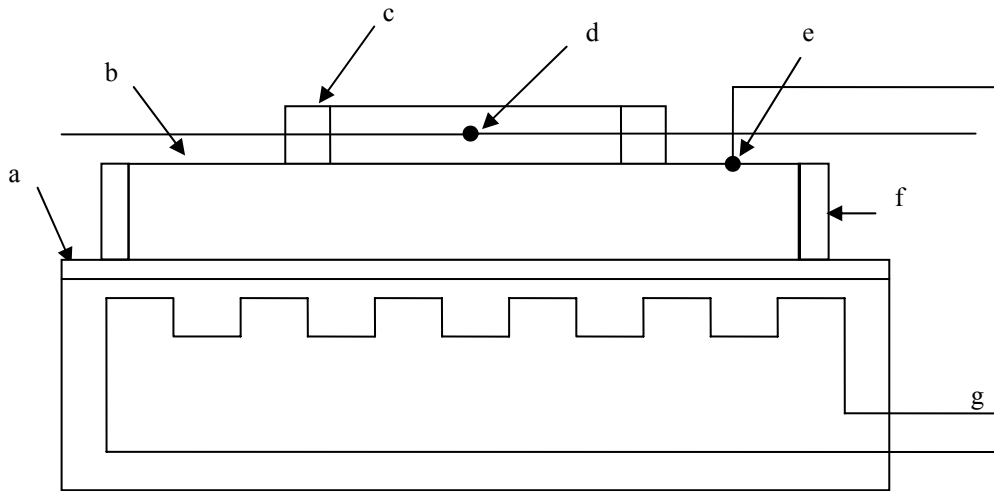


Figure 7 : Horizontal section of hot plate and thermocouple layout

a : Hot plate, 8.5inch diameter (Omega engineering ROPH-144)

b : Round shape aluminum plate, 1 inch thick, 8 inch diameter

c : Ring, 4 inch inner diameter, 5inch outer diameter, with 8 slots (1/8 inch width) to accommodate thermocouples at different heights (1/2, 3/4, 7/8, 15/16 inch depth from the top surface of the ring)

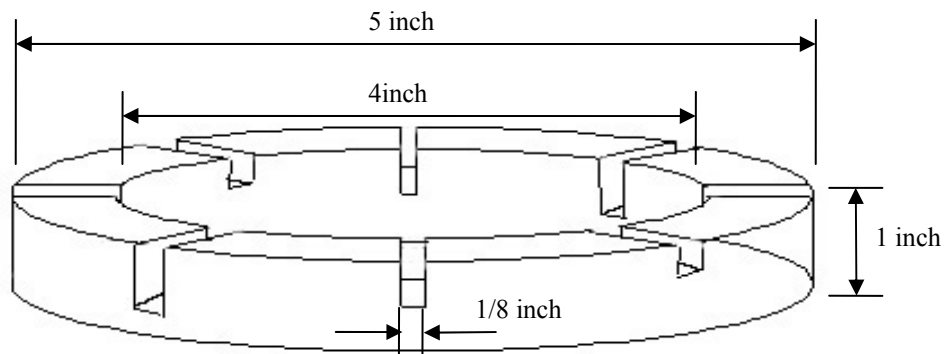


Figure 8 : Aluminum ring with slots to accommodate thermocouples

d: Dust layer thermocouple

e : Hot plate thermocouple (Omega engineering, CO1-K)

f : Insulating material, Cotronic's 390 ceramic paper

g : Power Supply from SSR for hot plate

h : Power supply for temperature controller

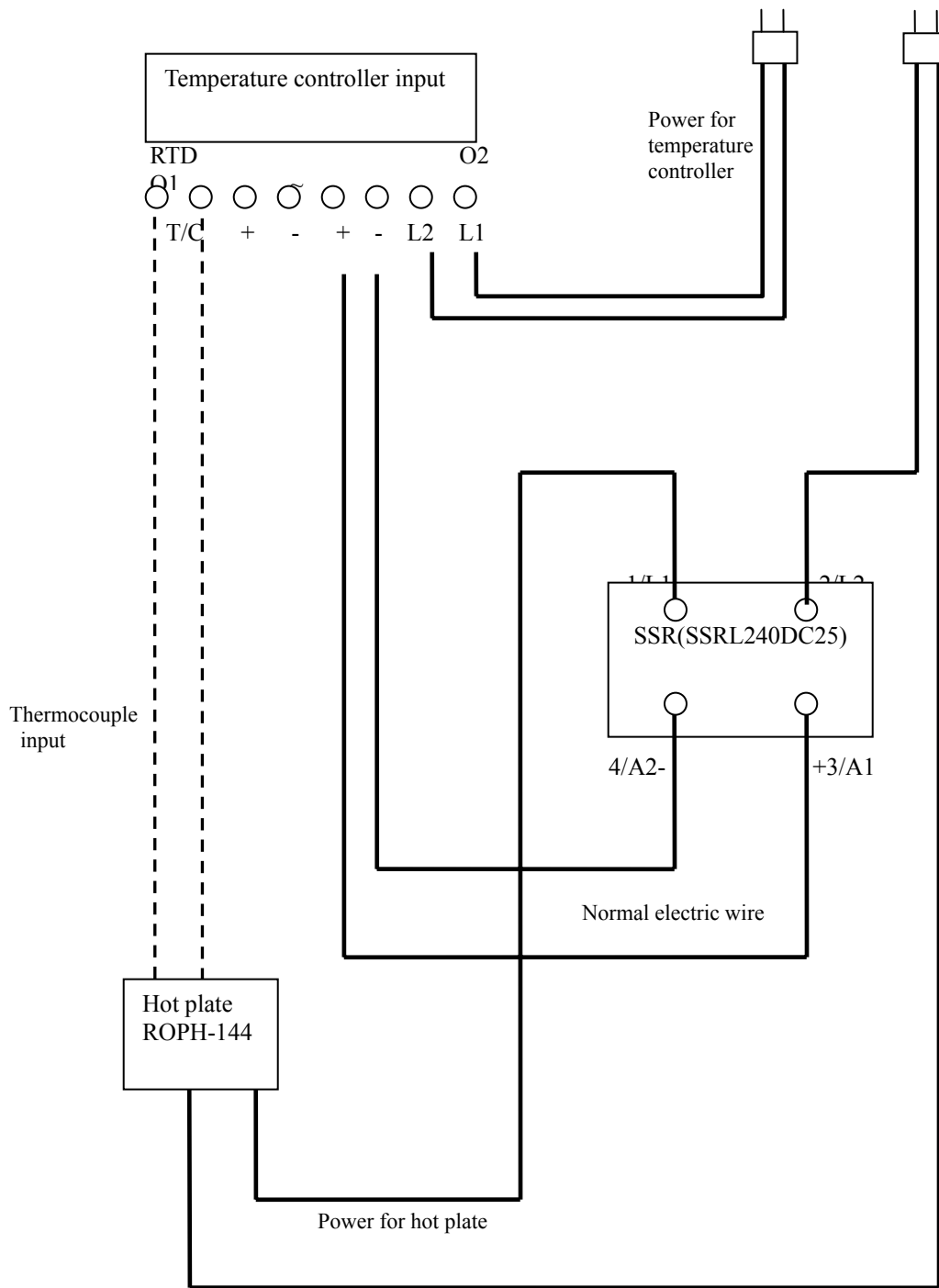


Figure 9 : Temperature controller, hot plate, and Solid State Relay layout

4.2.2. Test procedure

Test procedure for this topic is based on the ASTM E2021 standard test procedure. First, for safety issues, fire gloves are ready near the test site and fume hood is turned on. All equipment is plugged in and the intended temperature is set on temperature controller. Aluminum ring and thermocouples are positioned to the center of the hot plate and intended height. Monitoring the temperature of the hot plate with temperature controller, the thermocouples are checked to see whether they are working properly. When the hot plate temperature reached the set point and is stabilized, temperature recording software is run and the prepared dusts are poured carefully inside the aluminum ring. The amount of dust is predetermined. No compression is applied to the dust layer. The surface of dust is equally leveled with small piece of aluminum foil. After the test, the hot plate is turned off. Aluminum ring and dusts are removed a while after the hot plate is turned off.

4.2.3. Test environment

Tests were conducted on the test bench in the fire science laboratory in Higgins Laboratory of Worcester Polytechnic Institute. The ambient temperature was usually maintained around 25°C. To minimize the air flow near the hot plate, air conditioner was off and only fume hood located above the test bench was on. The air flow due to the fume hood on was different depending on the elevation above the test bench. For example, at 60 cm above the bench, 30 cm/s sideward air flow was measured. However, at the top surface of dust layer which was half inch above the hot plate surface, 0.5 cm/s air flow was measured in the ring. The air flow effect on the ignition temperature of dust layers was discussed further in section 4.11.

4.3. Uncertainty and experimental error

This thesis discusses the minimum ignition temperature of dust layer on a hot surface with and without combustible liquids. With regard to this topic, ASTM E2021 has specified the test method for “Hot-Surface Ignition Temperature of Dust Layers” which is very similar with the test method adopted to this paper. Therefore, most of the experimental procedure and uncertainty during the test are extracted from ATSM E2021.

4.3.1. Test equipment inherent errors

ASTM 2021 states several requirements of test apparatus.

4.3.1.1. The hot plate temperature should be maintained constantly within $\pm 5^{\circ}\text{C}$ throughout the time period of the test.

4.3.1.2. Once the hot plate temperature reaches a set point temperature, the temperature across the plate should be in the range of $\pm 5^{\circ}\text{C}$.

4.3.1.3. The hot plate temperature change should be within $\pm 5^{\circ}\text{C}$ during the placing of the dust layer on the hot plate and should be restored within 2°C of the previous temperature within 5 minutes of placing the dust layer.

4.3.1.4. Thermocouple and its readout device should be calibrated, and should be accurate to within $\pm 3^{\circ}\text{C}$.

4.3.1.5. About 4.3.1.1, temperature deviations of hot plate over the test period, up to one hour, at a set temperature were measured. At two different temperature ranges as above, and the error was found within

$\pm 1^\circ\text{C}$ as shown in figure 10 and 11. Two set temperatures, 225°C and 325°C , were selected based on the ASTM E2021, one in the range of between 200°C and 250°C and the other in the range of between 300°C and 350°C .

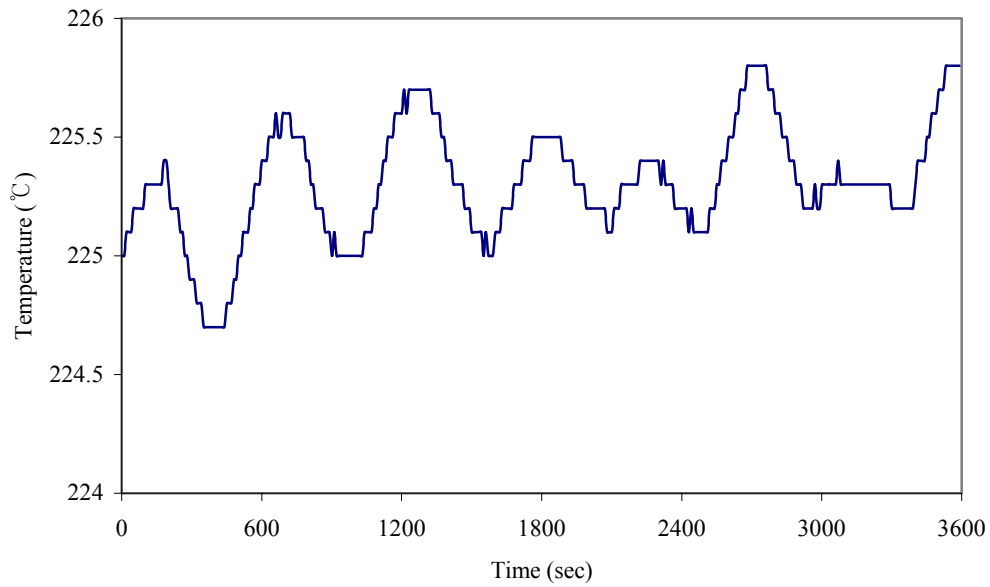


Figure 10 : Hot plate temperature deviation at 225°C

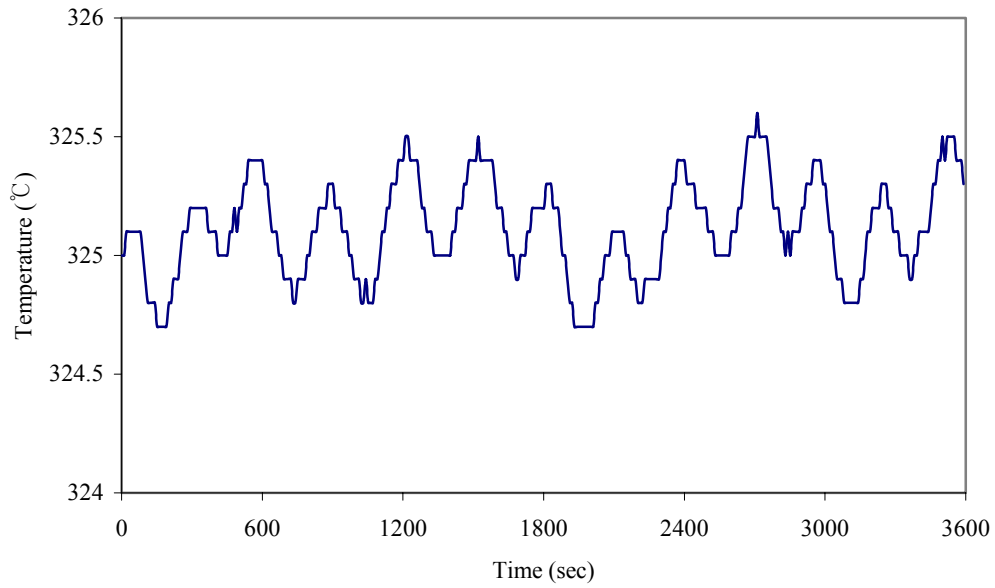


Figure 11 : Hot plate temperature deviation at 325°C

4.3.1.6. About 4.3.1.2, aluminum plate has the temperature distribution range within $\pm 1^\circ\text{C}$ as shown in figure 12.

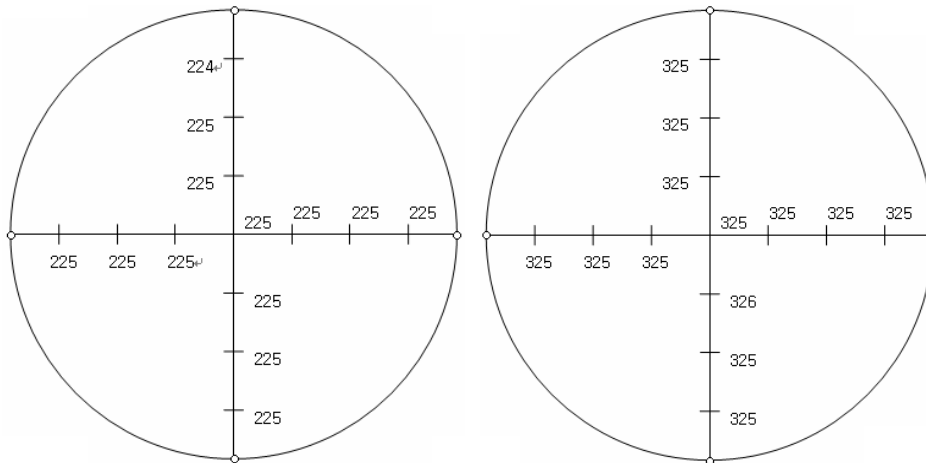


Figure 12 : Temperature distributions when hot plate temperatures are at 225°C and 325°C

4.3.1.7. About 4.3.1.3, there is no difference of hot plate temperature when placing the dust on the hot plate. The hot plate temperature was not affected, since the thermocouple for hot plate temperature is located a little distant from the center of the hot plate as shown in figure 13. According to the ASTM E2021, thermocouple is embedded in the aluminum plate. In our case, it is located on the surface of hot plate with insulating material on it. Thermocouple is very sensitive to the air flow velocity change near the thermal bid or non-uniform contact on the surface.

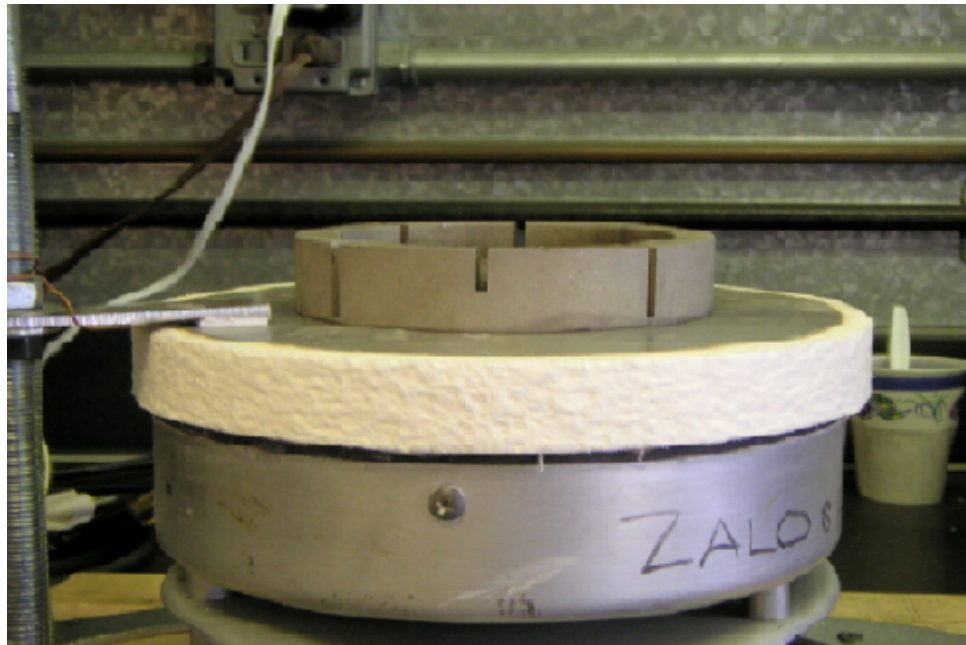


Figure 13 : Thermocouple position for the hot plate temperature

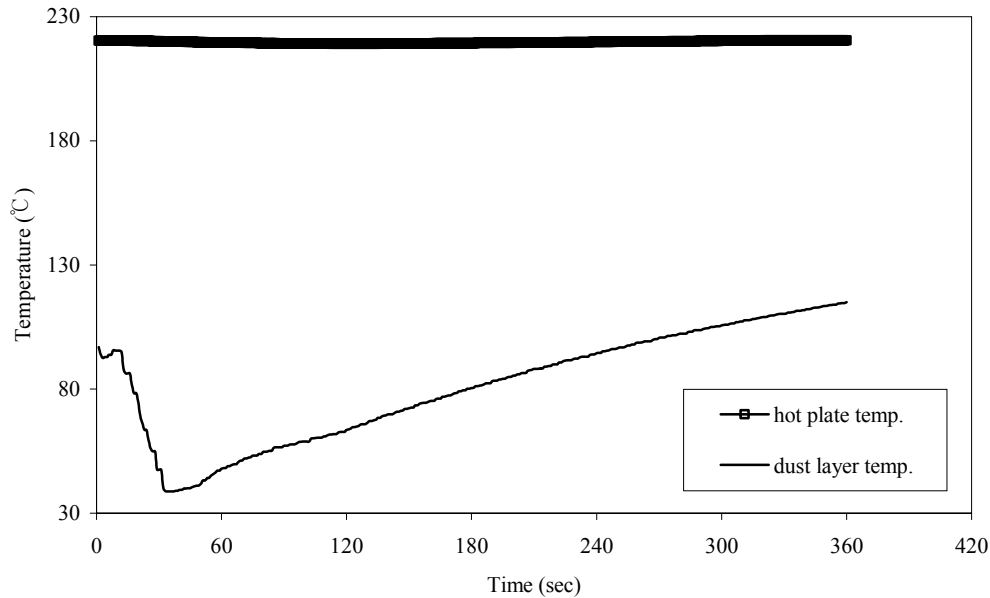


Figure 14 : Hot plate temperature when dust layer was placed on it

4.3.1.8. About 4.3.1.4, the test equipment’s deviations, the information of the equipment’s error range can be acquired by the manufacturer. First, Two different thermocouples were used for the test, surface temperature measuring thermocouple, CO1-K which is manufactured by Omega engineering, and on-site made dust layer thermocouple. Surface temperature measuring thermocouple is fabricated from ANSI “special limits of error” which is $\pm 1.1^{\circ}\text{C}$ or $\pm 0.4\%$ of the measured temperature. The maximum temperature applied to the test for this paper is 400°C . Therefore the temperature error range would be $\pm 1.6^{\circ}\text{C}$. Dust layer thermocouples were made in the lab and its error range is $\pm 2.2^{\circ}\text{C}$ or $\pm 0.75\%$, which results in $\pm 3^{\circ}\text{C}$ of error range based on the standard

limits of error of thermocouple. Thermometer, HH506RA made by Omega engineering has error range $\pm(0.05\% \text{ reading}+0.3^{\circ}\text{C})$, which is at most $\pm 0.5^{\circ}\text{C}$, and temperature controller, CN8592 also made by Omega engineering has error range $\pm 1^{\circ}\text{C}$

Table 4 : Comparison of test equipment inherent errors and ASTM requirements

List	ASTM	Actual test equipment
4.3.1.1	$\pm 5^{\circ}\text{C}$	$\pm 1^{\circ}\text{C}$
4.3.1.2	$\pm 5^{\circ}\text{C}$	$\pm 1^{\circ}\text{C}$
4.3.1.3	$\pm 5^{\circ}\text{C}$ and within 2°C	Satisfied
4.3.1.4	$\pm 3^{\circ}\text{C}$	$\pm 3^{\circ}\text{C}$

4.3.2. Experimental errors

The amount of dust filling the aluminum ring should be decided. ASTM recommends measuring the amount of dusts to fill the ring three times and the average value of the value be picked. However, very slight experimental errors are expected at this procedure. Below are the amounts of dusts to fill the half inch thickness inside the ring for each time and average values which were selected.

Table 5 : Average amount of dust to fill half of the ring (0.5 inch thick)

	First(g)	Second(g)	Third(g)	Average(g)
Pittsburgh seam coal	56.8	56.3	57.2	57
Brass powder	33.5	32.9	33.1	33
Gum Arabic powder	39.4	40.2	39.8	40
Paper dust	3	2.9	3	3

The positioning of thermocouple in dust layers at each run of test can not be the same. The slight difference of thermocouple bead's elevation may cause significantly different temperature readout. Test environment also cause experimental errors. The air flow (0.5 cm/s at the surface of dust layers) caused by fume hood located above the test bench can change the oxygen concentration inside the dust layer which can change the ignition temperature accordingly. It turned out that air flow did not change the ignition temperature of Pittsburgh seam coal dust layer, although it had some

effects on the time to ignition; time to ignition for the case of the fume hood on was 1000 sec longer than without airflow. Temperature variations by air flow were discussed combined with oxygen concentration later. Ambient temperature did not seem to affect the ignition temperature much.

The repeatability of tests results were examined with one material, Pittsburgh seam coal, by doing the same test three times at different date as a verification case. As shown in figure 15, the average value of maximum temperature differences among 1st, 2nd, and 3rd tests at 6mm high and 3mm high were 1.5°C and 1°C difference which were much smaller than ignition temperature resolution in this thesis, which was 10°C. The test results verified that the level of repeatability was satisfactory.

To examine air flow effects on the hot surface ignition temperature of dust layers, one preliminary test was conducted with Pittsburgh seam coal. One test was conducted with a 0.5 cm/s (average 0.5 cm/s with the highest value of 9 cm/s at a certain time) airflow at the top of the surface of dust layer, as driven by fume hood located above the bench. A second test was conducted in the adjacent lab where no air flow exists (average 0 m/s for two minutes, and the highest velocity was 2 cm/s at a certain time) at the top of the surface of dust layer. In both tests, Pittsburgh seam coal was ignited at 220°C and not ignited at 210°C. Figure 16 shows that the temperature variation at 210°C without air flow and with small air flow (0.5 cm/s at the elevation of surface of the dust layer) driven by the fume hood. The average temperature

differences are 3°C at 3mm elevation and 1.5°C at 6mm elevation.

Therefore, it was assumed that the effect of air flow on the hot surface ignition temperature on the test bench was in the acceptable range of experimental error. Since the test results were measured at every 10°C, which means hot plate temperature resolution was big enough not to be affected by the small air flow on the bench. Therefore, the air flow from fume hood was considered within the range of intended test resolution.

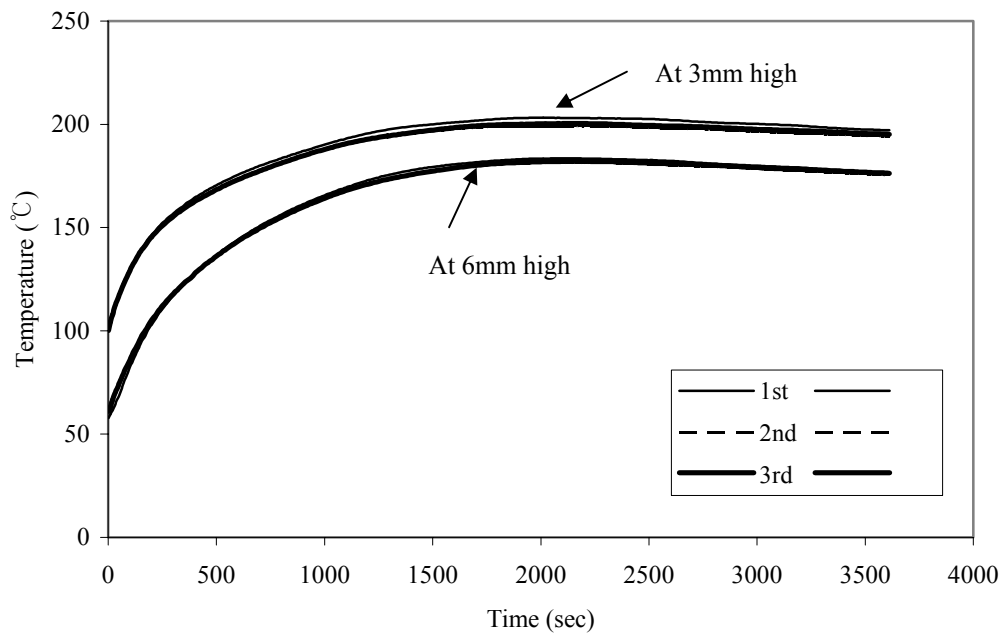


Figure 15 : Dust layer temperatures of Pittsburgh seam coal at 210°C

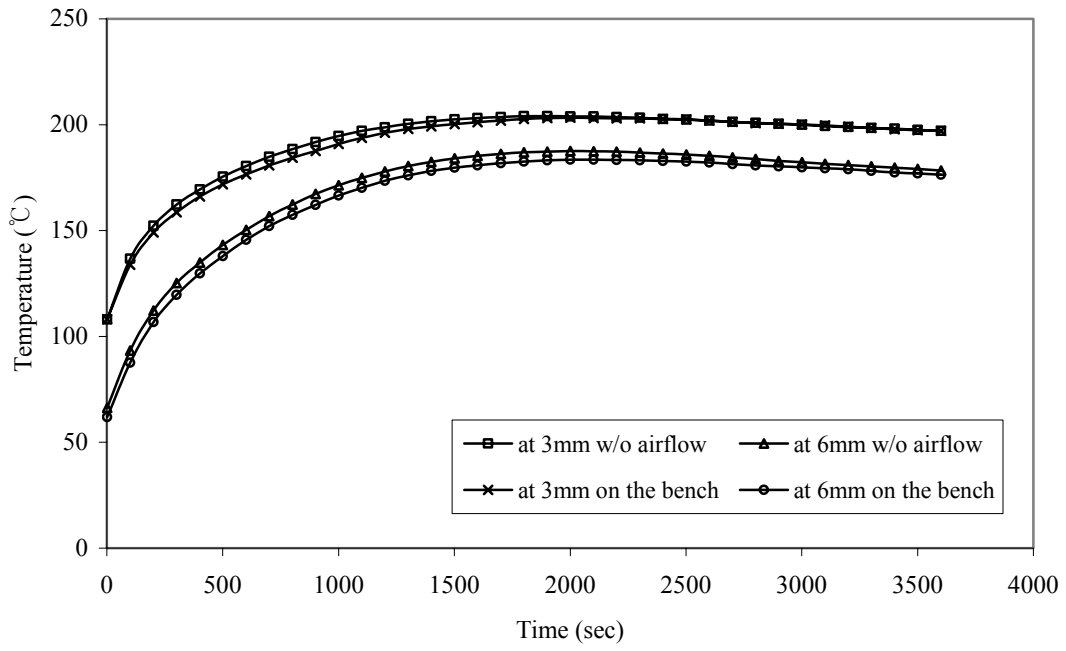


Figure 16 : Comparison of dust layer temperatures without airflow and on the bench at 210°C

4.4. Test material properties

4.4.1. Dust

Dusts' thermal properties are hard to measure and the purpose of this thesis is not only focused on the theoretical aspects of ignition of dust layers which requires exact values of thermal properties. Therefore, brief information such as bulk density, particle size and dust material supplier is listed in table 6. Bulk density was measured with the ring having 4inch inner diameter and 1 inch height without any compression on the dust. Therefore, inherent error due to the small scale measurement might be possible.

Dusts were sieved to measure the average particle size with a sieve shaker. On the sieve shaker, putting the coarser mesh sieves over the finer mesh sieves, sieving was continued until no more particles sieved from the coarser meshes. The change of the sieved amount of particles in the each sieve was checked by weighing the sieved particles.

Table 6 : Summary of dust properties and provider

	Bulk density(g/cm³)	Particle size(μm)	Material supplier
Pittsburgh seam coal	0.553	<75	NIOSH Pittsburgh research Laboratory
Gum Arabic powder	0.388	80% <105	Anonymous
Paper dust from printing press	0.029	<850, >425	Local newspaper company
Brass powder	0.320	<45	NEI-group

4.4.2. Combustible liquids and contaminants

Combustible liquids and other contaminants are key factors in this topic and their thermal properties are important. Flashpoints, AITs, and liquid suppliers are listed in table 7. Mobil DTE 24, and Citgo press oil 68 are hydraulic oils being used in a newspaper printing press. Citgo oil is formulated with premium paraffinic base oils and ashless antiwear additives which is not zinc-type. Other thermal properties such as specific heat, heat conductivity might be also important, but are not available. Since the main concern is about whether it promoted the ignition of dust layers, AIT and flashpoint were mainly concerned.

AITs of DTE24, and Citgo oil were measured by Kidde-Fenwal Combustion Research Center with the method of ASTM E659. Black ink's and ketone-based liquid solution's flashpoints were measured on-site with the pilot ignition source on an open hot plate. Therefore, it might not be exact value, but enough to give overall range of flashpoint. N-decane and kerosene's flashpoints and AITs were from the manufacturer's MSDS provided along with the products.

Ink was a black color newspaper printing ink containing high boiling point petroleum oil which is very similar to mineral oil as solvent, and using carbon black for its color. The ink also has small amounts of waxes, drying agents, and lubricants.

Table 7 : Flash point and Auto Ignition Temperatures of liquids

	Flash point(°C)	AIT(°C)	Liquid supplier
Mobil DTE24 Hydraulic oil	220(closed cup)	359	Mobile oil corp.
Citgo Hydraulic press oil 68	242(closed cup)	308	CITGO
n-decane	46(closed cup)	210	Spectrum chem.
Kerosene	38(closed cup)	210	Spectrum chem.
Black ink	265(open cup)		Newspaper company
Ketone-based liquid solution	90(open cup)		Anonymous supplier

4.5. Preliminary test

Preliminary tests were planned to verify the performance of test equipment. ASTM E 2021 describes three benchmarking test materials: Pittsburgh seam coal, coated brass flakes, and lycopodium. Specifications are as follows. Pittsburgh seam bituminous coal is up to 80% of minus 200 mesh, a mass median diameter of about $45\mu\text{m}$, and 36% volatility. Brass is 100% minus 325 mesh with less than 1.7% of stearic coating. The lycopodium is 100% minus 200 mesh and mass median diameter of about $28\mu\text{m}$.

The ignition temperatures are recorded in ASTM E2021 as 230~240°C for Pittsburgh seam coal, 155~160°C for brass flakes, and 240~250°C for lycopodium spores.

Dust layer temperatures were graphed right after putting dusts inside the ring, which usually corresponded to the first temperature drop. Related to this test procedure, inherent errors sometimes occurred. The temperature recorded - 9999°C or 9999°C when a sudden steep temperature change occurred at the thermocouple for dust layers. Usually this happened at the very early stage when dust layer was put on the hot plate causing sudden changes of the temperatures of the thermocouples.

Figure 18 is the magnified graph of the area surrounded a circle in figure 17. As shown in the figure 18, the initial thermocouple temperatures were 102.2°C and 85.6°C for 3mm and 6mm thermocouples respectively. When the dust was put on the hot plate just a little earlier than 20s, the temperatures dropped down to

44°C and 37°C. The first 20s refers to the period between turning on the temperature recording software and putting dusts inside the ring. Therefore, this 20s does not have any meaning and would be better not to be considered in calculating time to ignition. The first downward apex as the starting point to calculate time to ignition seems appropriate.

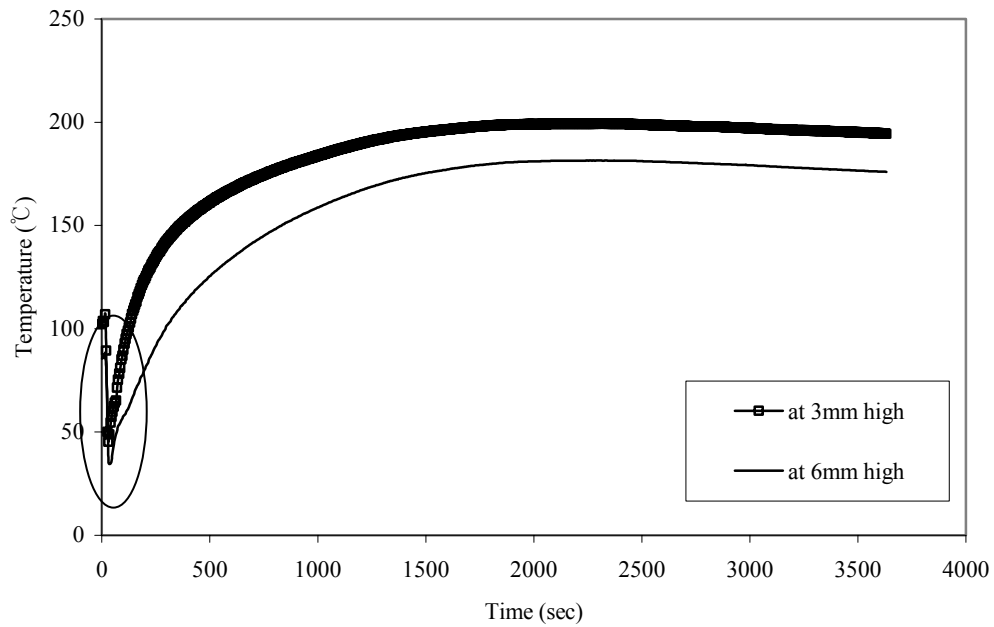


Figure 17 : Pittsburgh seam coal at 210°C

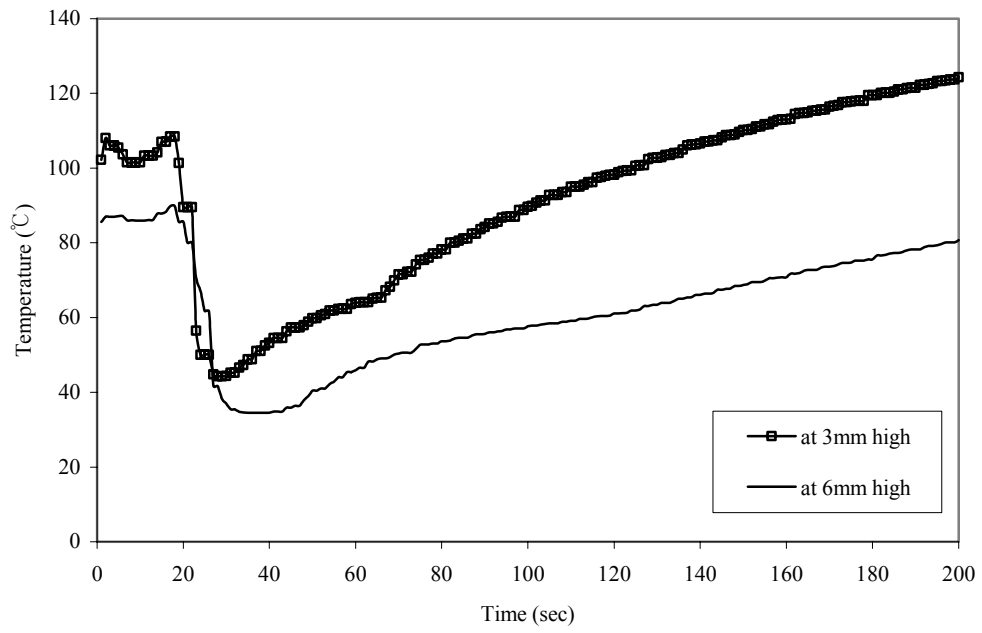


Figure 18 : Pittsburgh seam coal at 210°C for the first 200 sec

4.5.1. Pittsburgh seam coal

Pittsburgh seam coal was provided by NIOSH Pittsburgh Research Center Laboratory and had size distribution of 75.4% minus 200 mesh and 36.1% minus 325 mesh which satisfied the ASTM standard. The volatility of this Pittsburgh seam coal was not specified. 57g of Pittsburgh seam coal were tested at different hot plate temperatures.

The hot surface ignition temperature of Pittsburgh seam coal was 220°C which was 10~20°C below compared to the ASTM E2021 result. Although ASTM E2021 mentioned one hour as the maximum test period, the ignition symptom was shown almost at last minute of 3600 sec, the test was run longer than specified in ASTM E2021. At 210°C, Pittsburgh seam coal did not ignite. At 220°C, the time to ignition was 4060s when the thermocouple at 6mm high recorded 270°C. When the ignition occurred, there are some cracks on the surface of Pittsburgh seam coal as shown in the figure 19.

Temperatures measured at elevation of 3mm and 6mm in the dust layer are shown in figure 20 and 21. When ignition occurred, the temperature at 3mm high became higher than that of at 6mm high at about 4400 seconds. This can be explained by the relationship between temperature in the dust layer and oxidation of dust particles. Temperature is the representation of the extent of exothermic reaction, and exothermic reaction is dependent of oxygen concentration in this case. When the ignition occurred, oxygen access level at 6mm above the hot surface is larger than that of 3mm above because oxygen is

provided by the diffusion from the dust layer surface. This is explored in more detail in section 4.10.

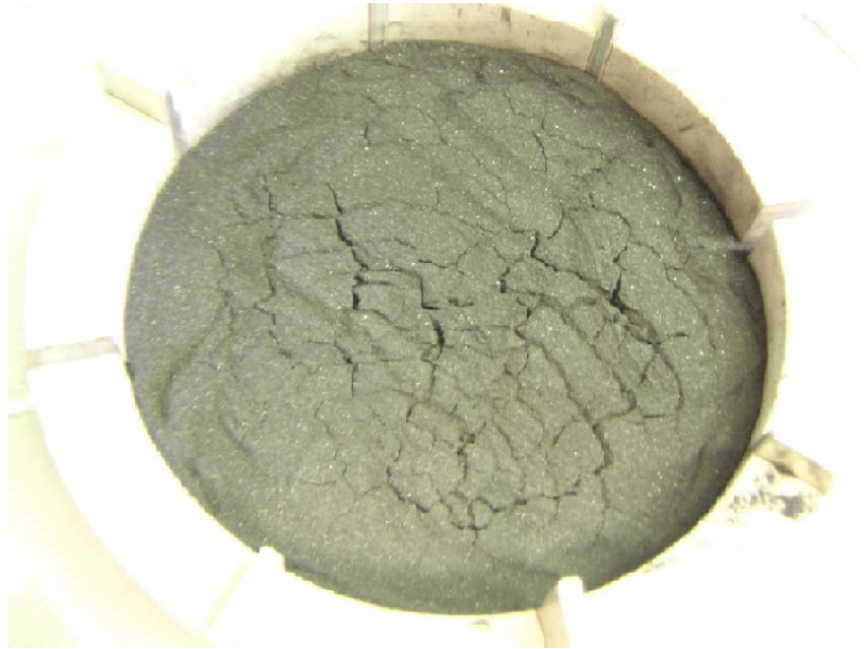


Figure 19 : Cracks in the Pittsburgh seam coal dust layer when ignition occurred

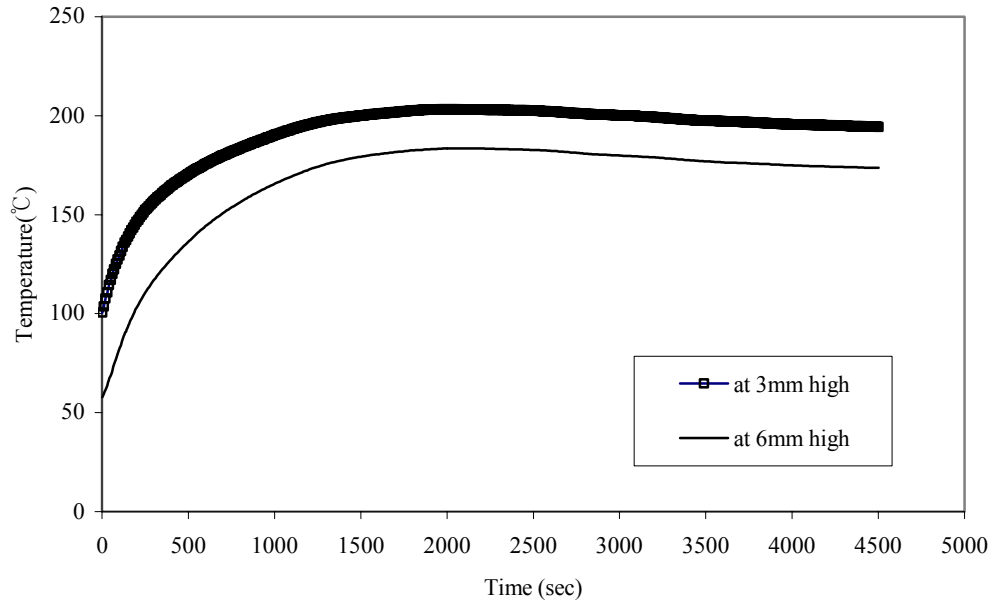


Figure 20 : Pittsburgh seam coal at 210°C

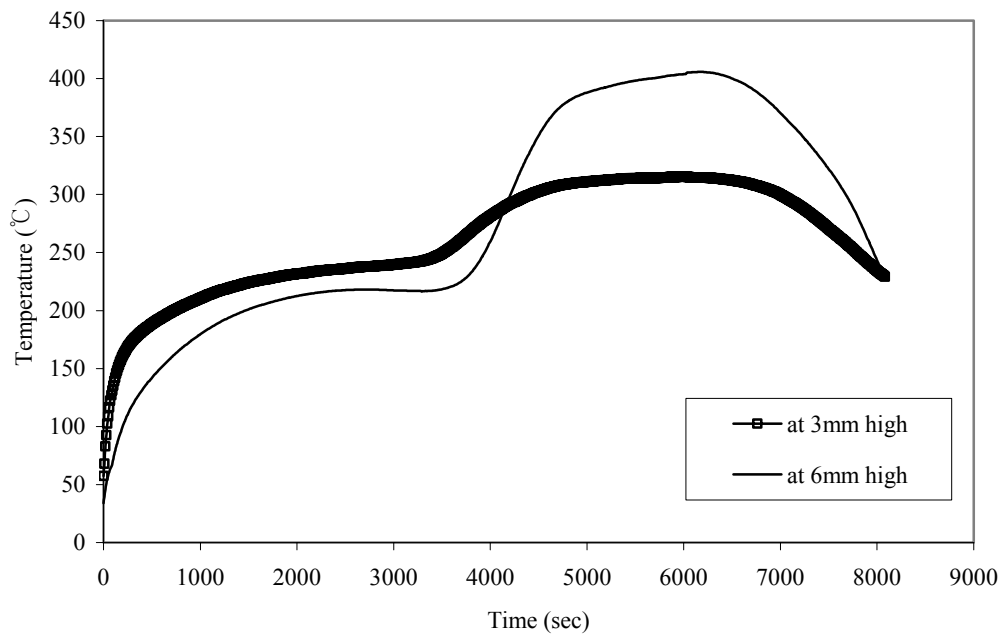


Figure 21 : Pittsburgh seam coal at 220°C

4.5.2. Brass powder

Brass powder, Super Brass 75, was purchased from NEI group New York office via www.easyleaf.com. It was not ignited until the hot plate temperature reached 400°C which is the maximum temperature of the hot plate prescribed by ASTM E2021. However, according to the ASTM E2021, the hot surface ignition temperature of brass powder is 155~160°C, which is much lower than the actual preliminary test here.

Previous paper by Yael Miron and Charles P. Lazzara mentioned the amount of stearic acid coating material can change the ignition temperature of brass. Since stearic acid amount of the brass powder used in this test was not known, it was possible that its ignition temperature was not the range in ASTM E2021. Further research about the effects of stearic acid was on ignition temperature was dealt with later section of this paper.

4.5.3. Analysis and summary

Through preliminary tests, test equipment and test procedure were verified. Although the tested materials were not the one exemplified in ASTM E2021, the temperature profile of Pittsburgh seam coal was very similar with ASTM 2021 test result. In case of brass, since the information about stearic coating level and its compound was not known, it did not seem proper to compare the test results.

4.6. Ignition temperatures of dust alone

4.6.1. Newspaper dust

Newspaper dust was provided by a local newspaper company. The particle size of newspaper dust was less than $850\mu\text{m}$ and bigger than $425\mu\text{m}$. The newspaper dust tended to stick together and was hard to sieve. It was not contaminated by any material such as printing inks. The paper dust picture figure 22 is taken right after putting paper dust on the hot plate which was $350\text{ }^{\circ}\text{C}$.

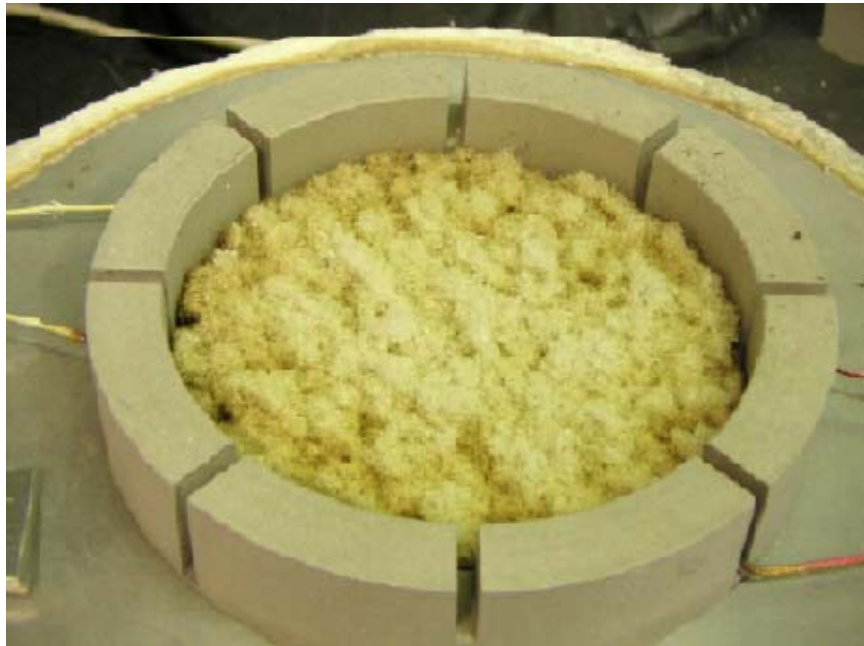


Figure 22 : Paper dust layer right after being leveled at $350\text{ }^{\circ}\text{C}$

As paper dust layer was heated, it generated sweet smell and some fumes. The amount of fumes was depending on the hot plate temperature.

The higher the hot plate temperature was, the more fumes were generated. The fume was not ignitable near the surface of dust layer with pilot ignition source.

As shown in figure 23, half inch thick paper dust alone did not ignite at 350°C reaching the maximum temperature of 334°C at 3mm high 165 sec. Dust layer temperatures remained at 306°C for 3mm, and 283°C for 6mm elevated thermocouples when the temperatures became stable. However, paper dust ignited at 360°C as shown figure 25. In figure 25, the fluctuation of temperatures both at 3 and 6mm represents the movement of glowing. After 1400 sec, the dust layer temperatures remained at 289°C and 255°C for 3mm and 6mm elevation respectively, which are lower than the 350°C of hot plate. This seemed to be caused by the paper dust layer which was shrunken as heated changing the thermocouple elevation.

Paper dust showed clear ignition symptom which was glowing as shown in figure 26. Glowing has started from the edge of the dust layer and traveled to the center of the paper dust layer. This can be explained by the effect of the hot aluminum ring. In the middle of the dust layer, while heat was only provided from the hot plate, at the edge of the dust layer where contacted by hot aluminum ring, heat was provided from both the hot plate and the ring. Oxygen concentration level might be another concern, but in case of paper dust, the bulk density seemed low enough to accommodate oxygen to the bottom of the dust layer.

At the end of the test, less than 1.5g of paper dust left which was less than half of the original amount. Before glowing was shown, the paper dust was shrunken forming chars on the bottom of the layer. When hot plate temperature was 350°C, charring occurred too, as seen in figure 24, but no glowing was observed. The temperature fluctuation which is shown in figure 25 represents the movement of glowing. When the glowing is near the thermocouple bid, the temperature jumped up.

There are some disconnections in temperature record, although this does not make it hard to read the temperature variation due to abrupt change of dust layer temperature.

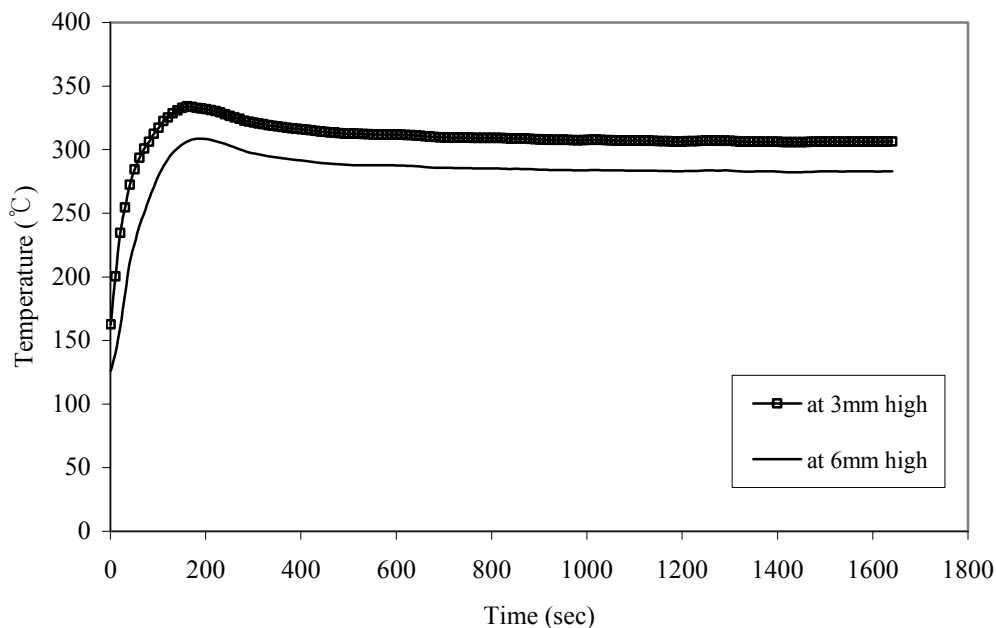


Figure 23 : Paper dust layer temperature at 350°C



Figure 24 : Chars formed on the bottom of paper dust layer at 350°C

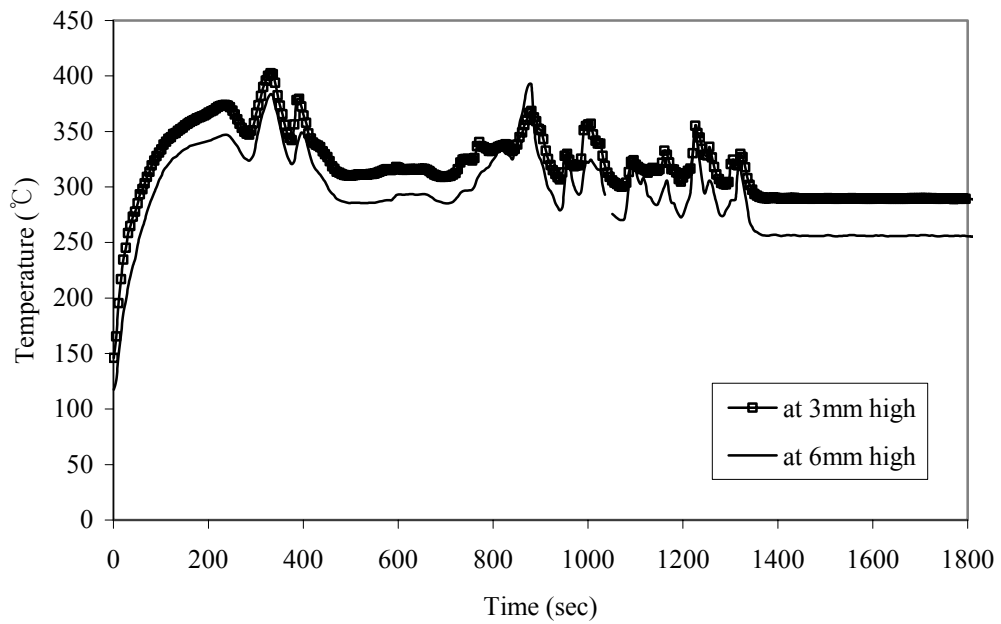


Figure 25 : Paper dust layer temperature at 360°C



Figure 26 : Glowing in the paper dust layer at 360°C

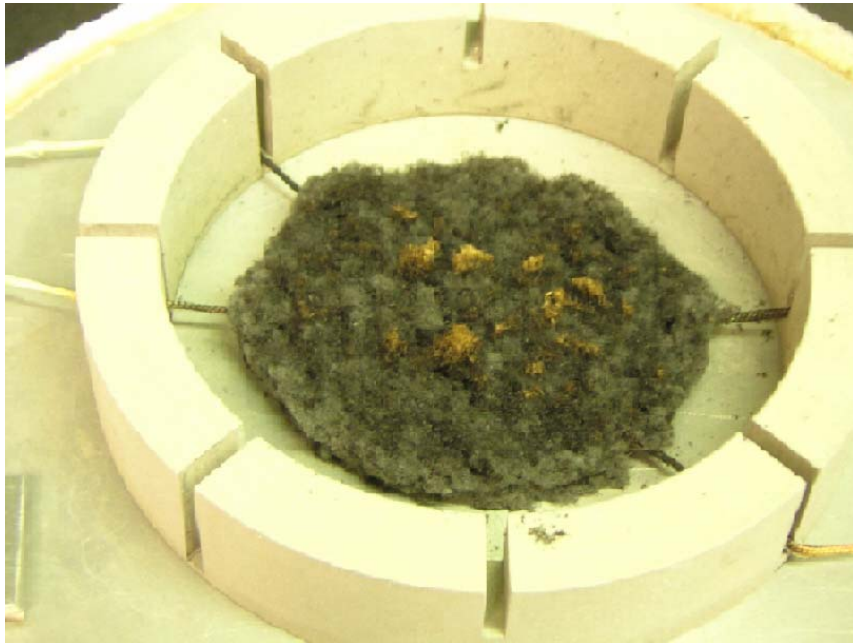


Figure 27 : Paper dust at the end of test at 360°C

4.6.2. Gum Arabic powder

Gum Arabic powder was provided by a company that does not want to be identified. The layer thickness for gum powder was one quarter inch (slightly above 6mm) which was different from other test materials. Two thermocouples were set at 3mm and 6mm high from the hot plate, too.

As shown in figure 28 and 30, gum powder was not ignited at 260°C, but ignited at 270°C. It did not show small hump before steady state temperature profile which was observed in Paper dust and Pittsburgh seam coal dust layers. It seems that the rate of endothermic decomposition and exothermic oxidation met together and raise the temperature gradually.

Its maximum temperatures were 566°C when ignition occurred from the thermocouple at 6mm high and was 198°C when ignition did not occur from the thermocouple at 3mm high which was in the middle of the dust layer.

Gum powder was shrunken a little bit, much less than paper dust. However, as the gum powder layer was heated, some cracks occurred on the surface of gum powder regardless of ignition as shown in figure 29, and it was clustered and hardened to semi-solid holding the thermocouples in it. As it is heated and shrunken holding the thermocouples, the elevation of thermocouples could be changed and subsequently, the temperature might be less accurate.

Gum powder generated sweet smell similar with paper dust, but stronger. It formed char on the bottom of the dust layer first and glowing was

observed later. However, the ashes were different. Paper dust left black ashes but gum powder generated white ashes which was lighter than that of paper dust. More complete combustion seemed to occur in gum powder case.

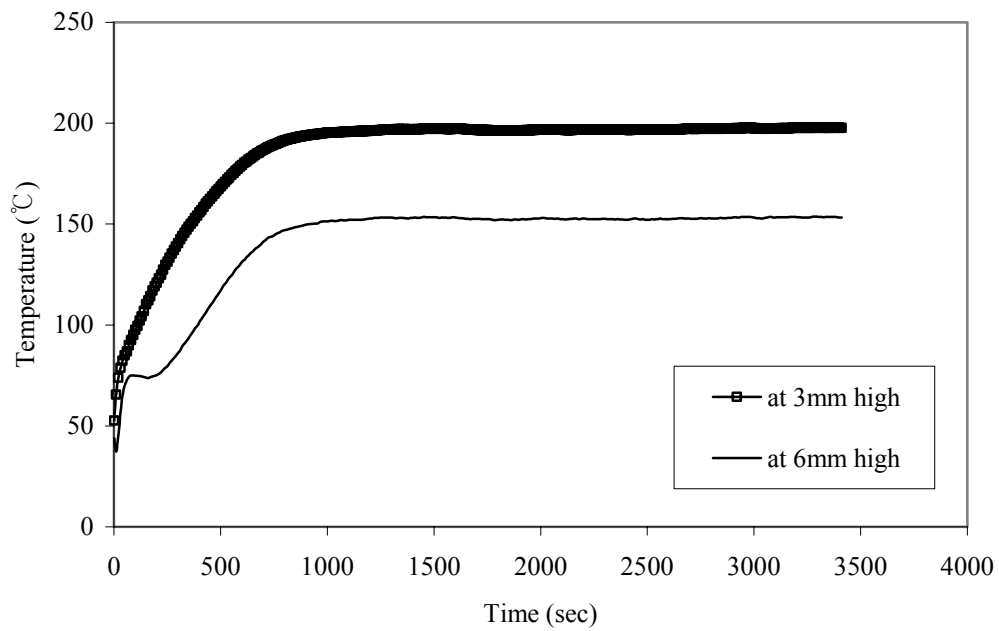


Figure 28 : Gum powder dust layer temperature at 260°C

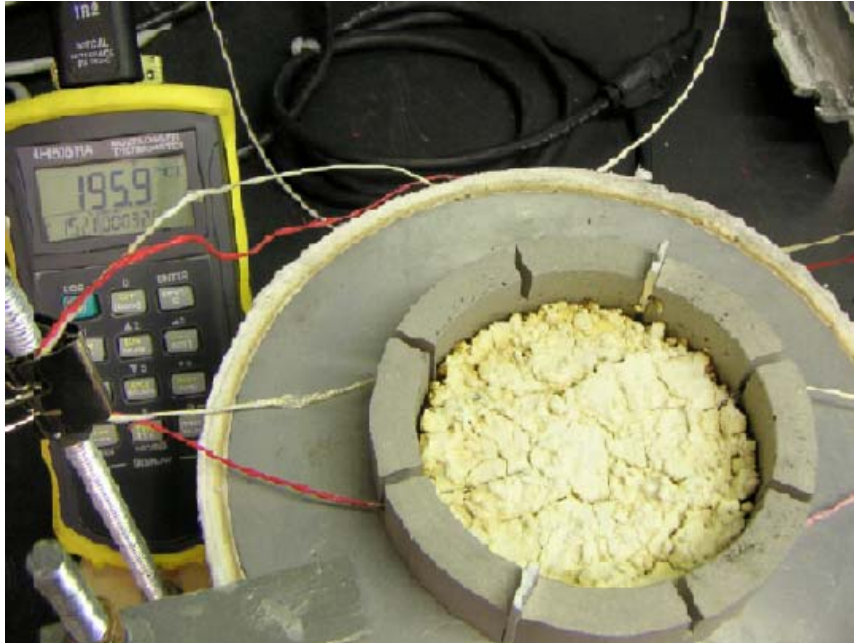


Figure 29 : Cracks in the gum powder dust layer at 260 °C

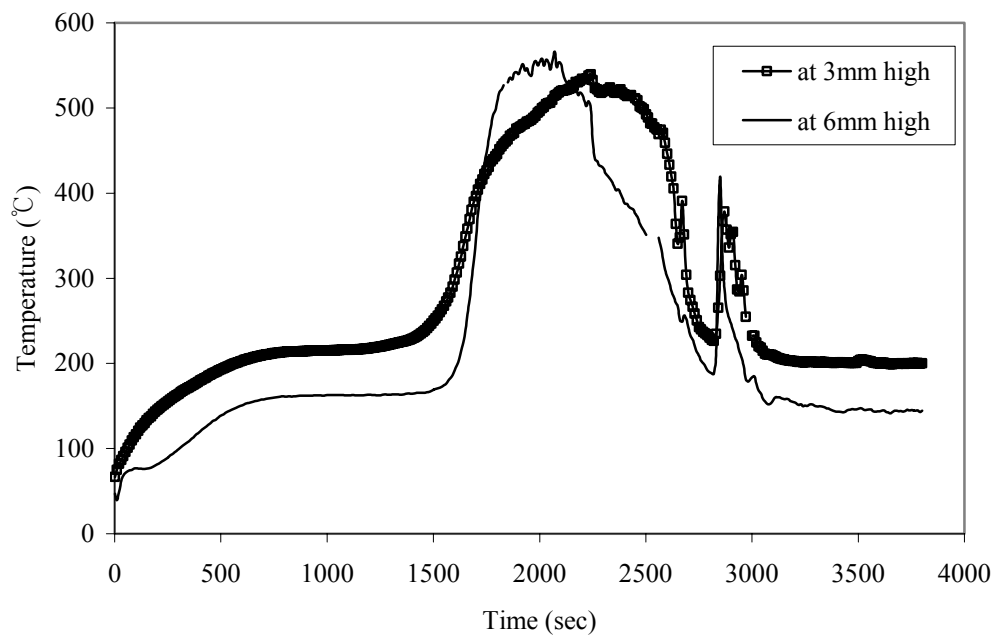


Figure 30 : Gum powder dust layer temperature at 270 °C

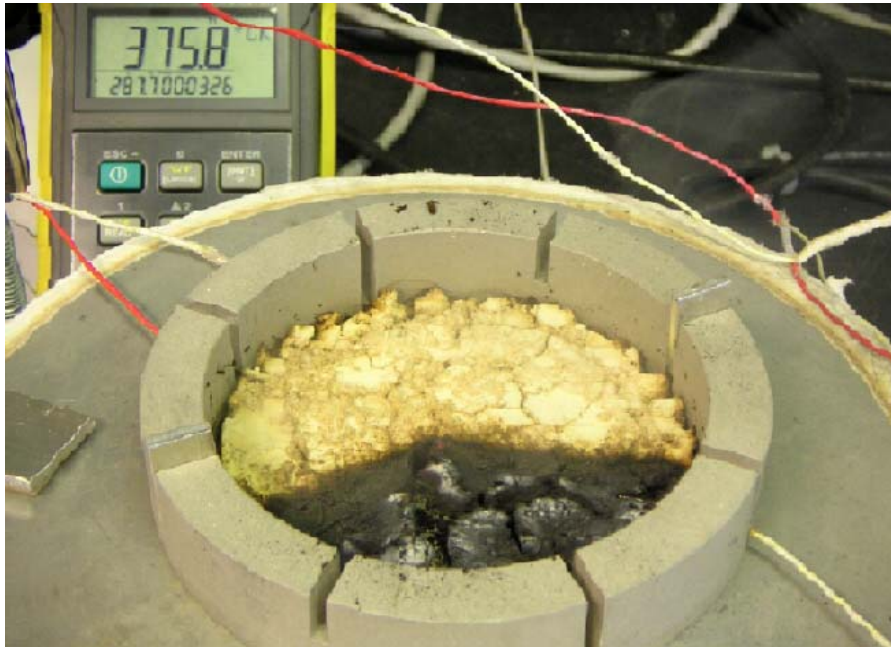


Figure 31 : Glowing in the gum powder dust layer at 270 °C

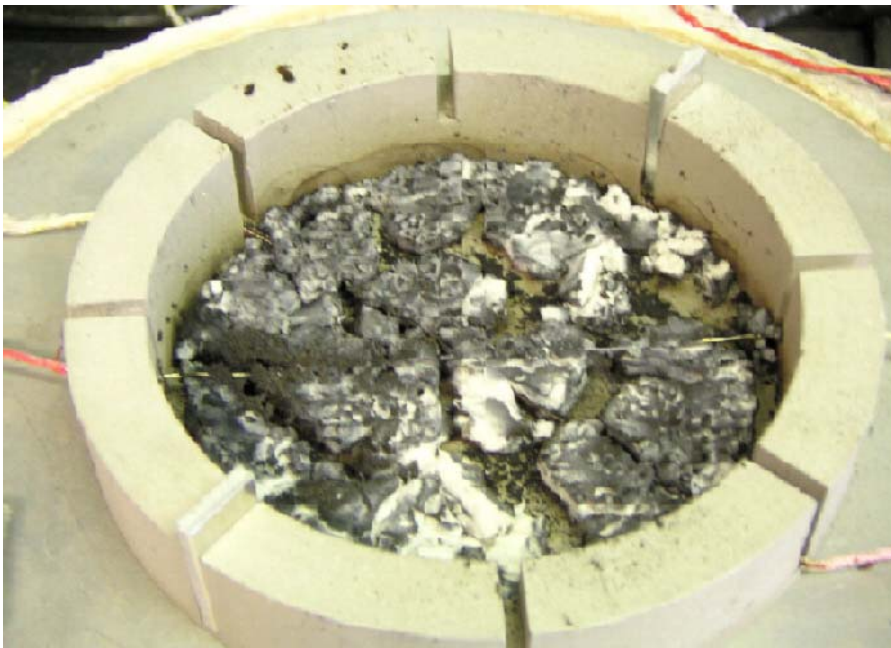


Figure 32 : Gum powder dust layer at the end of test at 270 °C

4.6.3. Analysis and summary

The mechanism of hot surface ignition of dust layers is a little different from that of solid ignition. The hot plate ignition of dust layers is related to the self-heating theory which was briefly dealt with in the literature review.

When a solid material is heated by external heat source, gas phase fuel is generated on the surface of the solid by the thermal decomposition. Exothermic chemical reaction can be the same cause for ignition for both solid and dust layer ignition. However, the surface area of solid material exposed to the oxygen is much less than the case of dust layers, since each particle in the dust layer is exposed to the surrounding oxygen molecules. In addition, the heat loss through conduction in the molecules and convection on the surface is much higher in case of solid material than a dust layer. The contact area of each particle in dust layer is much smaller than fully connected solid material leading smaller conductive heat loss.

Therefore, the crucial factor that decides the ignition temperature for dust layer is the surface-area/volume ratio of dust layer, the major difference between solid material and dust layer, which can decide the amount of oxygen access and heat loss to the ambient air. For example, dust layers having large surface area in low bulk density allowing more convective heat loss has fewer propensities for self ignition. From the past self-heating experiment, thermal runaway started from the middle of the dust layer where the minimum heat loss occurs.

The hot surface ignition temperatures were 360°C for paper dust, and 270°C for gum powder. Gum powder has shown similar temperature increase pattern with Pittsburgh seam coal which ignited at 220°C, a representative material for hot surface ignition test. After a certain incubation period while no ignition symptom was observed, the dust layer temperature increased steeply.

However, paper dust did not show incubation period before ignition. Temperature increased steeply from the beginning of the test, and when the peak temperature recorded, glowing, ignition phenomenon for paper dust, was observed. The ignition surface temperature of corrugated paper which is exposed to the external radiant heat flux is 370°C from the Industrial Fire Protection Engineering by Zalosh(2002, p.132) which is not much different from the hot surface ignition temperature of half inch paper dust layer.

From the fact that paper dust layer which was assumed to have lower hot surface ignition temperature due to self heating has similar ignition temperature with corrugated paper, the ignition of paper dust layer seemed to show less accordance to the F-K self-heating theory. This should be studied further to avoid improper conclusion, which might be able to draw a guideline for the application of F-K theory. However, much convection loss due to low bulk density can explain this.

4.7. Ignition temperatures of dust with combustible liquids

4.7.1. Newspaper dust

4.7.1.1. Paper dust with Citgo hydraulic/press oil

Citgo hydraulic/press oil was provided by a local newspaper company. It provides rust and corrosion protection to the printing press machine serving as gear and bearing lubricants. Its viscosity is 68 cSt at 40 °C and 8.5 cSt at 100 °C based on the ASTM D445 test method. It has 242 °C flashpoint, and 308 °C AIT from its MSDS and from Kidde-Fenwal Combustion Research Center report No.CRC-2556 (2005) which is attached in appendix B.

3g of paper dust was evenly mixed with 3g of Citgo hydraulic/press oil for hot surface ignition testing. The amount of fumes at early stage was much more than dust alone was tested. The mixture seemed to contain some residue of Citgo oil until the end of test, since the color of the mixture was much darker.

As shown in figure 33, the mixture was not ignited until the hot plate temperature reached 400 °C not showing glowing which was observed in paper dust alone. The layer temperature increase at 6mm high was not over 50 °C of hot plate set temperature. Its maximum temperatures were 401 °C at 3mm high and 346 °C at 6mm high.

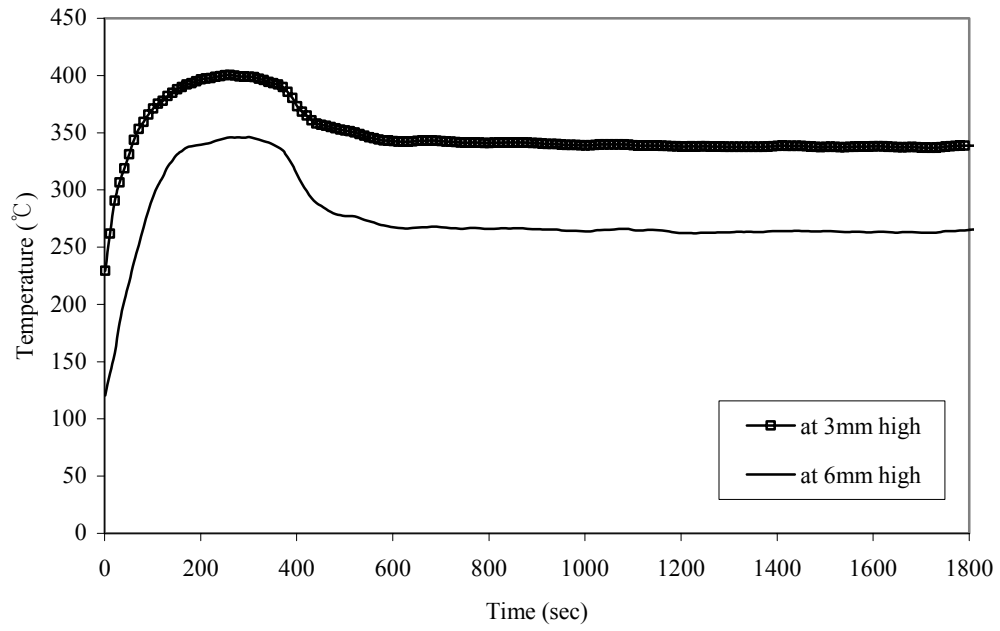


Figure 33 : Paper dust (3g) with Citgo oil (3g) at 400 °C

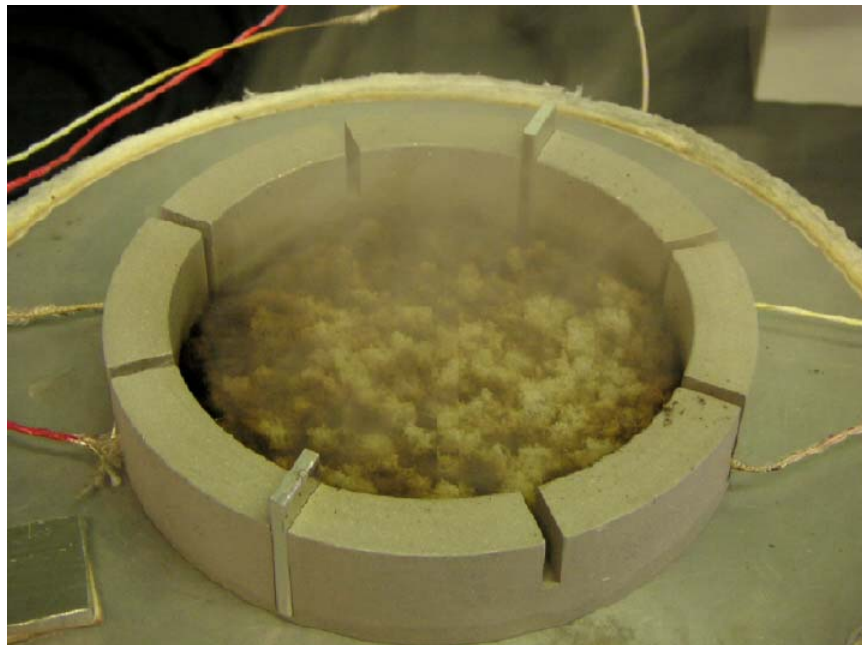


Figure 34 : Paper dust (3g) with Citgo oil (3g) at 400 °C, early stage



Figure 35 : Paper dust (3g) with Citgo oil (3g) at 400 °C, at the end of test

4.7.1.2. Paper dust with DTE 24

DTE 24 which was manufactured by Mobile Oil Corp. was provided by a local newspaper company, too. It is used also as hydraulic oil for gear or bearing lubricants. Its viscosity is over 29.8 cSt at 40°C and 5.3 cSt at 100°C. It has 220°C flashpoint, and 359°C AIT, which is slightly higher than Citgo oil from its MSDS which is also attached in the appendix B.

3g of paper dust and 3g of DTE 24 were mixed together and tested in the same way as Citgo oil. The ignition did not occur up to 400°C of hot plate temperature without glowing as shown in figure 36. The maximum temperatures of the test recorded 413°C at 3mm high at 390 sec, and 350°C at 6mm high at 280 sec. Color and smell of mixture at the end of test were almost the same with those of Citgo oil mixture.

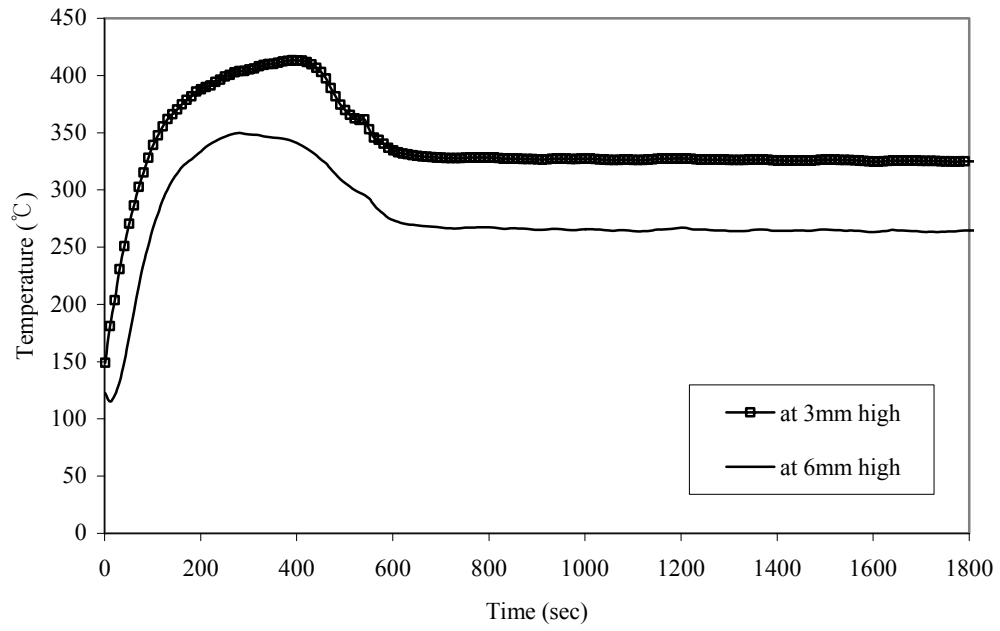


Figure 36 : Paper dust (3g) with DTE24 (3g) at 400 °C



Figure 37 : Paper dust (3g) with DTE24 (3g) at 400 °C, early stage



Figure 38 : Paper dust (3g) with DTE24 (3g) at 400°C, at the end of test

4.7.1.3. Paper dust with newspaper printing ink

Newspaper Black color printing ink manufactured by US Ink Corp. was provided by the same newspaper company. 3g of ink was evenly mixed with 3g paper dust. Its flash point is about 265°C and Auto Ignition Temperature was not known. Different from the previous two hydraulic oils and paper dust alone, the ignition temperature of ink-paper dust mixture was not clear, since there was no glowing observed when ignition occurred.

Referring to figure 40, at 350°C, there was no glowing observed throughout the test. However, the maximum temperature at 3mm high in the dust layer was more than 400°C which could have fulfilled the requirement of ASTM E2021 if ASTM E2021 stated that temperature at any point of dust layer can be a reference point for ignition. ASTM E2021 specified that locating thermocouple at the center of dust layers, i.e. at mid elevation.

Considering that paper dust alone did not really correspond to the self-heating theory and the temperature at 3mm high was much higher than the hot plate temperature, it was certain that some exothermic reaction was occurring in the dust layer which might be able to be considered as ignition, but not to be able to propagate to other dust particles showing glowing.

Therefore, 350°C was determined to be the ignition temperature of the

mixture of paper dust and newspaper printing ink.

At 360 °C and 380 °C, glowing was shown, although the temperature at 6mm high was not 50 °C higher than the hot plate temperature.

Table 8 : Max. temperatures of paper dust (3g) with ink (3g) at different hot plate temperatures

Hot plate temp.(°C)	Max. temp. at 3mm high (°C)	Max. temp. at 6mm high (°C)	
340	303	271	No glowing
350	408	332	No glowing
360	380	345	glowing
380	411	404	glowing

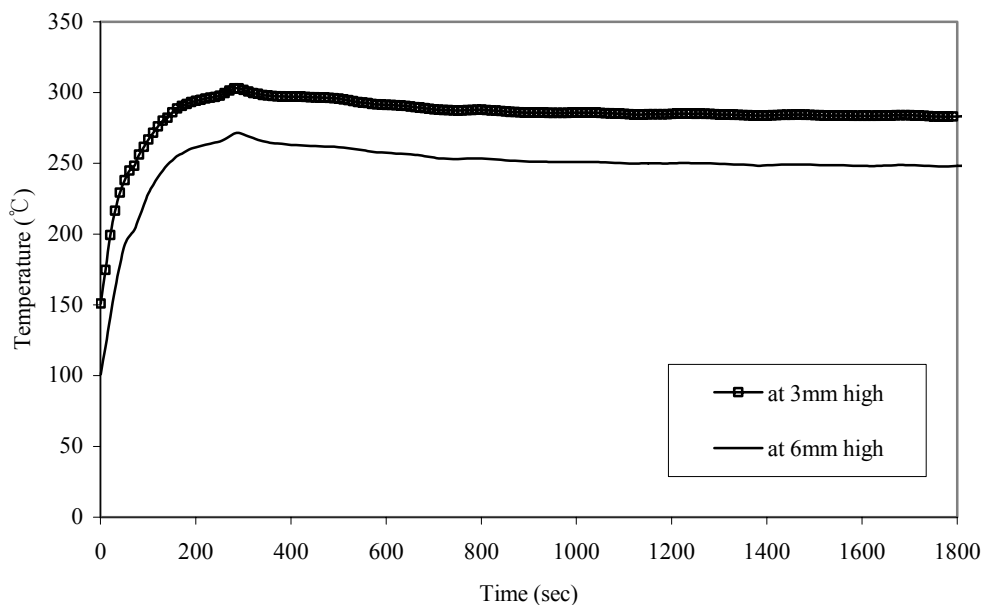


Figure 39 : Paper dust (3g) with newspaper printing ink (3g) at 340 °C

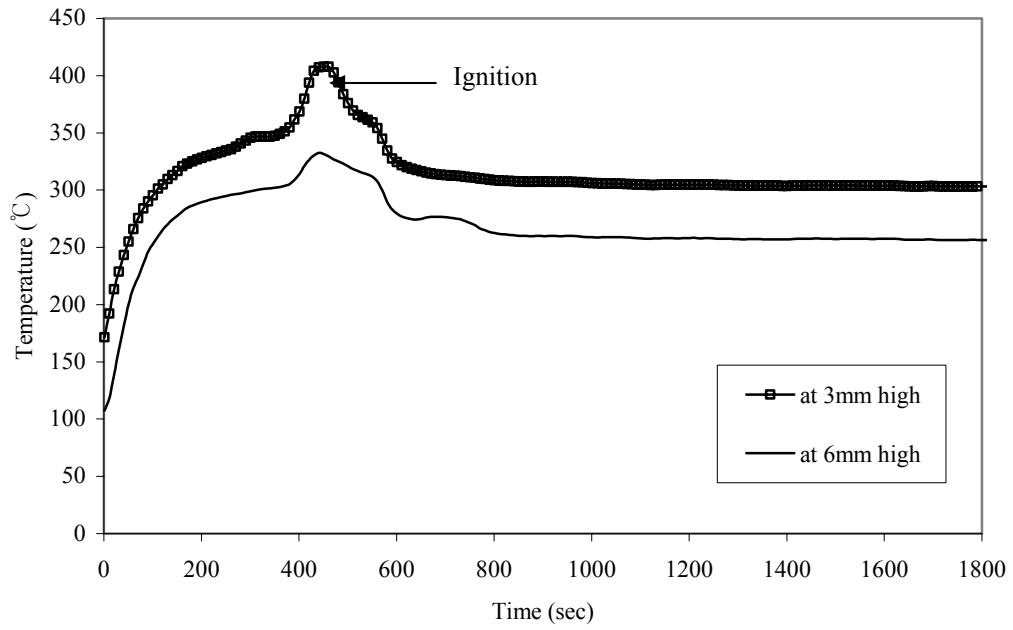


Figure 40 : Paper dust (3g) with newspaper printing ink (3g) at 350°C



Figure 41 : Paper dust (3g) with newspaper printing ink (3g) at 350°C, at the end of test

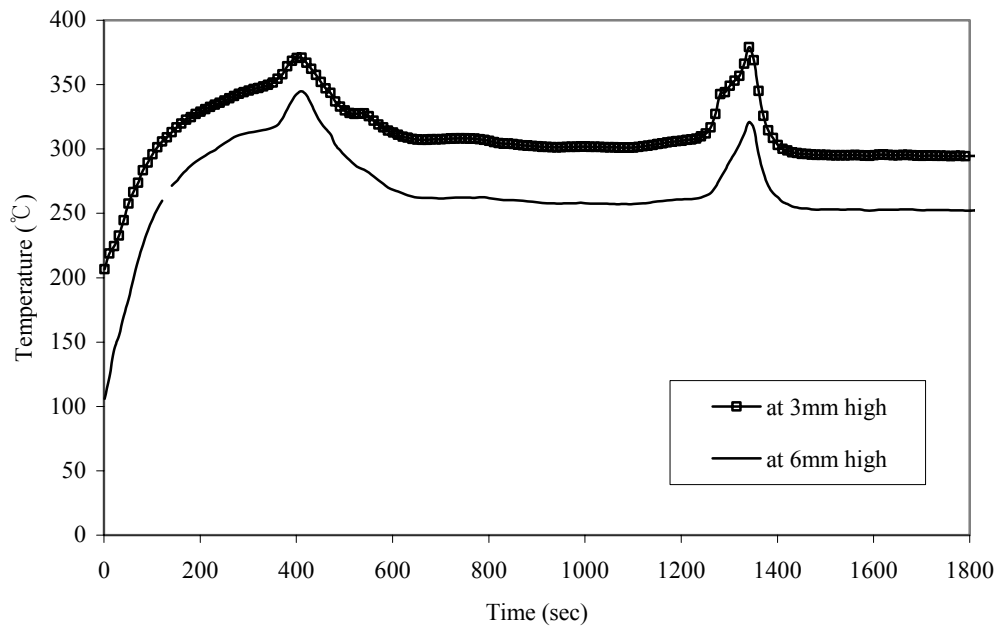


Figure 42 : Paper dust (3g) with newspaper printing ink(3g) at 360°C

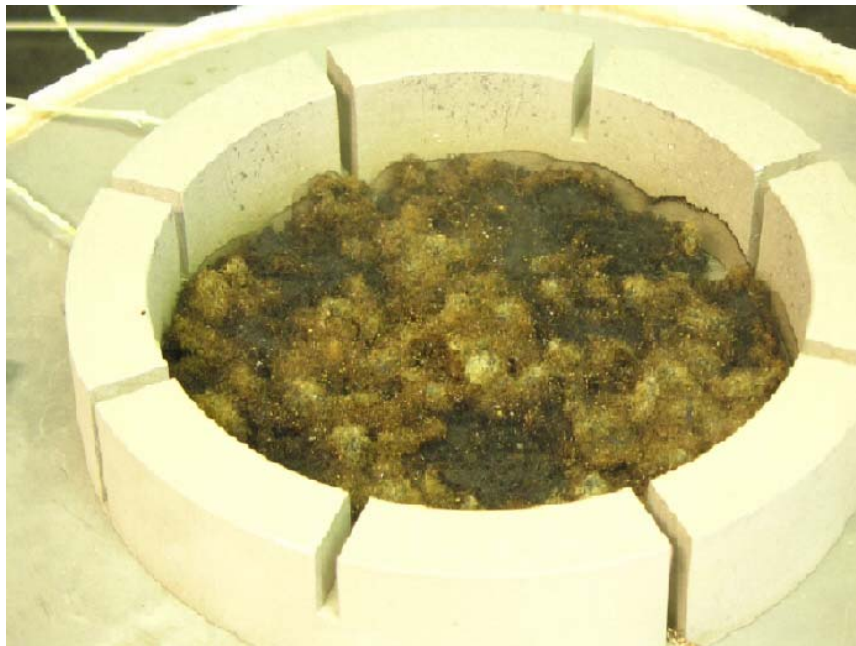


Figure 43 : Paper dust (3g) with newspaper printing ink (3g) at 360°C

4.7.1.4. Paper dust with n-decane

n-decane was purchased from Spectrum laboratory products, Inc.. It has 46°C of flashpoint, and 210°C of Auto Ignition Temperature from its MSDS. Compared to the previously tested combustible liquids, it has much lower flashpoint and AIT.

3g of n-decane was pre-mixed with 3g of paper dust and tested. 3g of n-decane was the amount with which paper dust was saturated, but with no liquids flowing on the hot surface. It was ignited at 360°C with glowing, but not ignited at 350°C as shown in figure 44 and 45. The maximum temperatures were 331°C at 3mm high and 276°C at 6mm high from figure 44, and 360°C at 3mm high and 349 at 6mm high from figure 45. Paper dust-n-decane mixture was shrunken as it ignited at 360°C.

The mixture also generated lots of vapors right after being touched on the hot plate surface. It seemed that the n-decane was evaporated right away since the hot plate temperature was much higher than its boiling point, 174°C.

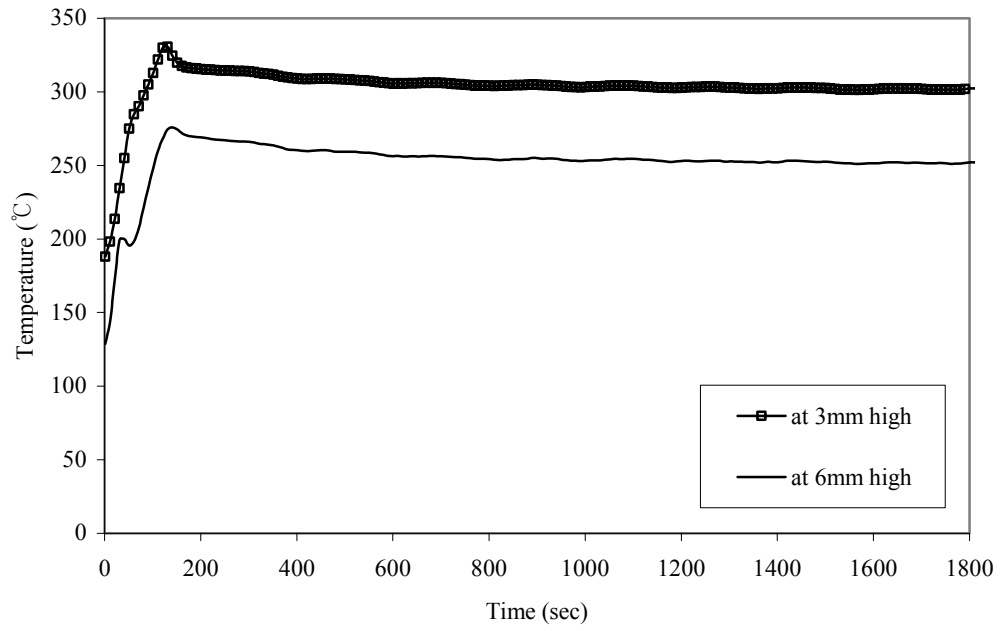


Figure 44 : Paper dust (3g) with n-decane (3g) at 350 °C

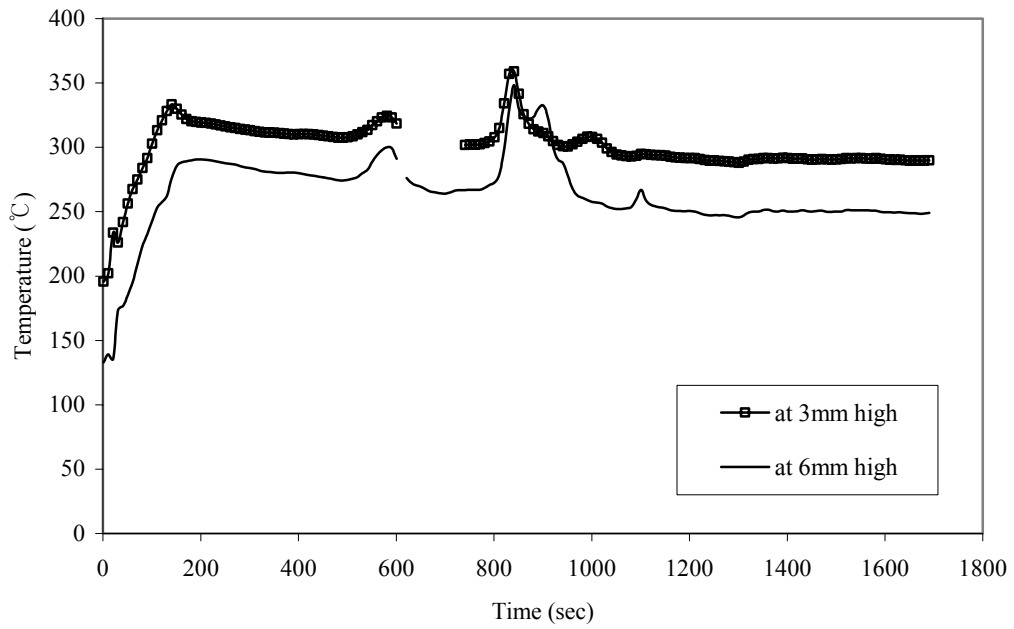


Figure 45 : Paper dust (3g) with n-decane (3g) at 360 °C

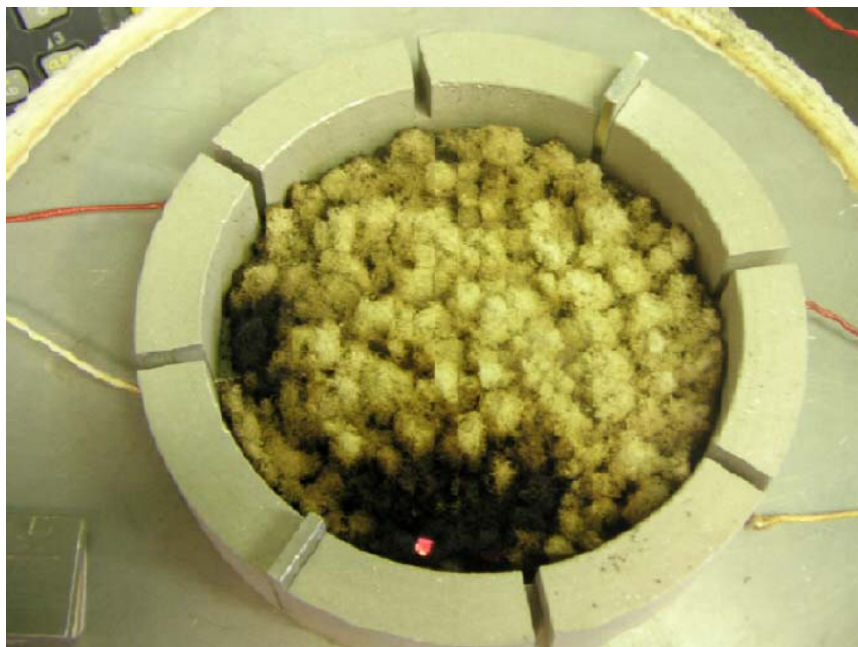


Figure 46 : Paper dust (3g) with n-decane (3g) at 360°C

4.7.1.5. Paper dust with kerosene

Kerosene was purchased from the same company, Spectrum laboratory products, Inc.. It has 38°C of flashpoint which is slightly lower than n-decane, and 210°C of Auto Ignition Temperature from its MSDS provided along with the kerosene.

The mixture of 3g of kerosene and 3g of paper dust ignited at 370°C with glowing and did not ignite at 360°C. At 360°C, the maximum temperatures were 339°C and 279°C for 3 mm and 6mm elevation respectively. At 370°C when ignition occurred, 417°C and 412°C recorded for 3mm and 6mm elevation as maximum temperatures.

The ignition procedure was almost same with n-decane. Large amount of vapors which seemed to be Kerosene were generated right after being on the hot plate.

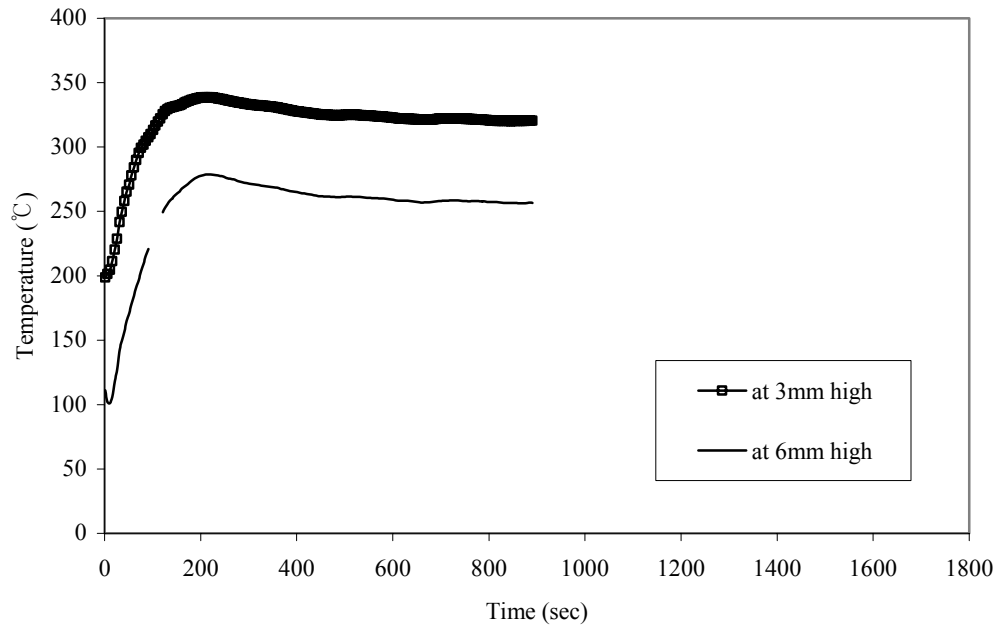


Figure 47 : Paper dust (3g) with kerosene (3g) at 360°C

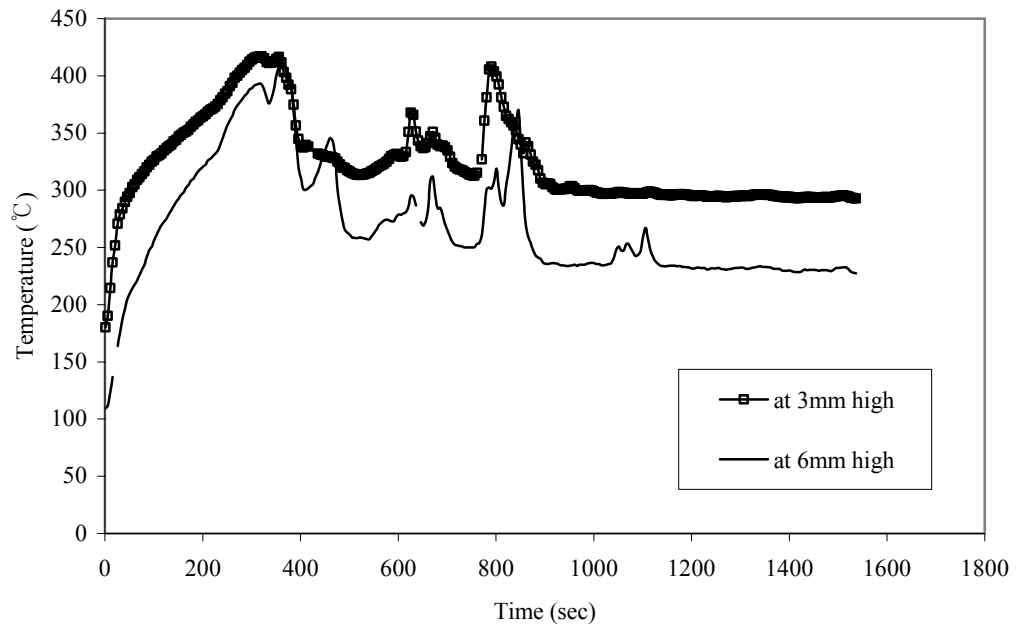


Figure 48 : Paper dust (3g) with kerosene (3g) at 370°C

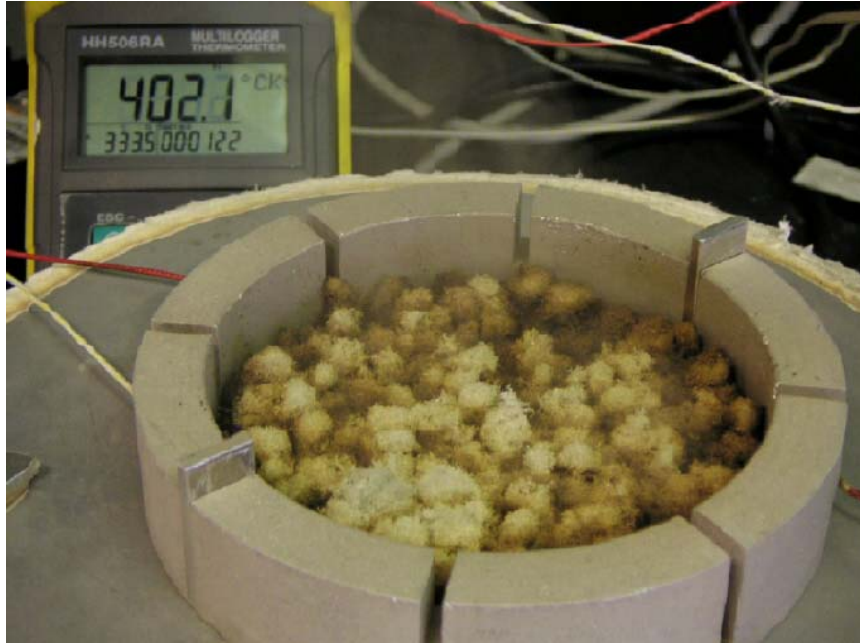


Figure 49 : Paper dust (3g) with kerosene (3g) at 370°C

4.7.2. Gum powder with ketone-based liquid solution

Ketone-based liquid solution was provided along the gum powder. The flashpoint of ketone-based liquid solution was measured on-site with pilot ignition source on the hot plate. 1 ml ketone-based liquid solution (11 cm diameter on the hot plate) was ignited when hot plate was about 90°C. The thickness of gum powder on the hot plate was one quarter inch. Therefore, the dust layer temperature at 3mm high was the criteria and main concern.

Different amounts of combustible liquid were mixed with gum powder and tested. 1g, 2g, and 4g were respectively added to 20g of gum powder and the ignition temperatures of them were 280°C. The vapors generated above the surface of the mixture with 4g of ketone-based liquid solution were ignited by a pilot flame source when the dust layer temperature at 3mm high was over 200°C, which was represented in figure 55. At 1000 sec, temperature dropping was due to the water application to the dust layer to extinguish flame which was ignited by pilot ignition source.

With 1g and 4g addition of ketone-based liquid solution to the gum powder, the maximum temperatures were 215°C and 168°C for 1g of liquid addition, and 221°C and 181°C for 4g of liquid addition at 3mm and 6mm high respectively. From the comparison of figure 50 and 51, with more ketone-based liquid solution, the temperature had more fluctuation at 6mm elevated thermocouple, although it was very small difference.

As figure 54 and 55 show, mixtures of gum powder with 2g and 4g of

ketone based liquid solution ignited at 280°C. The ignition temperature of gum powder alone was 270°C, 10°C lower than the gum powder mixture. With 2g addition, the maximum temperatures of dust layer were 463°C at 3mm high and 473°C at 6mm high. Glowing was observed. Although ignition did not occur at lower temperatures than 280°C, some chars were formed on the rim and bottom of the dust layer where dust layer was contacted with hot surface. After glowing has traveled, white ashes were left as gum powder alone was tested.

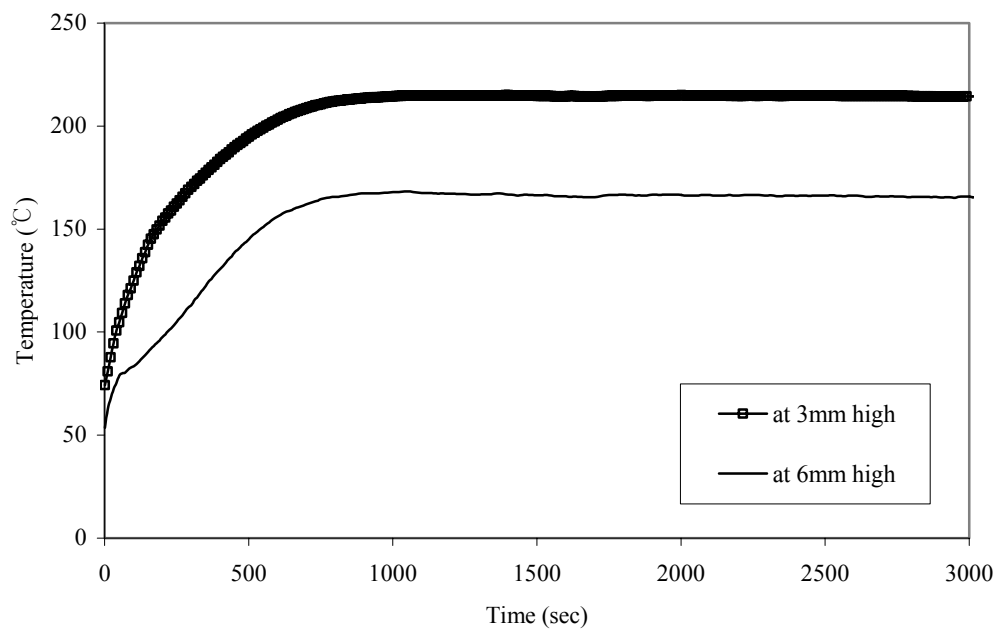


Figure 50 : Gum powder (20g) with ketone-based liquid solution (1g) at 270°C

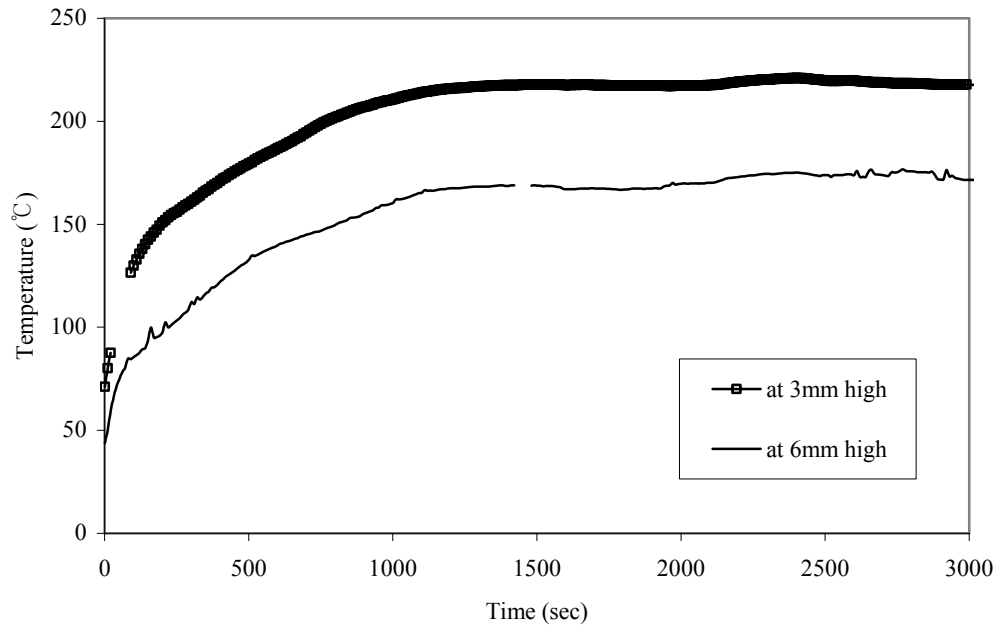


Figure 51 : Gum powder (20g) with ketone-based liquid solution (4g) at 270 °C



Figure 52 : Gum powder (20g) with ketone-based liquid solution(1g) at 270 °C, early stage



Figure 53 : Gum powder (20g) with ketone-based liquid solution (1g) at 270°C, at the end of test

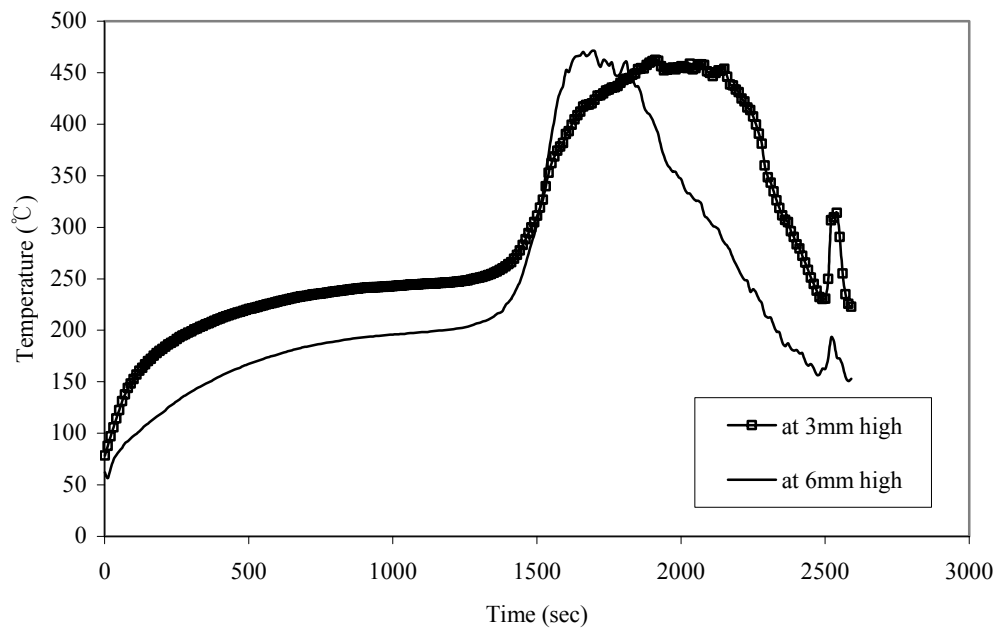


Figure 54 : Gum powder (20g) with ketone-based liquid solution (2g) at 280°C

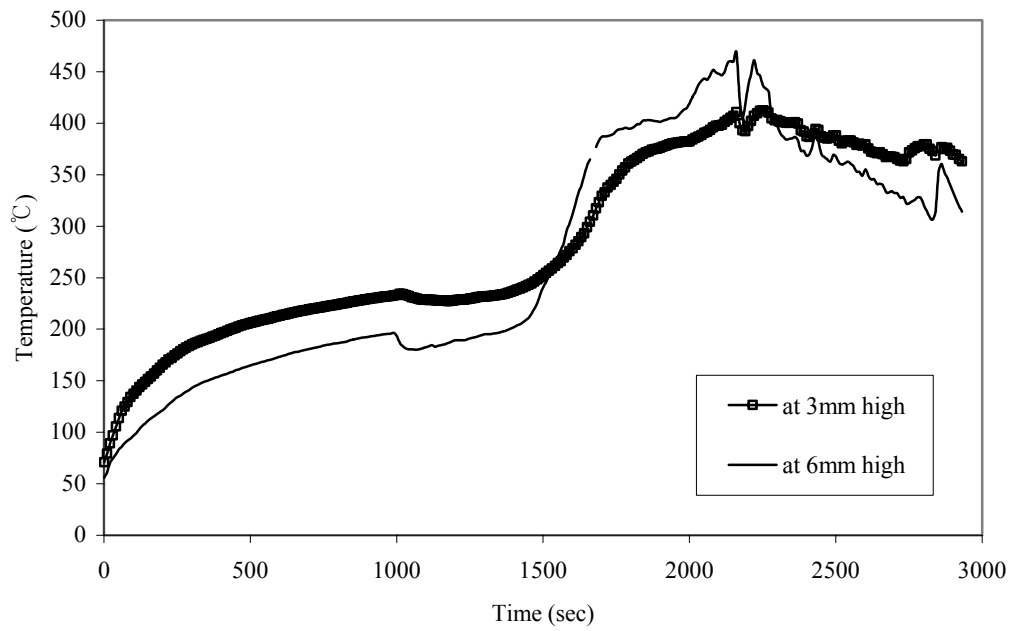


Figure 55 : Gum powder (20g) with ketone-based liquid solution (4g) at 280 °C

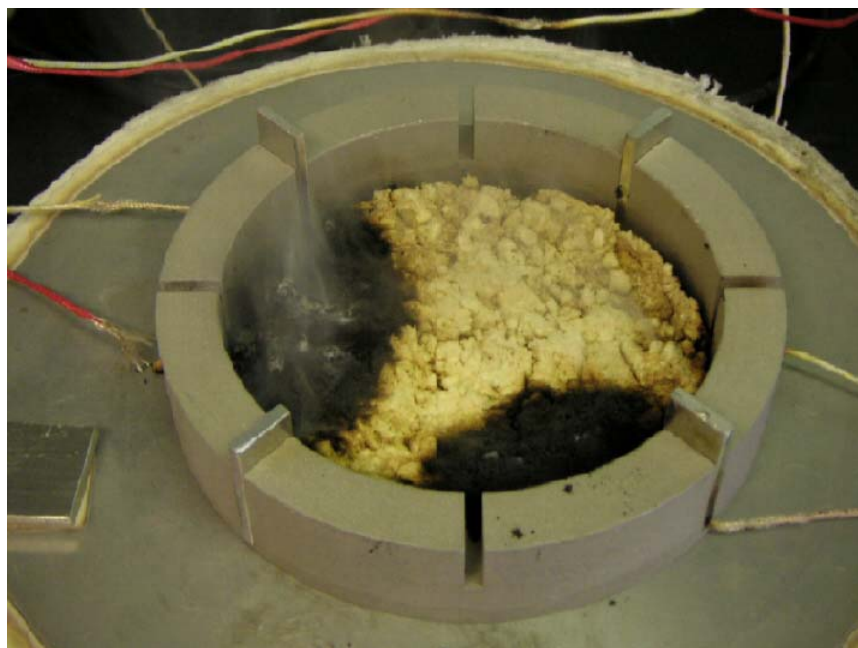


Figure 56 : Gum powder (20g) with ketone-based liquid solution (2g), ignition



Figure 57 : Gum powder (20g) with ketone-based liquid solution (2g), at the end of test

4.7.3. Analysis and summary

3g of two hydraulic oils (Citgo oil, and DTE 24), printing ink, n-decane, and kerosene were mixed with 3g of paper dust respectively and tested on the hot plate. The ignition temperatures were different from paper dust alone.

Table 9 : Comparison of ignition temperatures of paper dust mixture

	Amount	Ignition temp. (°C)	Maximum temp. at 6mm high(°C)
Paper dust alone	3g	360	415
Paper dust with Citgo oil	With 3g of Citgo oil	>400	346
Paper dust with DTE24	With 3g of DTE24	>400	350
Paper dust with ink	With 3g of ink	350	408 at 3mm high
Paper dust with n-decane	With 3g of n-decane	360	348
Paper dust with kerosene	With 3g of kerosene	370	412

Glowing was observed for n-decane, kerosene, and printing ink mixtures with paper dust, but not for the Citgo oil, and DTE 24 mixtures. One interesting thing in the mixture of paper dust was the temperature variation at 3mm high. ASTM E2021 specifies that thermocouple is located in the middle of dust layer, since the self-heating usually occurs in the middle of dust layer most. However, for the paper dust mixture with Citgo oil, and DTE 24, the temperature at 3mm high was higher than that of at 6mm high throughout the test. Moreover, temperature increase at 3mm high was more

than 50°C higher than hot plate temperature satisfying the ignition criteria of ASTM E2021. In case of printing ink mixture with paper dust, the ignition temperature was 10°C lower than paper dust alone. Printing ink is mainly composed of high boiling point petroleum oil based solvent and carbon black. Considering that DTE 24, and Citgo oil are also petroleum based, carbon black could be one of the reasons for lower ignition temperature of paper dust and ink mixture.

1g, 2g, and 4g of ketone-based liquid solution were mixed with 20g of gum powder. The ignition temperature of mixture was 10°C higher than gum powder alone for all cases. It showed similar temperature variation pattern with Pittsburgh seam coal dust layer. Ketone-based liquid solution did not help the ignition of gum powder layer.

Table 10 : Summary of other test results of gum powder mixture

Amount of ketone-based liquid solution	Hot plate temp.(°C)	Ignition	Maximum temp. at 3mm high(°C)
Gum powder alone	270	Ignition	566
1g	270	No ignition	215
2g	280	ignition	463
4g	270	No ignition	221
	280	Ignition	412

4.8. Comparisons of ignition temperatures with and without combustible liquids

4.8.1. Newspaper dust

As observed from previous test results of other materials, when ignition occurred, the temperature at 6mm high was increased more, so the peak temperature was not recorded at 3mm high thermocouple. Initially, as the dust layer or dust layer mixtures were heated, thermocouple at 3mm high from the hot surface is more closely located than 6mm high thermocouple, which consequently leads higher temperature at 3mm high in the dust layer. However, when ignition occurred, temperature at 6mm high increased more. This is because higher oxygen concentration at 6mm than at 3mm providing more active exothermic oxidation leading higher temperature.

However, this phenomenon was not observed in paper dust alone, and paper dust mixture. Oxygen provision in case of paper dust and its mixture seemed to be high enough through the bottom of the dust layer. This seemed to be related to the paper dust bulk density and void fraction. It was 0.029 g/cm^3 without compression which was much lower than other materials: 0.553 g/cm^3 for Pittsburgh seam coal, 0.338 g/cm^3 for gum powder.

Table 11 : Dust particles' volume fraction and bulk density

	bulk density (g/cm ³)	Particle density (g/cm ³)	Void fraction
Paper dust	0.029	0.61~0.69	0.95~0.96
Pittsburgh seam coal	0.553	1.35	0.59
Gum Arabic powder	0.338	1.08	0.69

In addition, the air in the dust layer could allow more convective heat loss. Non-dimensional heat generation variable in eq.(2.4.12) also confirmed that heat generation was also proportional to the density of dust layers, which means more heat can be generated in denser dust layers in self-heating.

Another consideration on this paper dust test was the interpretation of ignition time. Since the glowing started from the edge of the dust layer and traveled into the center of the dust layer, the maximum temperature of the dust layer did not correspond to the time when glowing started, since the temperature measuring thermocouple was located at the center of the dust layer. However, glowing was first observed about 3minutes at which the first peak temperature was recorded. The next peak temperature was recorded when the glowing reached to the thermal bid at the center of the dust layer.

From figure 58, the temperatures of paper dust alone and mixture with ink were almost same until about 50 sec at 350°C, and from then on to about 200 sec, the mixture of paper dust and ink recorded lower dust layer temperature at 6mm high. If the heat of vaporization was the reason, the

temperature should have been lower from the beginning of the test. For the first 50 sec, major portion of fumes were already generated and only small portion of fumes were observed.

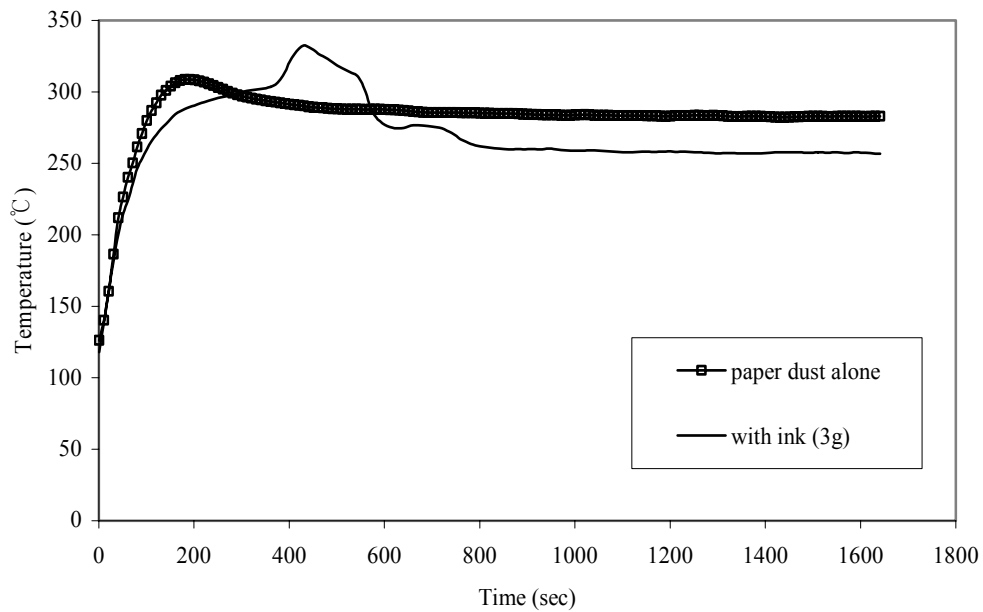


Figure 58 : Paper dust (3g) alone and with ink (3g) at 6mm high at 350 °C

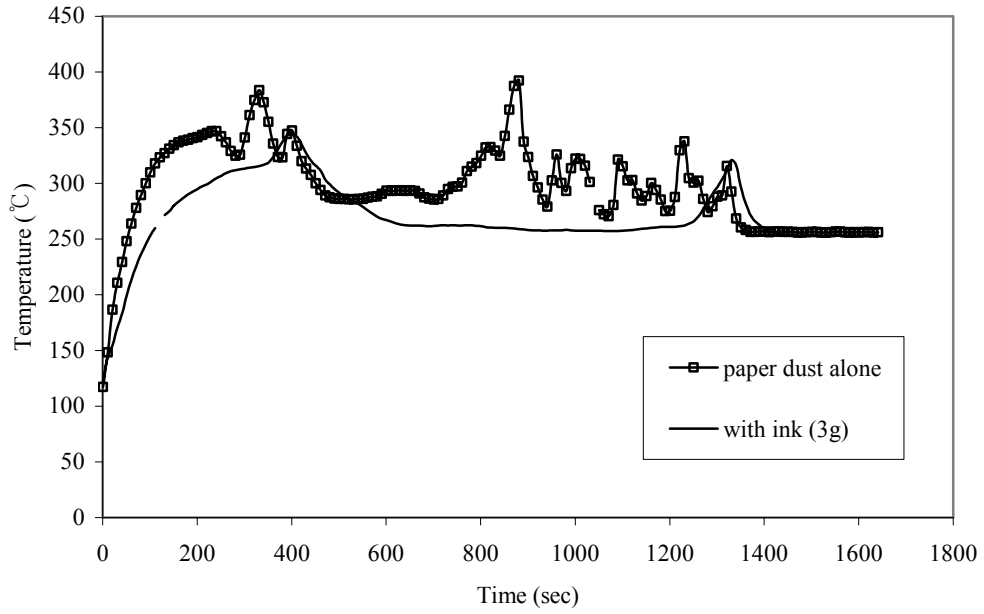


Figure 59 : Paper dust (3g) alone and with ink (3g) at 6mm high at 360 °C

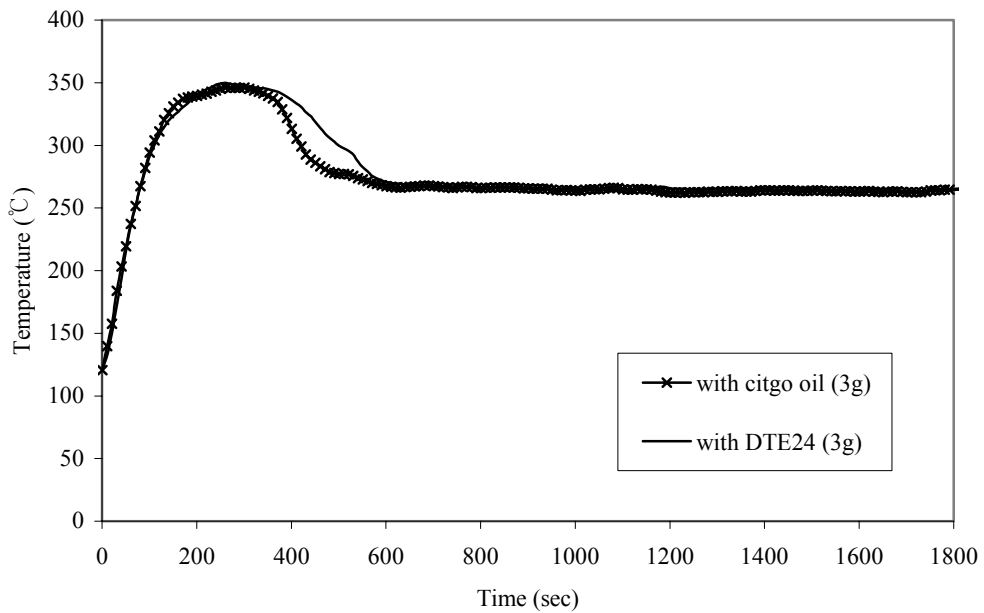


Figure 60 : Paper dust (3g) with Citgo oil (3g) and DTE 24 (3g) at 400 °C

The temperatures of paper dust mixture with Citgo oil and DTE 24 at 6mm high showed very similar temperature variation throughout the test period. Those two combustible liquids have very similar flashpoints and AITs. However, it was revealed that paper dust mixture with Citgo oil and DTE24 have higher ignition temperature than paper dust alone.

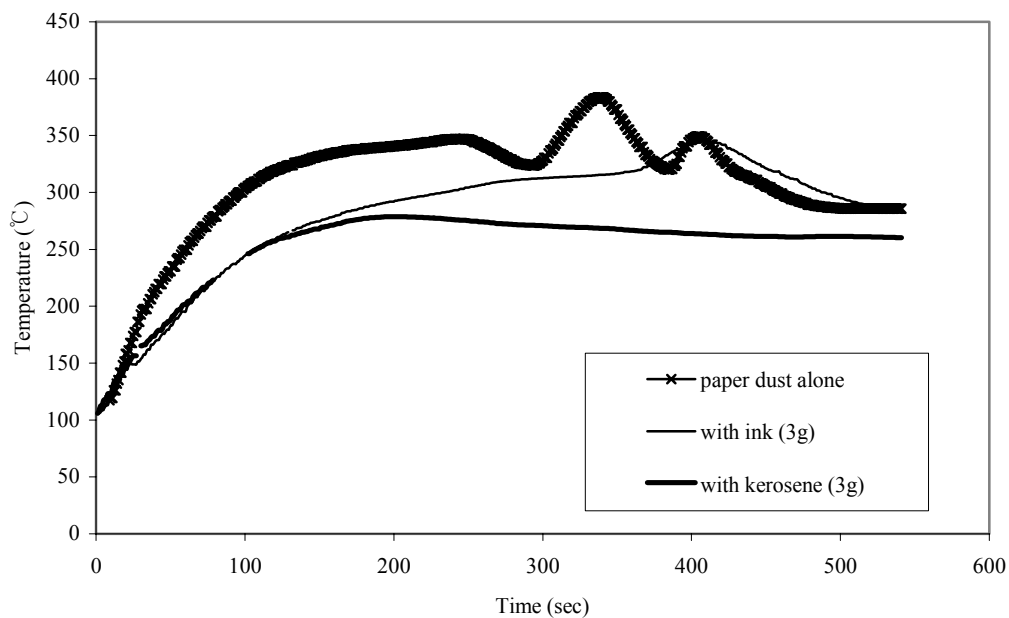


Figure 61 : Paper dust (3g) alone, with ink (3g), and kerosene (3g) at 360 °C, first 600s

The temperatures at 6mm high of three different cases for the first 600 sec at 360 °C were compared in figure 61. For the early 120 sec, the paper dust mixture with ink and kerosene showed very similar temperature development as different from the paper dust alone. At least early stage of hot plate test, paper dust seemed to have higher temperature than other mixtures. This

indicates that the liquid saturated paper had a higher heat capacity than paper dust alone.

4.8.2. Gum Arabic powder

270°C and 280°C were recorded as ignition temperatures for gum powder alone, and for the mixture of gum powder and a ketone-based combustible liquid respectively. From figure 62, gum powder alone ignited at 270°C, but the mixture of 4g ketone-based liquid solution did not ignite at this hot plate temperature. Until 250 sec, ketone-based solution recorded average 7°C higher temperatures than gum powder alone, and from then on to 1200 sec, gum powder alone showed average 8°C higher temperatures. From the figure 63, temperature variations were not much different up to 800s when ignition seemed to occur at a gum powder temperature of 235°C. Before 800s, major portion of ketone-based combustible liquid seemed to be evaporated and some small amount of residue or non-evaporating components were left in the layer. Those components might affect the ignition phenomena of gum powder mixture by delaying exothermic reaction of the gum.

Both gum powder, and gum powder mixture were both ignited at 280°C. However, the time to ignition in case of gum powder mixture was longer than the case of gum powder alone. Larger heat capacity or endothermic reaction energy of the mixture seemed to be the reason.

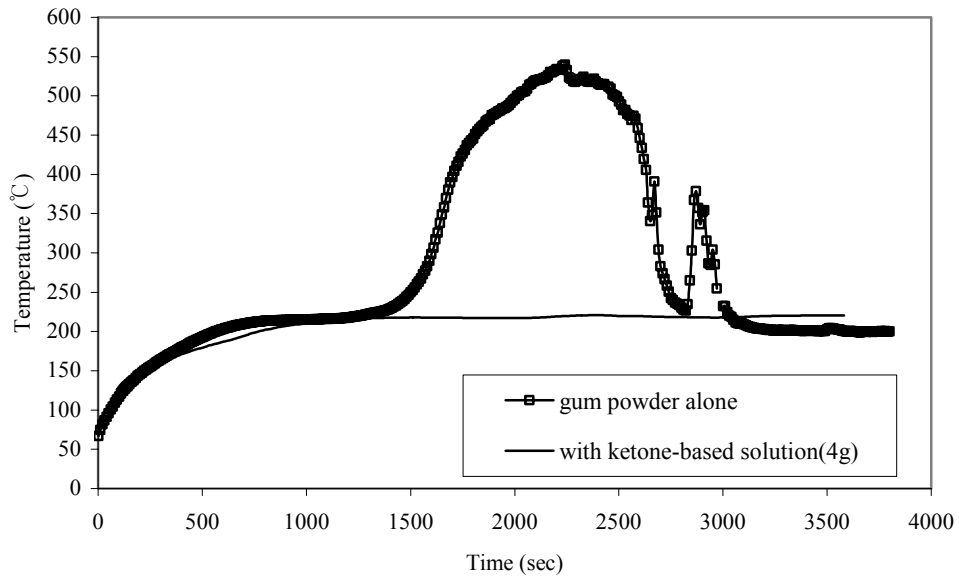


Figure 62 : Gum powder (20g) alone and with ketone-based liquid (4g) at 3mm high at 270 °C

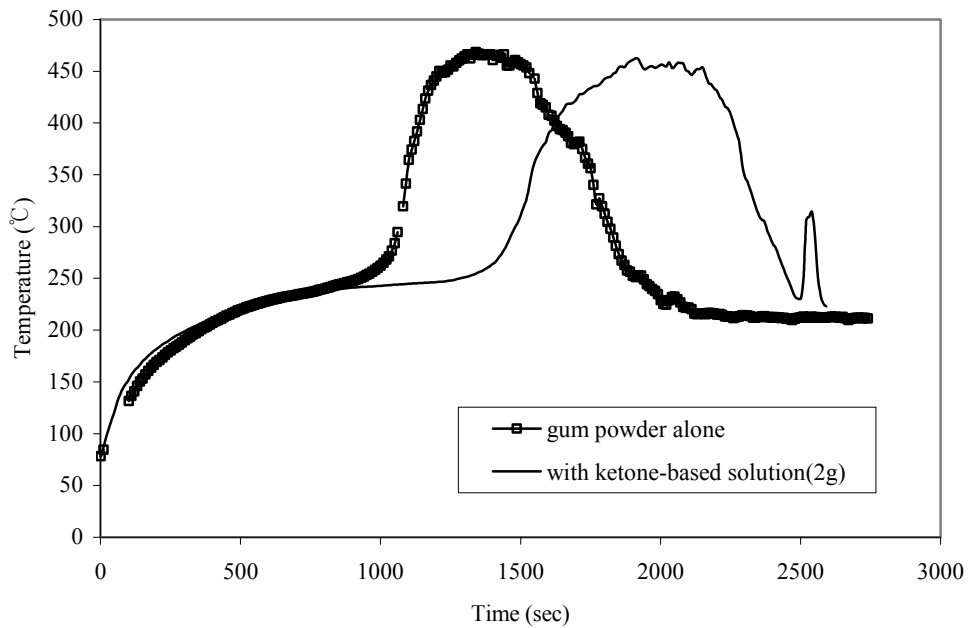


Figure 63 : Gum powder (20g) alone and with ketone-based liquid (2g) at 3mm high at 280 °C

4.9. Ignition temperature of Brass powder with stearic acid

With 10 wt % of stearic acid addition, the ignition temperature of brass powder mixture was measured. In addition, 2, 4, 6, and 10 wt % of stearic acid were tested with 30g of brass powder respectively. Stearic acid is usually used as a brass powder coating material to prevent corrosion. It is not combustible. Its melting point was 69.4°C on the hot plate. Therefore, right after being put on the hot plate, the brass powder mixture generated stearic acid vapors which was not shown when brass powder alone was tested. Discoloration of brass powder layer was also observed in the stearic acid mixture when it was heated which was not observed in brass powder alone. As the mixture was heated, stearic acid was melted and some of them seemed to be left in the dust layer having the particles get together. At the end of test, brass powder was hardened and formed a semi-solid chunks as shown in the figure 70 which was not observed in brass powder alone.

When the 3g (10 wt %) of stearic acid was mixed with 30g of brass powder, the hot plate ignition temperature was 180°C. When the ignition occurred, the period of peak temperature was very short compared to the Pittsburgh seam coal and gum powder as shown in figure 65. The amount of brass powder involved to the ignition seemed to be little or only part of brass powder where stearic acid left in the dust layer seemed to be related to the ignition.

2, 4, 6, 10 wt % of stearic acid were mixed with 30g of brass powder to see the effect of different amount of stearic acid on the ignition temperature. The more amount of stearic acid were added, the lower ignition temperatures were recorded.

Figure 64 and 65 show the temperature variation of the mixture of brass powder with 3g of stearic acid. At 160°C, it was not ignited recording the maximum temperature of 160°C at 3mm high, but at 170°C, ignition occurred showing the maximum temperature of 234°C at 6mm high. As Pittsburgh seam coal and gum powder, temperature at 6mm high was higher than 3mm at ignition. Figures from 66 to 69 show the temperature variation of dust layers at 3mm and 6mm high with addition of 2, 4, 6, 10 wt % of stearic acid, and the results is summarized in table 12. With more addition of stearic acid, the time to the maximum temperature was increased indicating that higher heat capacity of the mixture and higher temperatures.

Table 12 : Summary of brass powder (30g) with different amount of stearic acid addition at 400°C

Addition amount Wt% (weight, g)	Maximum temp. at 6mm high (°C)	Time to Maximum. temp. (s)
2 (0.6)	352	260
4 (1.2)	415	306
6 (1.8)	462	450
10 (3)	559	506

From figure 66, the brass powder mixture of 2 wt % stearic acid did not ignite at 400°C. According to the ASTM E2021, stearic coating less than 1.7 wt % ignited at 155~160°C. The difference between these two cases with similar amount of stearic acid contamination seems the difference of coating vs. blending. Coating

generates oxide layer on the surface of brass powder and it can decrease heat conduction between particles holding higher temperature than simply mixed cases. Another factor could be the vaporization of stearic acid being occurred right after being located on the hot plate.

Brass powder is referred to a benchmarking test material in ASTM E2021. However, the fact that the brass powder manufacturer mentioned in ASTM E2021 is not available any more, and that brass powders available in the market are composed of various compositions having unknown coating level make it not appropriate as a benchmarking test material.

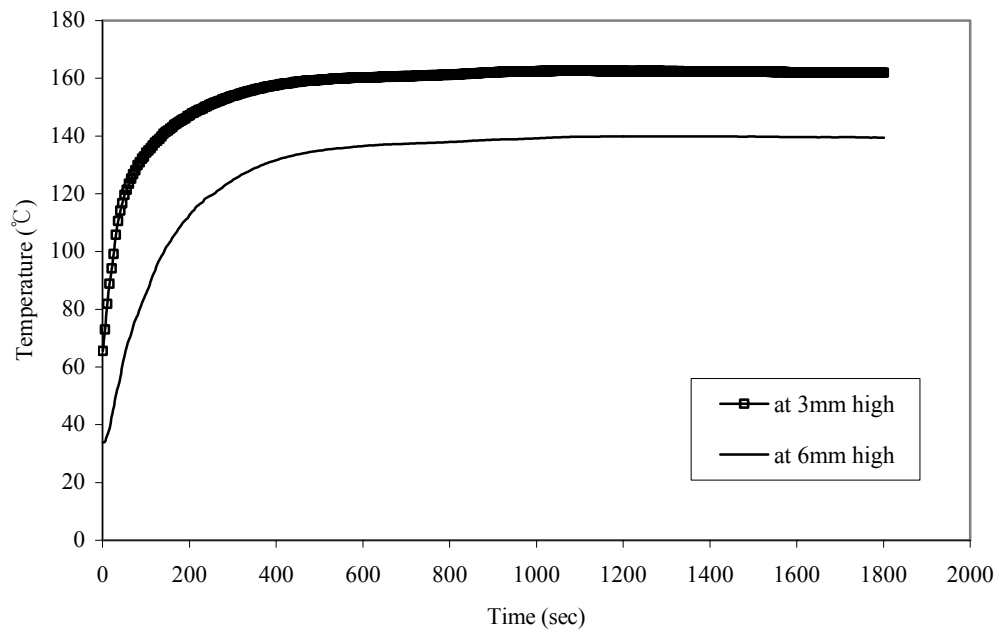


Figure 64 : Brass powder (30g) with stearic acid (3g) at 170 °C

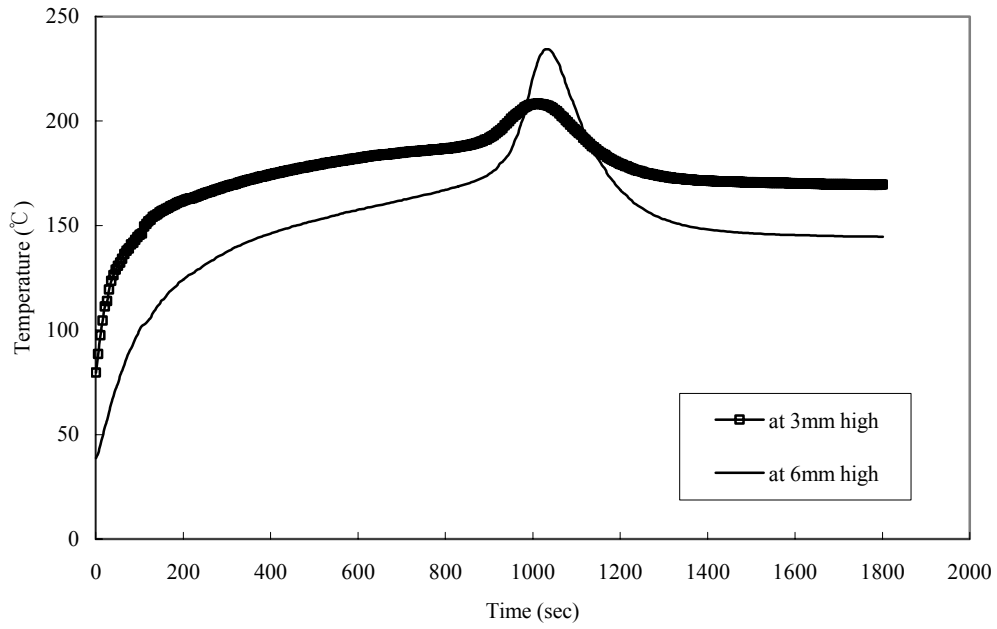


Figure 65 : Brass powder (30g) with stearic acid (3g) at 180 °C

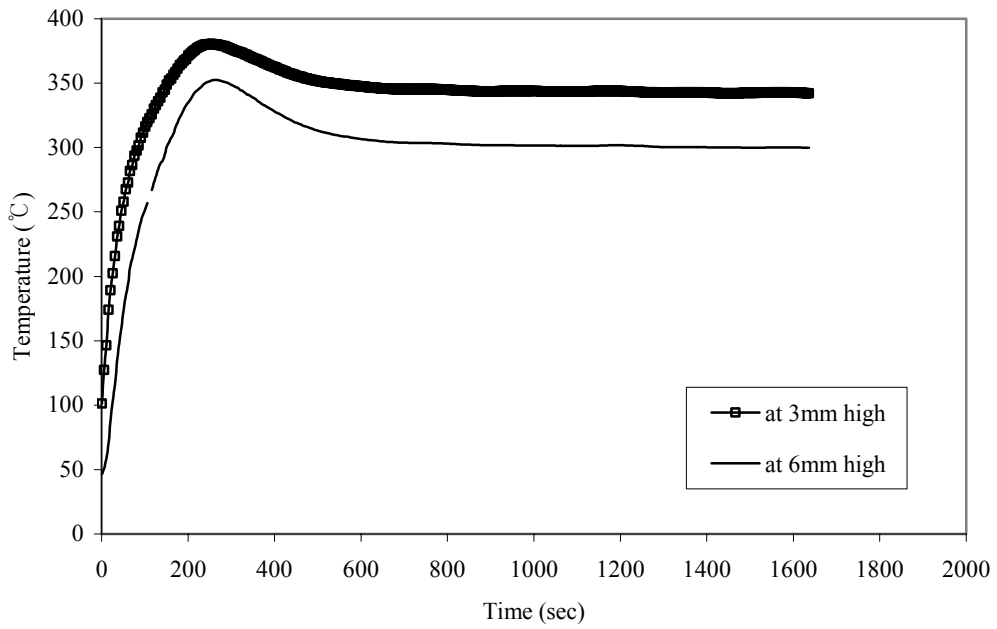


Figure 66 : Brass powder (30g) with stearic acid (0.6g) at 400 °C

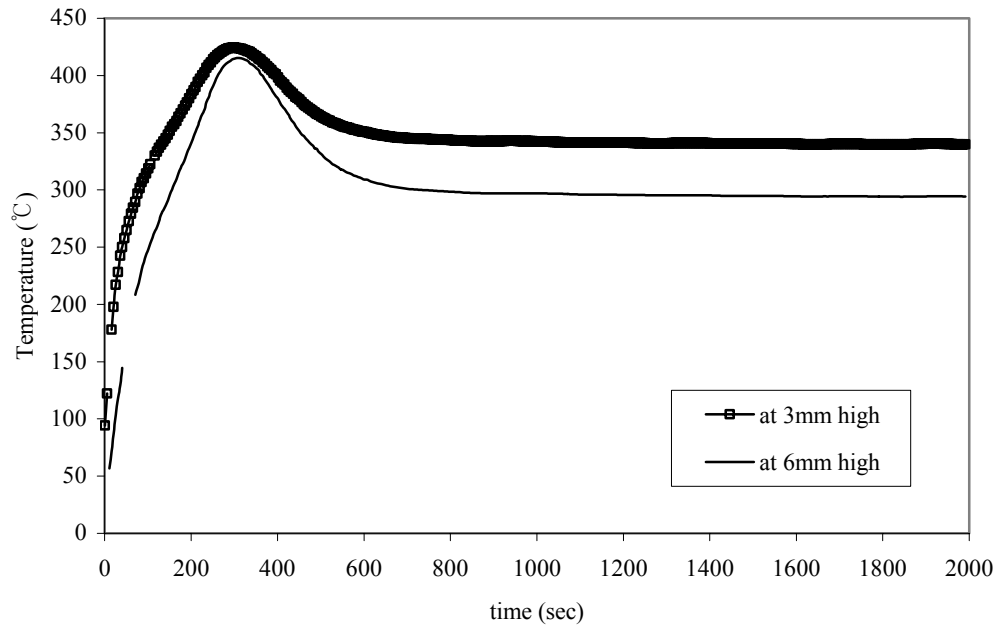


Figure 67 : Brass powder (30g) with stearic acid (1.2g) at 400 °C

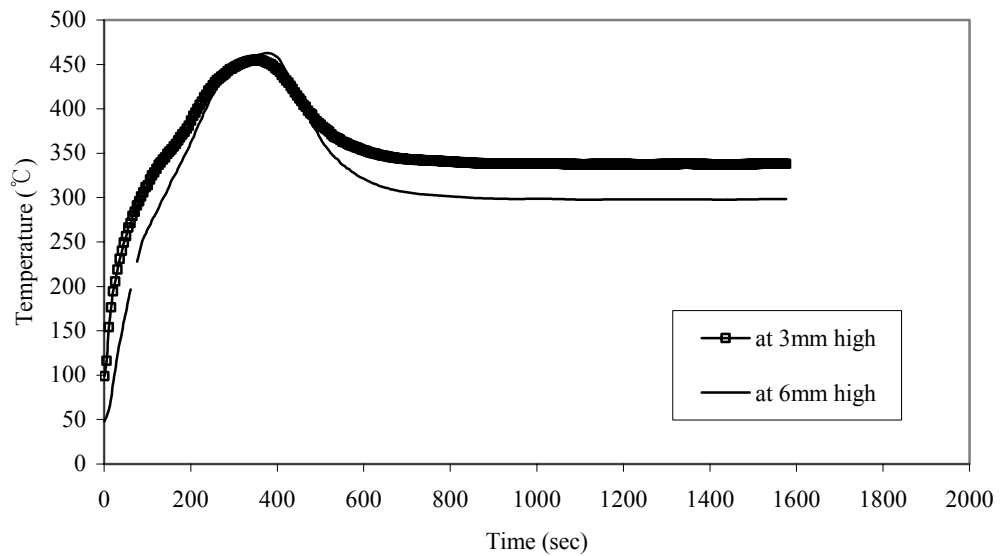


Figure 68 : Brass powder (30g) with stearic acid (1.8g) at 400 °C

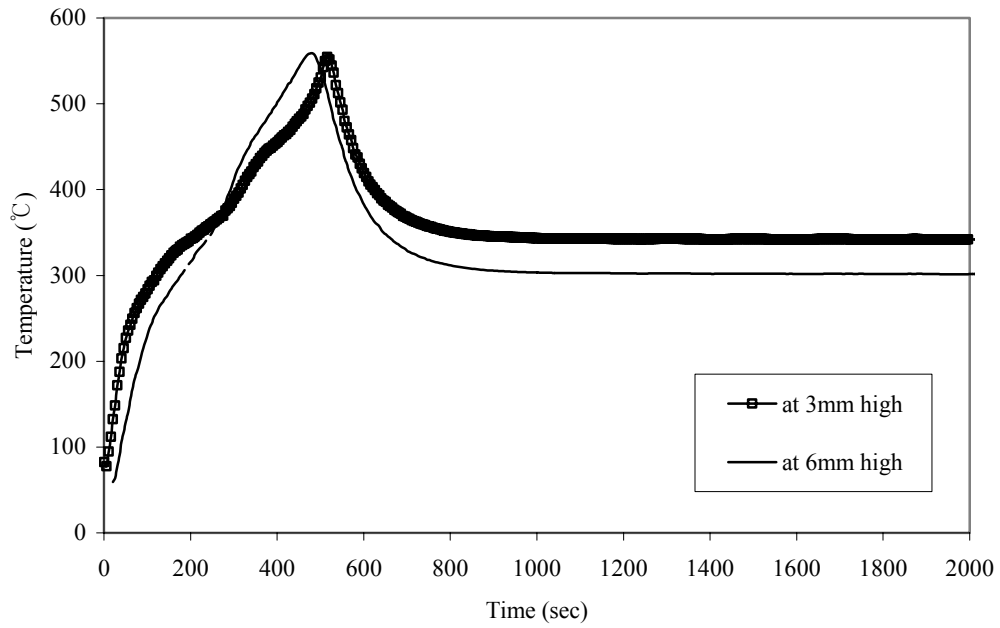


Figure 69 : Brass powder (30g) with stearic acid (3g) at 400 °C

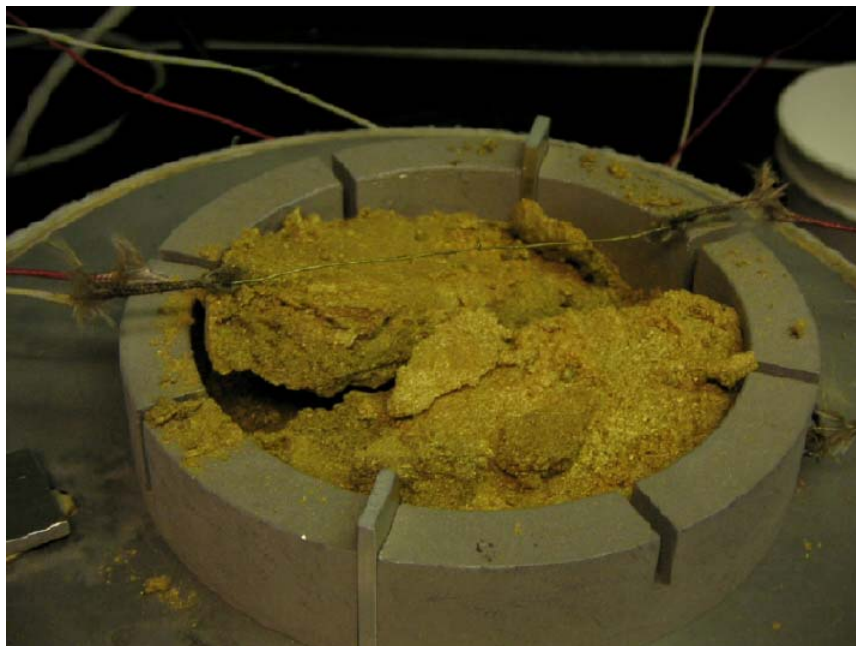


Figure 70 : At the end of test of brass powder with 4% stearic acid at 400 °C

4.10. Oxygen concentration in the Pittsburgh seam coal layer

How critical is oxygen concentration in the ignition of dust layers? Is ignition controlled or limited by the oxygen concentration in the dust layer, or is the limited oxygen concentration caused by ignition chemical reaction in dust layer? Due to the distance from the layer surface, and particles' oxidation as they are heated, the oxygen concentration in the dust layer is not the same as in ambient air condition. More oxidation would occur when dust particles heated more resulting in less oxygen concentration level in the dust layer, and consequently, less oxygen concentration can limit the oxidation possibly ending in not increasing temperature any more.

By comparing the oxygen concentrations when ignition occurred and did not occur, the relationship between oxygen concentration and temperature variation can be explained to some extent. More oxidation of dust particles can increase dust layer temperature and increased temperature will boost oxidation again at over a critical temperature of hot plate.

Oxygen concentration was measured at 6mm above the hot plate in the Pittsburgh seam coal dust layer using oxygen analyzer in a cone calorimeter. The oxygen analyzer sampled air from the exhaust hood through a plastic tube and analyzes it based on electric voltage difference corresponding to a certain oxygen concentration difference. A small brass tube having some holes which was set in the dust layer to sample air was connected to the plastic tube of cone calorimeter.

Ten small holes were made on the brass tube of 1/32 inch inner and 1/16 inch

outer diameter to sample enough amount of air to analyze. The number of holes was decided based on several experiments. 24 gage thermocouple cover was used to wrap the brass tube to prevent small Pittsburgh seam coal dust particle from being sucked with sampled air to the oxygen analyzer. The rate of sampled air maintained at 200ml per minute for more exact analysis. The sampled air passes through all the filters, which are fiber glass heavy particulate filter, 10 μm filter, HEPA filter, acid filter, and then maintained at constant temperature and moisture passing through the cold trap. Then, two drierite desiccants, and sodalime remove remaining moisture and carbon monoxide in the sampled air. At last, oxygen analyzer measures the oxygen concentration at the end of these filters.

The oxygen analyzer was calibrated first with 100 % nitrogen gas (0 % oxygen) and ambient air (20.9% oxygen), and was spanned. 40sec of time lag was observed between actual oxygen concentration in the dust layer and the values calculated from the oxygen analyzer.



Figure 71 : Oxygen analyzer

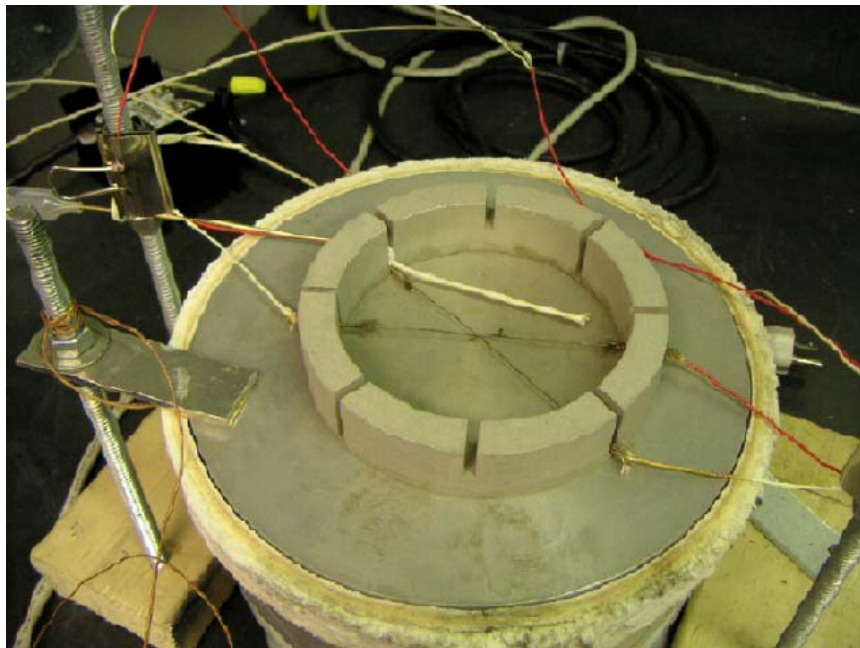


Figure 72 : Brass tube covered by thermocouple cover at 6mm above the hot plate

4.10.1. When ignition occurred

Pittsburgh seam coal dust alone was ignited at 220°C. However, some of heat was taken out of the dust layer with hot sampled air. Therefore, at 220°C, Pittsburgh seam coal dust with brass tube in it did not ignite at 220°C, but 230°C. As shown in figure 73, around 2000 sec, the rate of sampled air from the brass tube in the dust layer dropped all of a sudden to the 10~20 ml per minute which is one tenth of recommended air flow rate for the oxygen analyzer. Therefore, after 2000 sec, the oxygen concentration does not seem to be exact. At the end of test, the brass tube cover was blocked and stuck by the oxidized Pittsburgh seam coal dust particles.

The minimum oxygen concentration recorded 6.2% at 2076 sec. Oxygen concentration has changed from 19% to 6% within 1000°C between about 1000s and 2000s while temperature has changed only about 50°C. After this oxygen concentration drop, dust layer temperature increased steeply. Rolf K. Eckhoff(2003, p. 583) mentioned the fundamental aspect of dust cloud explosion in his *Dust Explosion in the Process Industries*. In the process of dust clouds ignited by hot surfaces, Oxygen concentration through the dust clouds is one of the limiting factors in table 9.1. 6.2% oxygen concentration is lower than the Limiting Oxygen Concentration for coal dust cloud flame propagation, which is in the range of 12 ~ 15% from NFPA 69 table C.1(c), *Limiting Oxidant Concentrations for Combustible Dust Suspensions When Using Nitrogen as a Diluent*. This might not be directly analogous to the dust

layer on the hot surface, but the oxygen limitation in the dust layer seemed to be one of the factors that prevented flaming ignition.

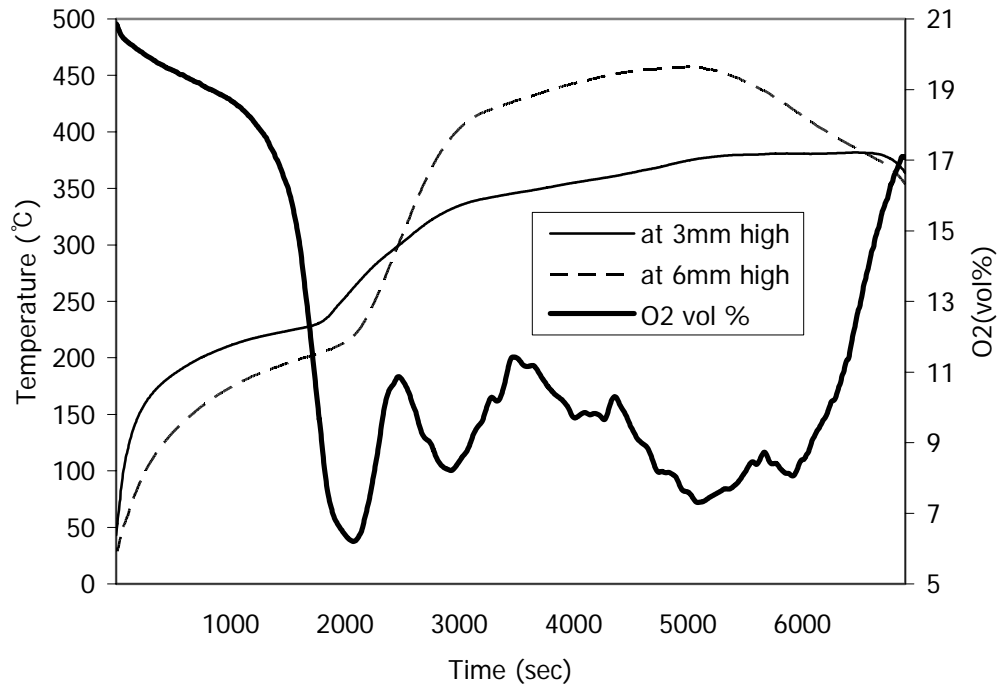


Figure 73 : Oxygen concentration at 6mm high, Pittsburgh seam coal at 230°C



Figure 74 : Pittsburgh seam coal when ignition occurred

4.10.2. When ignition did not occur

Ignition did not occur at 220°C as shown in figure 75. At 220°C, Pittsburgh seam coal dust was ignited without air sampling brass tube. With brass tube in it, heat was taken away with air, and same amount of new cool air filled the space in the dust layer. Oxygen concentration was dropped to 19.8% around 950 sec and maintained for about 300 sec until 1250 sec. At this period, dust layer temperature did not change much, only about 6°C from 199°C to 205°C. At early stage, until 500s, temperature has changed a lot more than other periods. Oxygen concentration change corresponded to the temperature change to some extent, but it only showed general trends, not proportional relationship.

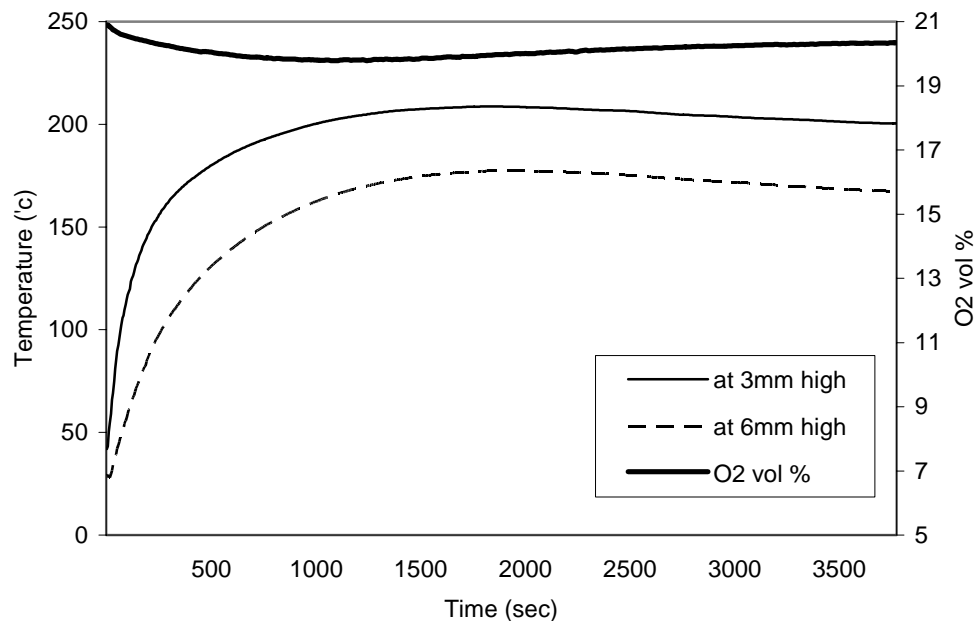


Figure 75 : Oxygen concentration at 6mm high, Pittsburgh seam coal at 220°C

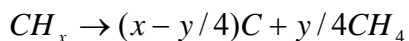
4.10.3. Analysis and summary

Comparison temperatures at 6mm high and oxygen concentrations for the first 3000 sec would be meaningful to see the relationship between oxygen concentration and ignition.

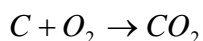
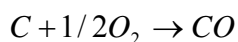
From figure 76, The oxygen concentrations were not different between two cases, ignition at 230°C and no ignition at 220°C, until the first 60s. However, the oxygen concentration on the hot plate of 230°C became much lower than the other one after 60 sec when the dust layer temperature was 50°C. Temperatures were almost same until about 500 sec showing only 4°C difference, 135°C and 131°C for 230°C and 220°C respectively. The temperature increases for this period, 60 sec to 500 sec were almost same, which means oxygen concentration was not reflected in temperature of dust layer at 6mm elevation right away.

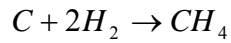
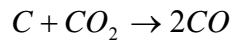
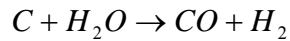
From Solomon et al. Pittsburgh No. 8 bituminous coal particle is mainly composed of C (82.1%), and small portion of other components such as O(8.2%), H (5.6%), S (2.4%), and N (1.7%) composing hydrocarbons and CO during the reaction.

Pyrolysis reaction

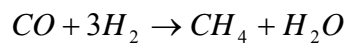
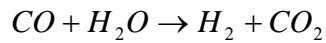


Gas-solid reactions





Gas-gas reactions



When the particle is heated, the first reaction is endothermic pyrolysis reaction or devolatilization in which hydrocarbons are divided into carbon and methane. And then exothermic gas-solid reactions producing carbon monoxide, carbon dioxide, hydrogen, and methane are followed. In this period, the major portion of exothermic reaction occurred in carbon monoxide and dioxide production. As exothermic oxidation occurred generating more carbon monoxide and dioxide, more heat was generated to increase the temperature of dust layer, but not right away. There was some thermal lag time between exothermic oxidation and the increase of dust layer temperature. This can be explained by heat transfer lag time in the dust layer. Although oxygen concentration was decreased which means exothermic reaction occurred in the dust layer, most of the heat energy were stored as source heat energy to increase oxidation more in the dust layer until when the dust layer temperature reached 400 °C. In addition, the major portion of oxygen drop did not occur in this period. Between 1000 sec and 1500 sec, oxygen dropped

pretty fast and corresponding temperature increase from 170°C to 195°C was observed in figure 76. Then, the oxygen concentration most steeply decreased indicating the most active oxidation reaction in the dust layer and this was represented in the dust layer temperature increase from 200°C to 400°C.

As shown figure 74, when ignition occurred, the Pittsburgh seam coal particles near the brass tube collapsed and quite large cracks appeared in the dust layer. Some small particles were carried into the tube with air flow and the each particle volume seemed to be smaller by oxidation. Some white ashes were observed near the brass tube representing more complete reaction.

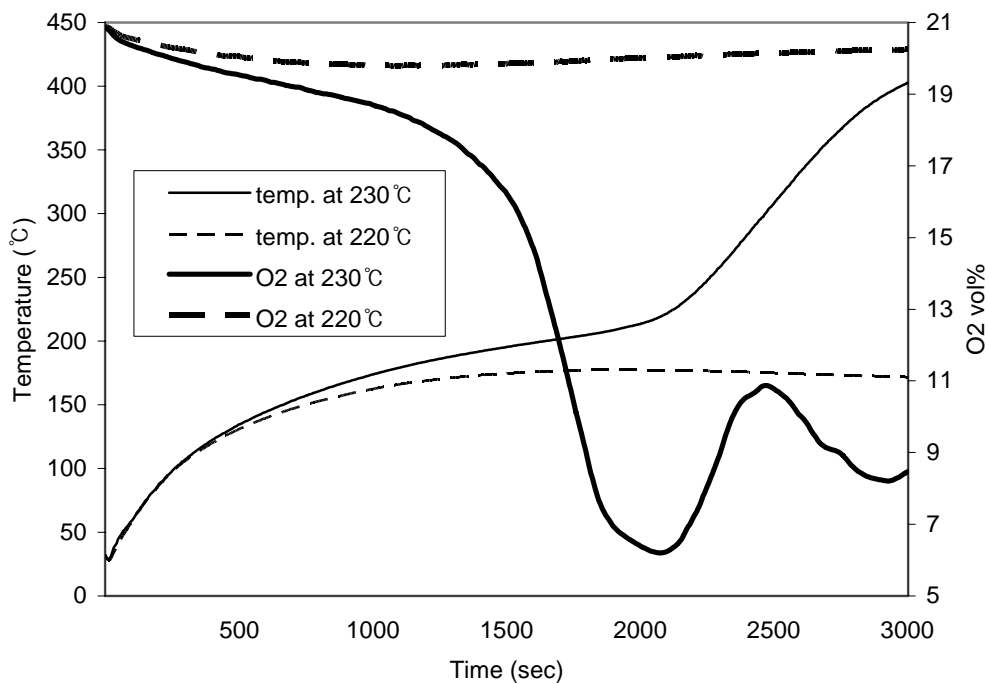


Figure 76 : Oxygen concentrations and temperatures at 6mm above the hot plate when ignition occurred and did not occur

4.11. Air flow effects on ignition temperature of Pittsburgh seam coal layer

The ignition temperature of dust layers in an environment with air flow was measured to see if there is any ignition temperature difference or time to ignition. Since air flow can increase the oxygen concentration in the dust layer accommodating more oxidation reaction. On the other hand, air flow on the surface of dust layer can cool down the layer preventing oxidation reaction in the dust layer.

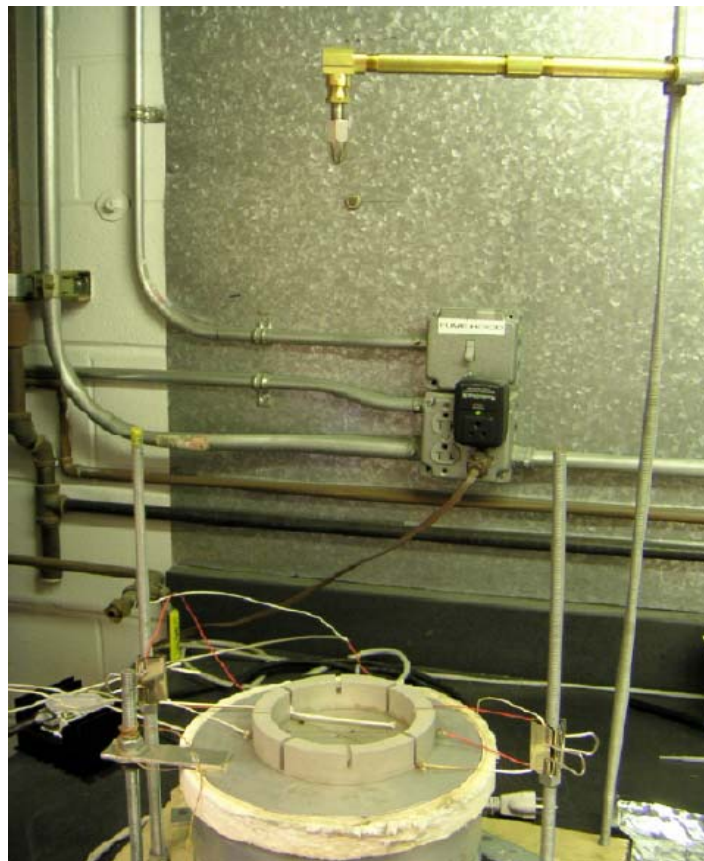


Figure 77 : Downward air flow on the hot plate

1103SS stainless steel Super Air nozzle which was purchased from Exair.com was used to provide downward airflow. The location of air nozzle which was 17 inch (43 cm) above the hot plate was decided based on the air distribution pattern shown in figure 78. 4 inch inner diameter of the ring was the target area of the air flow provision.

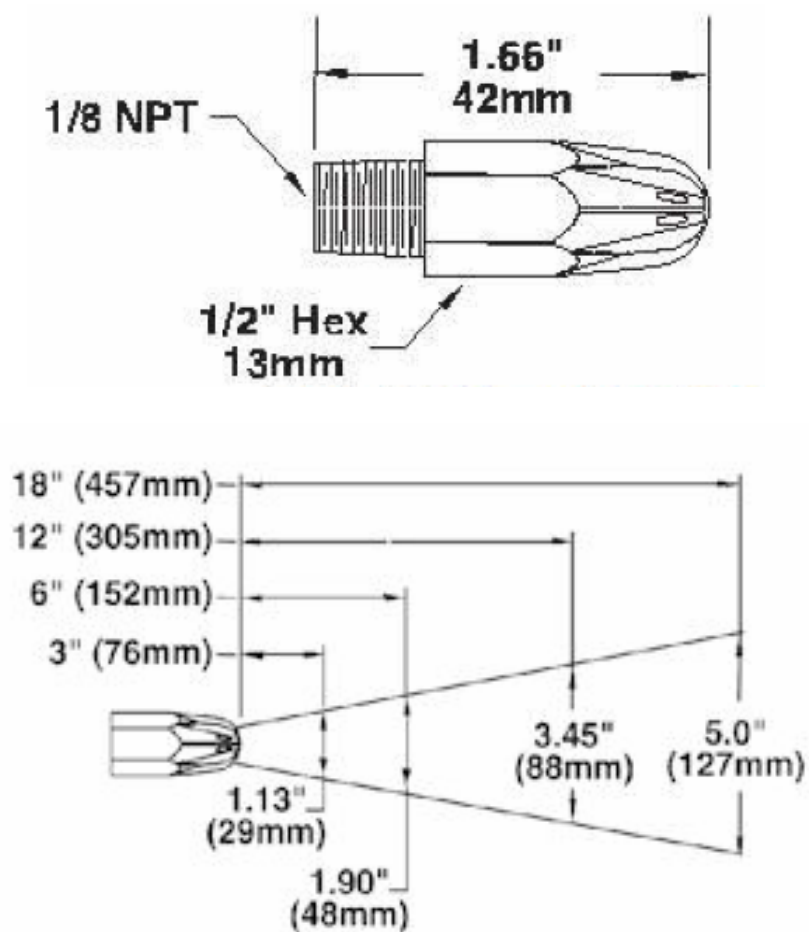


Figure 78 : nozzle shape and air distribution pattern from the nozzle

Air was provided from the air supply valve in the fire science lab. To control and maintain the air flow rate through the air nozzle, an air flow meter

with 5~ 60 SLPM capacities was installed between the air nozzle and built-in air supply in the fire lab. Air flow was provided throughout the test, from when hot plate was turned on, to the end of test. Air flow (cm/s) was measured on the surface of half inch elevation inside ring by air velocity measuring instrument, which is “Velocical model 8355.” for two minutes and average values were selected. It has 2.5% uncertainty range in terms of air velocity between 0.15m/s to 50m/s.

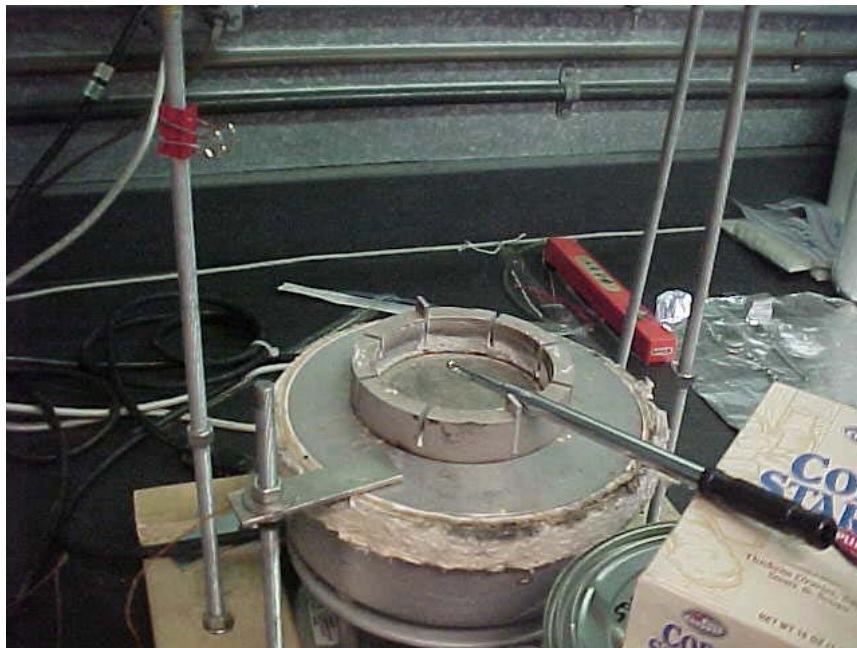


Figure 79 : Air flow velocity measurement

Dust layer temperature variations at 220°C and 230°C without air flow were used as references as exact test results. However, all tests were conducted on the test bench in the fire laboratory where inherent air flow exists due to the fume hood located above the test bench; temperature comparison should be conducted

to verify the test results. With fume hood turned on, the air velocity at the 6mm elevation corresponding to the top surface of dust layer in the ring was average 0.5 cm/s, which did not seem to affect the test results, though.

In addition, to see the effect of downward air flow on the dust layer temperature, 6 SLPM and 15 SLPM air flow with fume hood turned on was provided to the Pittsburgh seam coal dust layer. Air flows at the rates of 6 SLPM and 15 SLPM corresponded to 2.5 cm/s and 33 cm/s respectively with the fume hood turned on.

4.11.1. Without air flow, and with inherent air flow on the bench

In the laboratory without any air flow (average 0 cm/s on the surface of dust layer for two minutes at 220 °C), dust layer temperatures of pittsburgh seam coal measured at 220 °C and 230 °C. As the tests are conducted on the test bench where 0.5 cm/s air flow was measured due to the fume hood, it ignited at 220 °C as shown in figure 80 and not ignited at 210 °C as shown in figure 15. The hot surface ignition temperatures were not different, but the time to ignitions were different as shown in the figure 81. Ignition of Pittsburgh seam coal tested without air flow occurred about 1000 sec earlier than the test with 0.5 cm/s downward air flow provision. This seemed to be due to cooling effect of air flow caused by the fume hood. Dust particles were oxidized generating heat energy and reached the critical temperature where thermal runaway occurred. This referred to the moment of steep temperature increase. Air flow on the bench promoted oxygen concentration increase in the dust layer, but also decreased the dust layer temperature by promoting more convective and conductive heat transfer in the dust layer. Between those, the latter were more dominating and resulted in longer time for ignition.

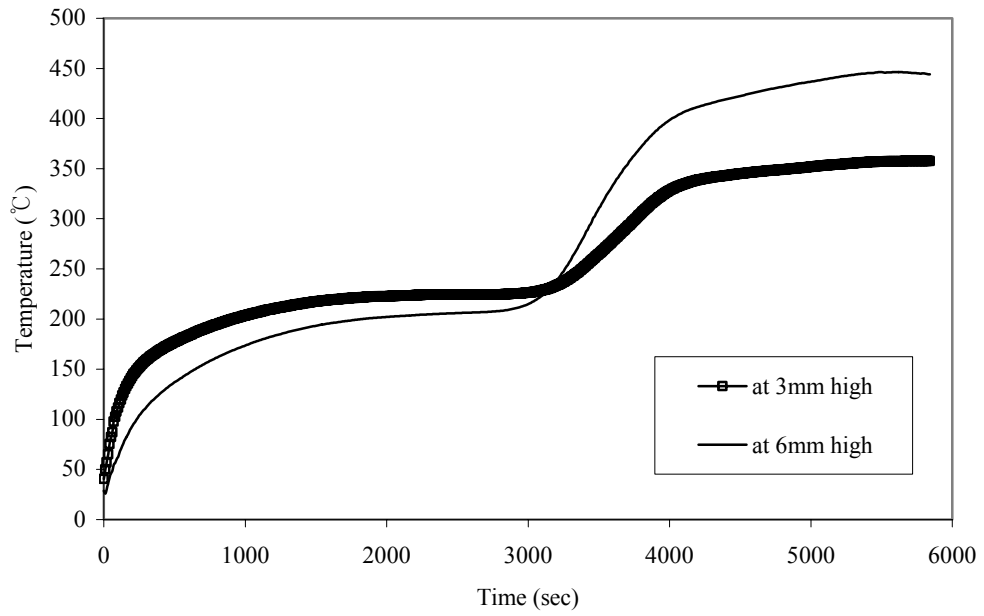


Figure 80 : Pittsburgh seam coal without air flow at 220 °C

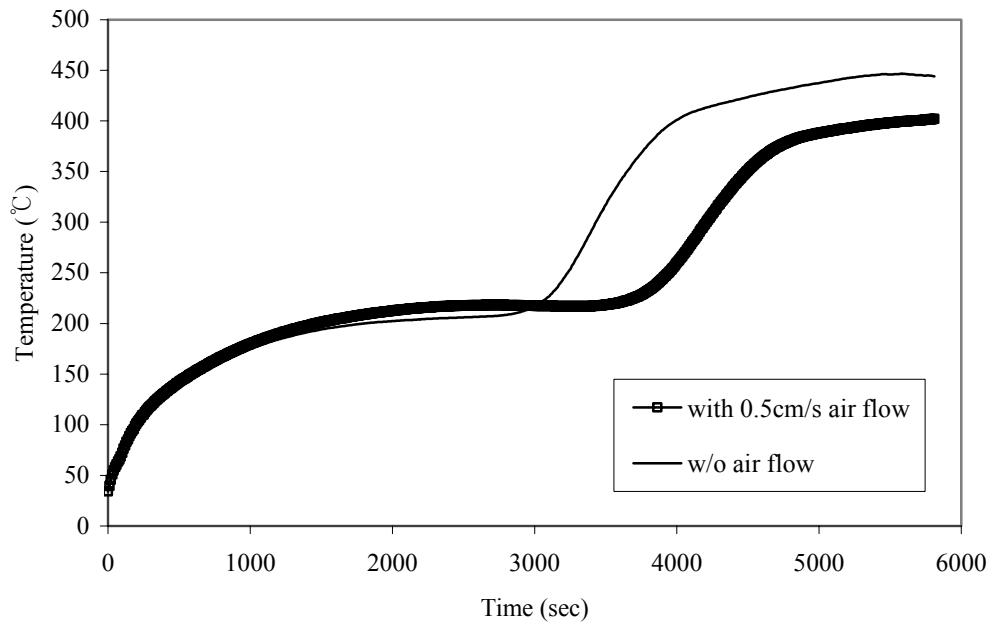


Figure 81 : Pittsburgh seam coal temperatures at 6mm high with and w/o air flow at 220 °C

4.11.2. With downward air flow

6 SLPM (average 2.5 cm/s at the surface of dust layer) downward air flow was provided to the Pittsburgh seam coal dust layer at 220 °C, and the temperature variation was compared with the result without air flow. Figure 82 shows different dust layer temperatures at 6mm high without air flow, and with 6 SLPM (average 2.5 cm/s) downward air flow. Ignition time of the test conducted with 2.5 cm/s downward air flow was longer than the test without air flow due to the cooling effect. The maximum temperature was recorded almost same as about 450 °C at 5650 sec.

Increased air flow rate (15 SLPM) was provided to the Pittsburgh seam coal dust layer on the bench to see if there is ignition temperature difference. Without extra downward air flow, the dust layer was ignited at 220 °C, but with 15 SLPM air flow, the ignition did not occur in the dust layer at 230 °C, as is evident from the temperature data in figure 83. 15 SLPM corresponded to the air velocity of about 33 cm/s at the elevation of the top surface of the dust layer inside the ring.

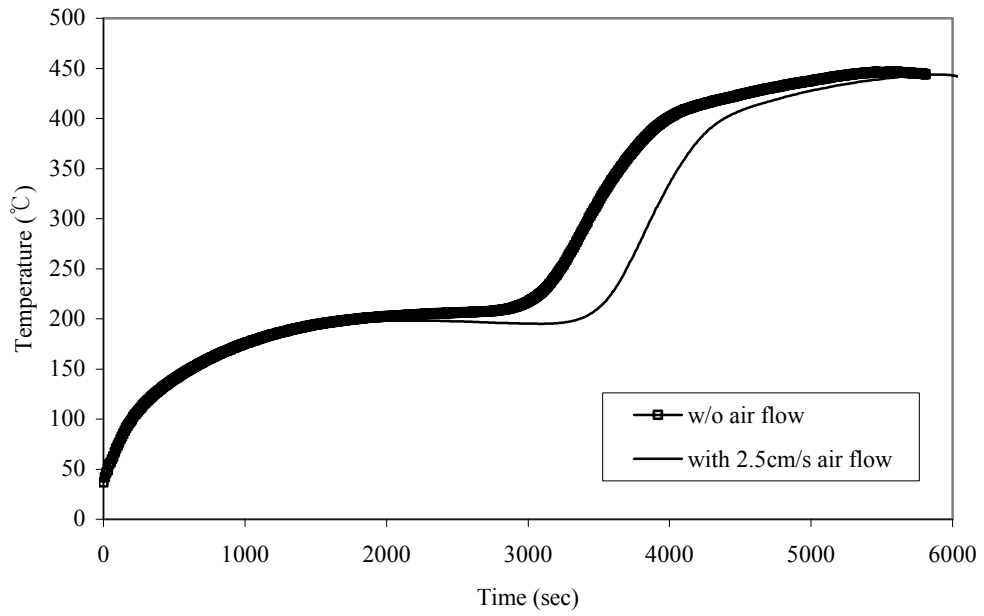


Figure 82 : Comparison of dust layer at 6mm high with and without air flow at 220°C

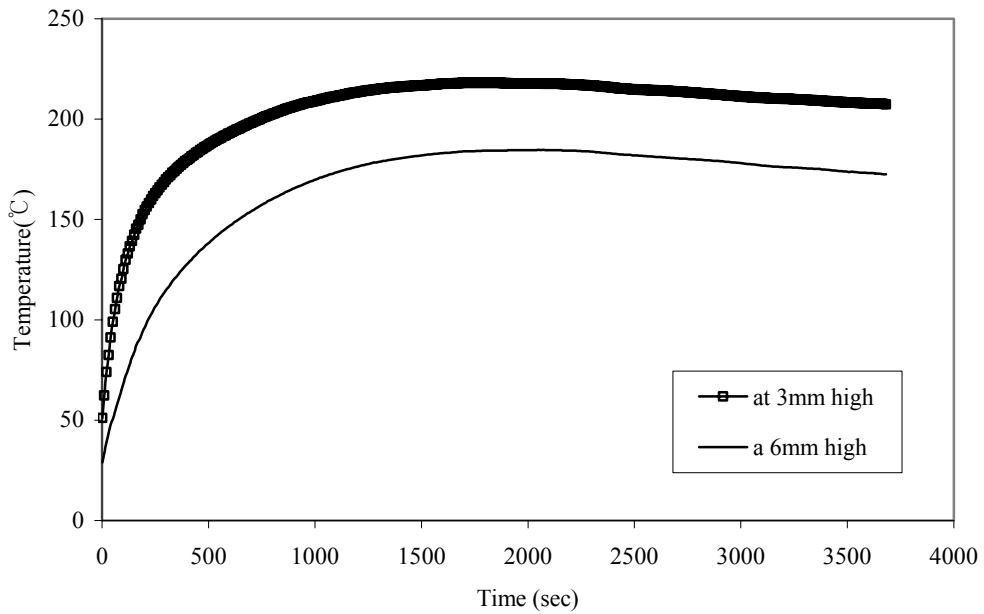


Figure 83 : Pittsburgh seam coal with 15SLPM downward air flow on the bench at 230°C

4.11.3. Analysis and summary

It was revealed that the cooling effect of 2.5 cm/s air flow on the Pittsburgh seam coal dust layer increased the time to ignition. Oxygen diffusion into the Pittsburgh seam coal dust layer by the downward air flow is manifest, but not as strong as cooling effect. With 33 cm/s downward airflow on the bench, Pittsburgh seam coal was not ignited at 230°C which is 10°C higher than the ignition temperature without airflow.

In addition, considering the oxygen concentration level when ignition did not occur from figure 75, the lowest oxygen concentration is about 19% which seemed to more than enough to accommodate ignition of Pittsburgh seam coal dust layer. The dust layer temperature seems more important factor than oxygen concentration level, even by external airflow at least for this test environment. For highly piled Pittsburgh seam coal dust layer, in the middle of which oxygen level might be much lower than the test cases in this thesis, oxygen concentration can be a critical issue for ignition.

5. Application of test results to ASTM E2021 Standard

ASTM E2021 provides a very good test procedure for the hot plate ignition temperature of dust layers. However, the Standard should have at least consider adding more specific information on benchmarking test materials, air flow requirements, and contaminant effects, as explained below. It would also be advisable to use two thermocouples in the dust layers to allow a more reliable indication of ignition, as will also be explained below.

Two of the benchmark combustible dusts cited in the standard cannot easily be obtained now. In particular, the stearic acid coated brass powder is no longer commercially available, at least not from the original supplier. Test results in this thesis show that a mixture of 10 weight percent stearic acid in uncoated brass flakes has an ignition temperature of 170°C. If this temperature can be confirmed by tests at another laboratory, it would make a good candidate benchmark material.

The air flow effects measured in this thesis demonstrate that fume hood air velocities of about 0.5 cm/s and imposed air velocities of 2.5 cm/s at the elevation of the dust layer surface do not affect test results, but an air velocity of 33 cm/s did cause an increase in the minimum hot surface ignition temperature. Therefore, the Standard should specifically prohibit air currents greater than about 4 or 5 cm/s during testing.

The contaminant effect testing in this thesis showed that addition of as little as 6 weight percent stearic acid can significantly reduce the hot surface ignition temperature of brass powder. Therefore, the Standard might specify that the test

results only apply to materials that have no more than 1 or 2 wt% added components to the nominal composition of the test material.

Whenever ignition occurred with the combustible powders alone, the temperature measured at the 6 mm elevation in the dust layer eventually became higher than the temperature at the 3 mm elevation. This inversion of temperatures did not occur without any ignition. Therefore, a new criterion for ignition could be the use of two thermocouples in the layer, with the higher thermocouple temperature becoming greater than the temperature of the lower thermocouple. Since this inversion did not always occur when combustible liquid added to paper dust resulted in ignition, this temperature inversion criterion should not entirely replace some minimum temperature rise criterion. Instead, it is offered as a second criterion to produce clear evidence of oxidation at the mid elevation of the dust layer, and an oxygen-limited combustion at the lower elevation. As one of the ignition criteria in the hot plate ignition test condition for some dust, temperature inversion of at 3mm and 6mm high from the hot plate might be possible.

Another reason for the use of two thermocouples is that the highest temperature was not always recorded in the middle of a dust layer. For example, as shown in figure 40, ignition was observed from the thermocouple at 3mm high in the mixture of paper dust with ink. This ignition criterion is based on the ASTM E2021 standard, which is the dust layer temperature increase more than 50C above the hot plate temperature. Therefore, when ignition occurred, the highest temperature can be recorded at different elevations, not always in the middle of the dust layers.

Although tests were not conducted with varying bulk densities of a particular material, heat and oxygen mass transfer considerations suggest that the bulk density can be an important factor in hot surface ignition temperature of dust layers. Thus, the bulk density should be reported in ASTM E2021 tests.

6. Conclusions and Recommendations

The minimum hot plate ignition temperatures of various dust materials were measured with and without addition of combustible liquids. A half inch thick layer of paper dust alone in the 4 inch inner diameter ring on a hot plate was ignited when the hot plate temperature was at or above 360°C with addition of 50 weight percent of two hydrocarbon base hydraulic oils commonly used on printing presses, the paper dust mixtures did not ignite until the hot plate temperature reached 400°C. With the same 3g addition of newspaper printing ink (50 weight %), the ignition temperature of paper dust mixture with a newspaper printing ink was reduced to 350°C which was 10°C lower than news paper dust layer alone. Overall, paper dust test results demonstrated that the addition of combustible liquids does not seem to lower the hot surface ignition temperature by more than 10°C, and in most cases increase the hot surface ignition temperatures.

Gum powder mixed with a ketone-based liquid solution, which is of the gum powder processing, resulted in a slightly higher than hot surface ignition temperature. The hot plate ignition temperatures were 270°C for gum powder alone, and 280°C for the mixture of gum powder with 0.5 to 2 wt% ketone-based liquid solution.

Downward air flow was provided to see if there is any effect on the hot surface ignition temperatures of dust layers. With 15 SLPM downward air flow (33 cm/s at the top of dust layer), the Pittsburgh seam coal did not ignite at 230°C. Without air

flow, it was ignited at 220°C. When the ignition did not occur, the oxygen concentration was above 19 vol% which is higher than the 17 vol% Limiting Oxygen Concentration for combustion of coal dust clouds. Therefore, the slightly reduced oxygen concentration in the Pittsburgh seam coal dust layer is not the critical factor that can change the hot plate ignition temperature, for dust layer bulk densities from about 0.03 to 0.55 g/cm³ of tested materials. Since there is sufficient oxygen to support combustion in the absence of air flow, the reduced hot surface ignition temperatures with air flow are probably due to the increased convective heat loss at the dust layer free surface.

Stearic acid was added to the brass powder dust layer. Half inch brass powder did not ignite until the hot plate temperature reached 400°C. However, small amount of stearic acid addition resulted in large decrease of hot plate ignition temperature. 30g of brass powder with 3g of stearic acid addition was ignited at 180. This is more than 200°C different from the ignition temperature of brass powder alone. Since brass powder is used as a benchmarking test material in ASTM E2021, it may be advisable to change the current imprecise specification of a stearic acid coating which is <1.7 wt %, to a more precise mixture of uncoated brass powder with 10 wt % stearic acid addition to produce a 180 hot surface ignition temperature.

Clearer criteria for ignition definition in the ASTM and IEC hot surface ignition standards should be considered. Although ASTM E2021 stated 50°C or more difference between the hot plate temperature and the thermocouple in the middle of

dust layer, as observed in the case of paper dust mixture with ink, the temperature in another location of dust layer, not in the middle of dust layers, can be higher than in the middle of dust layer. In many other tests, the temperature at the lower elevation was greater than the temperature at the mid elevation prior to ignition, but became less than the mid elevation temperature after combustion occurred in the layer.

References

¹Y. Miron and C. P. Lazzara, Hot-surface Ignition Temperatures of Dust Layers, Fire and Materials, Vol. 12, p. 115~126, 1988

²P. C. Bowes and S. E. Townshend, Ignition of Combustible Dusts on Hot Surfaces, BRIT. J. APPL. PHYS, Vol. 13, 1962

³G. A. Lunn, Testing Methods for Electrical Apparatus Installed in a Dusty Environment with a Potential Risk of Explosion, SMT-CT98-2273, 2001

⁴B. J. Tyler and D. K. Henderson, Spontaneous Ignition in Dust Layers: Comparison of Experimental and Calculated Values, IChemE Symposium Series No. 102, p.45~59, 1987

⁵ASTM E2021-01, Standard Test Method for Hot-Surface Ignition Temperature of Dust Layers, 2001

⁶AIChE, Guidelines for Safe Handling of Powders and Bulk Solids, chapter 4, Assessing particle hazards, 2004

⁷Robert G. Zalosh, Industrial Fire Protection, p. 132, 2002

⁸Rolf K. Eckhoff, Dust Explosions in the Process Industries, p.583, 2003

⁹Vytenis Babrauskas, Ignition Handbook, p.207-210, p.369~383, 2003

¹⁰Dougal Drysdale, An Introduction to Fire Dynamics, 2nd ed. p. 197~200, 2001

¹¹SFPE Handbook, 3rd ed. p.2-211~2-227

¹²N. Jackson, Boston globe, personal communication to R. Zalosh, 2004

¹³Michael A. Nowack et al. Coal Conversion, Encyclopedia of Energy, Vol. 1, p. 425~434, 2004

¹⁴Kiddie-Fenwal, report No. CRC-2556, November 8, 2005

¹⁵ B. R. Bhandari et al. Flavor Encapsulation by Spray Drying: Application to Citral and Linalyl Acetate, J of food sciences, Vol. 57, No.1, 1992

¹⁶<http://www.paperonweb.com/density.htm#density>

¹⁷http://www.mcelwee.net/html/densities_of_various_materials.html

Appendix A: AITs of hydraulic oils

Tests conducted

Auto ignition temperature of liquid chemicals (AIT)

Test Method

ASTM E 659

1. Results

The Reaction Threshold Temperature (RTT), Cool Flame Temperature (CFT), and Auto-Ignition Temperature (AIT) were determined at atmospheric pressure in air. The results are tabulated below.

	Test Material		Reference Materials	
	CITGO Hydraulic/ Press Oil 68	DTE 24	n-Heptane	Ethyl Alcohol
RTT ¹ (°C)	290	281	207	363
CFT ¹ (°C)	293	284	N/A	380
AIT ¹ (°C)	308	359	215	388

1. ASTM Definitions:

RTT: Reaction threshold temperature for nonluminous pre-flame reaction. Typically, this is evidenced by a weak and gradual temperature rise, which then falls off to the base temperature.

CFT: Cool-flame autoignition temperature. Cool flames may occur at lower flask temperature than hot flames. It is typically evidenced by a temperature rise of less than 100 °C.

AIT: Hot-flame autoignition temperature. It is usually evidenced in these tests by hot flames of various colors, usually yellow, red, or blue. Normally hot-flames produce sharp temperature rises of at least a few hundred degrees or more.

2. All tests were conducted at Barometric Pressure of 29.8 inHg ± 0.2.

Table 1

Test Material: CITGO Hydraulic/ Press Oil 68

Auto-ignition Temperature (AIT): 308 °C

Cool Flame Temperature (CFT): 293 °C

Reaction Threshold Temperature (RTT): 290 °C

Test No.	Sample Amount (mg)	Flask Temp. °C	Result Go /No Go	Time Lag Sec.	RTT °C	CFT °C	AIT °C
1	100	250	No Go	-			
2	100	280	No Go	-			
3	100	295	No Go	-	295		
4	100	310	No Go	-	310		
5	100	319	No Go	-	319		
6	100	349	Go	20		349	
7	100	379	Go	6			379
8	100	370	Go	7			370
9	100	361	Go	20		361	
10	100	364	Go	40		364	
11	100	367	Go	30		367	
12	100	322	Go	-		322	
13	100	325	Go	-		325	
14	100	328	Go	-		328	
15	100	334	Go	-		334	
16	100	340	Go	-		340	
17	150	340	Go	20		340	

18	150	355	Go	9			355
19	150	349	Go	30		349	
20	150	352	Go	30		352	
21	150	329	Go	30		329	
22	150	320	Go	-		320	
23	150	323	Go	-		323	
24	150	326	Go	-		326	
25	150	311	Go	-		311	
26	150	305	No Go	-	305		
27	150	308	Go	-		308	
28	200	308	Go	10			308
29	200	293	Go	-		293	
30	200	299	Go	-		299	
31	200	302	Go	-		302	
32	200	305	Go	-		305	
33	250	305	Go	-		305	
34	200	287	No Go	-	287		
35	200	290	No Go	-	290		

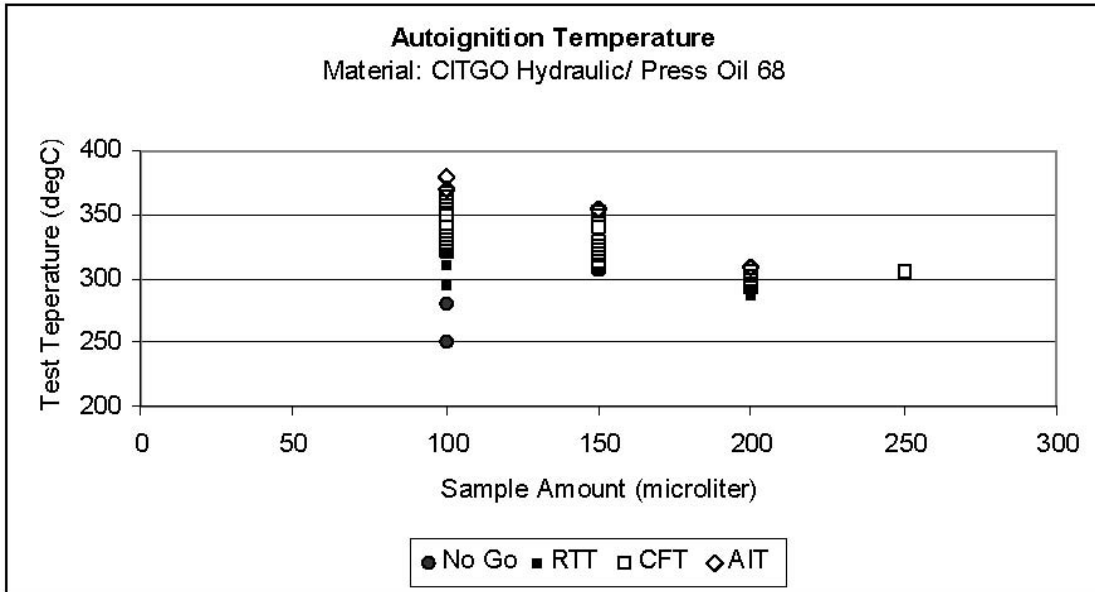


Table 2

Test Material: DTE 24

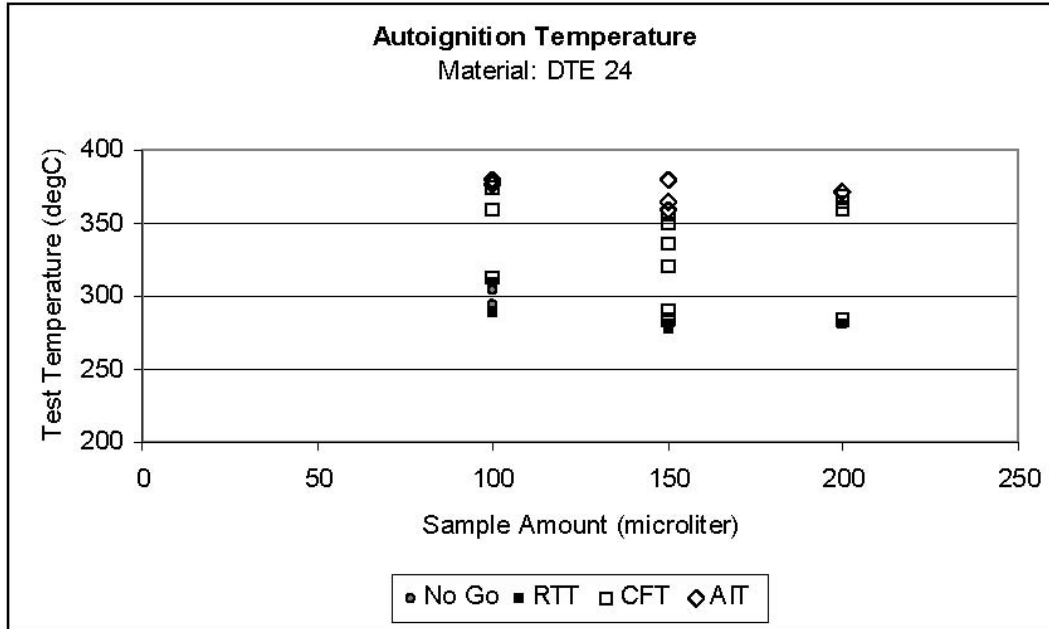
Auto-ignition Temperature (AIT): 359 °C

Cool Flame Temperature (CFT): 284 °C

Reaction Threshold Temperature (RTT): 281 °C

Test No.	Sample Amount (mg)	Flask Temp. °C	Result Go /No Go	Time Lag Sec.	RTT °C	CFT °C	AIT °C
1	150	290	Go	-		290	
2	150	284	Go	-		284	
3	150	278	No Go	-	278		
4	150	320	Go	-		320	
5	150	335	Go	-		335	
6	150	350	Go	-		350	
7	150	380	Go	3			380
8	150	365	Go	7			365
9	150	356	Go	-		356	
10	150	359	Go	9			359
11	150	281	No Go	-	281		
12	200	281	No Go	-	281		
13	200	284	Go	-		284	
14	200	359	Go	-		359	
15	200	365	Go	-		365	
16	200	371	Go	4			371
17	200	368	Go	-		368	

18	100	359	Go	-		359	
19	100	374	Go	-		374	
20	100	380	Go	5			380
21	100	377	Go	5			377
22	100	289	No Go	-	289		
23	100	295	No Go	-			
24	100	304	No Go	-			
25	100	313	Go	-		313	
26	100	310	No Go	-	310		



Appendix B: sieve size

Sieve number	Theoretical opening size(μm) (US mesh)	Sieve size opening ASTM 2(μm)
18	1000	1000
20	841	850
25	707	710
30	595	600
35	500	500
40	420	425
45	354	355
50	297	300
60	250	250
70	210	212
80	177	180
100	149	150
120	125	125
140	105	106
170	88	90
200	74	75
230	63	63
270	53	53
325	44	45
400	37	38
500		32
600		25